VAGINAL DELIVERY OF A HYDROPHOBIC ANTIRETROVIRAL DRUG CSIC FOR HIV PREVENTION: NOVEL FORMULATION STRATEGIES FOR IMPROVED DRUG SOLUBILIZATION AND LYMPHATIC TARGETING

By

Tiantian Gong

BS, China Pharmaceutical University, 2007

Submitted to the Graduate Faculty of

School of Pharmacy in partial fulfillment

of the requirements for the degree of

Doctor of Philosophy

University of Pittsburgh

2015

UNIVERSITY OF PITTSBURGH

SCHOOL OF PHARMACY

This dissertation was presented

by

Tiantian Gong

It was defended on

August 10, 2015

and approved by

Byron Ballou, PhD, Molecular biosensor and imaging center (MBIC), Carnegie Mellon

University

Kerry Empey, Pharm D, PhD, Department of Pharmaceutical Sciences, School of Pharmacy,

University of Pittsburgh

Michael A.Parniak, PhD, Department of Microbiology & Molecular Genetics, School of

Medicine, University of Pittsburgh

Song Li, MD, PhD, Departmental of Pharmaceutical Sciences, School of Pharmacy,

University of Pittsburgh

Dissertation Advisor: Lisa C. Rohan, PhD, Department of Pharmaceutical Sciences, School of

Pharmacy, University of Pittsburgh

VAGINAL DELIVERY OF A HYDROPHOBIC ANTIRETROVIRAL DRUG CSIC FOR HIV PREVENTION: NOVEL FORMULATION STRATEGIES FOR IMPROVED DRUG SOLUBILIZATION AND LYMPHATIC TARGETING

Tiantian Gong

University of Pittsburgh, 2015

HIV epidemic is an ongoing health concern globally. Sexual transmission accounts for the overwhelming majority of new infections. Vaginal microbicides are under investigation as pre-exposure prophylaxis (PrEP) products for HIV prevention. Although progress has been made, the development of more efficacious products is warranted. Cervicovaginal tissue and draining lymph nodes contain an adequate amount of HIV target cells and play critical roles in HIV replication and sedimentation at the early stage of infection. Improved efficacy can be achieved with the use of specially designed drug delivery systems which achieve greater drug concentrations in these two sites of action.

In this dissertation, we hypothesized that the hydrophobic microbicide candidate CSIC can be formulated in a polymeric vaginal film and a nanocrystal formulation with high loading capacities using multiple formulation strategies. We further hypothesized that the nano-delivery strategy can improve cervicovaginal tissue drug penetration and achieve lymphatic drug delivery. Series of preformulation studies were conducted to evaluate the physicochemical and biological properties of the drug candidate CSIC. The major challenge for CISC formulation development

was identified as its hydrophobicity. Therefore, a cosolvent system comprising PEG 400, propylene glycol, and glycerin at a ratio of 5:2:1 has been optimized and utilized in a polymer based vaginal film formulation for increased drug solubility, long term stability, and lack of leakage. Additionally, a CSIC nanocrystal formulation, with a particle size of 243nm and near neutral surface charge, was developed. CSIC nanocrystals have been proved to possess increased drug saturation solubility, rapid mucus penetration properties, and improved drug permeation in the cervicovaginal tissue. More importantly, the pharmacokinetic study provided the first evidence of lymphatic targeting after intravaginal application without causing any epithelial damage. Furthermore, CSIC was able to release from the nanocrystals in a sustained mode, indicating its potential use as a coitally independent PrEP product that could improve user adherence. In summary, this work sets the stage to create new opportunities for sexually transmitted HIV prevention through the development of a novel dual targeting delivery system. The developed approaches can be used to deliver other drugs that lack solubility or require lymphatic targeting.

TABLE OF CONTENTS

LIST OF TABLES

LIST OF FIGURES

PREFACE

Completing my graduate training and dissertation work was never possible without the support and guidance from many people.

My greatest gratitude goes to my advisor Dr.Lisa Rohan. Her mentorship and scientific guidance lead me to develop essential professional skills and scientific thinking and to become an independent scientist. Her support and help in many aspects of my personal life helps me to be a more mature individual.

I would like to express my deepest gratitude to my committee members: Dr. Byron Ballou, Dr. Michael Parniak, Dr. Kerry Empey, and Dr. Song Li, for their invaluable input and guidance over the past five years. I would not have been able to complete my dissertation work without their support.

I also want to extend my special thanks to Dr. Judith Yanowitz, Dr. Robert Powers, and Dr. Ida Washing for their help on live cell imaging, IACUC application, and animal studies.

I am grateful to all of the lab members of the Rohan Lab, both past and present, for their support, help, and friendship. Special thanks to Dr. Ayman Akil, Dr. Wei Zhang, Dr. Lindsay Kramzer, Dr. Tian Zhou, and Dr. Haitao Yang, for sharing their knowledge, experience, and technique with me. Thanks also go to my classmates and friends in the School of Pharmacy, especially to Dr.Osama Alshogran and Kacey Anderson, for their support and accompany in the years of graduate courses.

I am extremely gratefully to my parents, Aiguo and Geli for all they sacrificed for me and for allowing me time away from the family stuff to complete my dissertation writing. They has been encouraging, supportive, and shown belief in me. Without their help, it would have been impossible for me to get the best education I can ever have.

Lastly, but most importantly, I would like to thank my dear husband Yi and our sweet little boy Luke. Their love and smile are my endless motivation. Without which, I cannot be where I am today.

This thesis is dedicated, with love, to my husband Yi and our son Luke.

LIST OF ABBREVIATIONS

ACN	Acetonitrile
AIDS	Acquired ImmunoDeficiency Syndrome
APC	Antigen Presenting Cell
API	Active pharmaceutical ingredient
ATCC	American Type Culture Collection
BP	British Pharmacopeia
BSA	Bovine serum albumin
BV	Bacterial vaginosis
CAP	Cellulose acetate phthalate
CBQCA	3-(4-carboxybenzoyl) quinoline -2-carboxaldehyde
CCR5	C-C motif receptor 5
CD4	Cluster of Differentiation 4
CDC	Center for Disease and Control
CMC	Critical micelle concentration
CONRAD	Contraceptive Research and Development
CXCR4	C-X-C motif receptor 4
CSIC	
DC	Dendritic Cell
DIC	Differential Interference Contrast
DLS	Dynamic light scattering
DMSO	Dimethyl sulfoxide
DPV	Dapivirine
DSC	Differential scanning calorimetry
DMEM	Dulbecco's Modification of Eagles Medium
DMSO	Dimethyl sulfoxide
DNA	Deoxyribonucleic acid
EC_{50}	Half Maximal Effective Concentration

FD	Free drug
FDA	Food and Drug Administration
GI	Gastrointestinal
H & E	Hematoxylin and Eosin
HIV-1	Human Immunodeficiency Virus type 1
HPH	High pressure homogenization
HPLC	High performance liquid chromatography
HPMC	Hydroxypropylmethylcellulose
HPTN	HIV Prevention Trials Network
IACUC	Institutional Animal Care and Use Committee
IC50	Inhibitory concentration that inhibits 50%
ICH	International Conference on Harmonization
IRB	Institutional Review Board
IVR	Intravaginal ring
LC	Langerhans cells
LC-MS/MS	liquid chromatography coupled online with tandem mass spectrometry
LOD	Limit of Detection
LOQ	Limit of Quantification
LSC	Liquid scintillation counter
MALDI-TOF MS	Matrix assisted laser desorption ionization–time of flight (MALDI-TOF) mass spectrometry (MS)
MIP	Macrophage inflammatory protein
MTT	3-(4,5-dimethyl-thiazol-2-yl)-2,5-diphenyl tetrazolium bromide
MWCO	Molecular weight cut off
N-9	Nonoxynol-9
NC	Nanocrystals
NEC	New chemical entities
NIAID	National Institute of Allergy and Infectious Diseases

NNRTI	Nucleoside/Nucleotide Reverse Transcriptase Inhibitor
NtRTI	Non-Nucleoside Reverse Transcriptase Inhibitor
P_{app}	Apparent permeability coefficient
PBS	Phosphate Buffered Saline
PdI	Polydispersity Index
PEG	Polyethylene glycol
PPO	poly(propylene oxide)
PrEP	Pre-Exposure Prophylaxis
PVA	Polyvinyl Alcohol
Qdots	Quantun dots
rDHPE	Rhodamine B 1,2-Dihexadecanoly-sn-Glycero-3-phosphoethanolamine, Triethylammonium salt
RH	Relative Humidity
RNA	Ribonucleic acid
RSD	Relative standard deviation
RT	Reverse transcriptase
SD	Standard Deviation
SDS-PAGE	Sodium Dodecyl Sulfate Polyacrylamide Gel Electrophoresis
SEM	Scanning electron microscope
SHIV	HIV-1/SIV chimeric virus
SIV	Simian Immunodeficiency Virus
SMST	Standard Microbicide Safety Test SMST
STDs	Sexually Transmitted Diseases
STIs	Sexually Transmitted Infections
TEM	Transmission electron microscope
TFV	Tenofovir
UHPLC	Ultra-high performance liquid chromatography
UNAIDS	Joint United Nations Programme on HIV/AIDS
USP	United States Pharmacopeia

VCF   vaginal contraceptive films

VFS   Vaginal Fluid Simulant

1.0   INTRODUCTION AND SPECIFIC AIMS

1.1   HIV -1 FEMALE SEXUAL TRANSMISSION

1.1.1   HIV/AIDS epidemic

Human immunodeficiency virus (HIV) infection has spread rapidly around the world following the earliest reported cases of Acquired Immunodeficiency Syndrome (AIDS) in the 1980s. Since that time the AIDS epidemic has become a major global public health issue. In 2013, 2.1 million people were newly infected by HIV, and 1.5 million people died from AIDS-related diseases. Despite the declining numbers of new HIV infections and AIDS related deaths in the past decade, the epidemic is still alarming. By the end of 2013, approximately 35 million people were living with HIV[1]. Among all the HIV positive people eligible for HIV treatment under the 2013 World Health Organization guidelines, only 34% (9.7 million) received antiretroviral therapy. Reasons for this extreme lack of treatment include the unawareness of infection, poverty, and HIV related stigma and discrimination. The existence of this large untreated population arouses a great social panic as they increase the risk of HIV transmission.

In addition to the antiretroviral drug treatment, prevention is critical to protect people at risk from HIV acquisition, thus curbing the growth of the HIV/AIDS epidemic. Preventative strategies including condom use, male circumcision, reduction in number of sexual partners, and

less risky sex have drawn a great amount of attention in the past decades. Among other options, a new approach called Pre-Exposure Prophylaxis (PrEP) has been approved by FDA to prevent HIV infection. The target population for PrEP intervention is the HIV negative and at substantial risk of getting infection. To date, Truvada is the only drug product that has been approved for the purpose of oral PrEP. It is a combination of the nucleotide reverse transcriptase inhibitor (NtRTI) tenofovir (TFV) and the nonnucleoside reserve transcriptase inhibitor (NNRTI) emtricitabine. Other than oral PrEP, substantial efforts have been made towards the development of injectable PrEP and topical PrEP. Currently, the HIV Prevention Trials Network (HPTN) has launched two phase II clinical studies, HPTN 076 and HPTN 077, which are designed to evaluate the safety and acceptability of long-acting injectable antiretroviral drugs. These injectable products are very promising since they can stay in the body for several months and protect people at risk of HIV infection. Topical PrEP refers to the category of products administrated vaginally or rectally. Success has been achieved in topical PrEP studies such as the TFV 1% vaginal gel and dapivirine (NNRTI) vaginal ring. Both products are under investigation in Phase III clinical studies for efficacy [2-4]. Despite the progress that has been made, the development of more efficacious products is warranted. Improved efficacy can be achieved with the use of specially designed drug delivery systems which achieve greater drug concentrations where needed.

1.1.1   Physiological factors related to HIV infections in women

Women account for 52% of HIV positive people in the low-and middle –income countries. In sub-Saharan Africa, 76% of the infected population in the 15-24 age group are female [5]. The overwhelming majority of the new infections in women (84% in 2010) were

caused by heterosexual contacts [6]. Numerous reasons account for the high vulnerability of women, including physiological factors, gender disparities, sexual norms, violence, poverty, and limited access to education [7]. Physiologically, women are more susceptible to HIV acquisition than their male partners. The male to female HIV transmission rate is approximately two times as likely compared to the female to male transmission during vaginal intercourse [8]. The increased susceptibility is associated with the use of hormonal contraceptives, ovulation, and pregnancy [1, 9-12]. It is well known that the immune system in the female reproductive tract is mainly regulated by sexual hormones such as estradiol, progesterone, luteinizing hormone, and the follicle-stimulating hormone. When sexual hormones suppress the innate, humoral, or cell-mediated immune systems, viral infectivity in the female reproductive tract will be enhanced. In addition, previous investigations have shown that both ulcerative and non-ulcerative sexually transmitted diseases (STDs) also facilitate HIV transmission by boosting HIV infectiousness and susceptibility [13]. The promoted HIV infectiousness is achieved by increased HIV shedding and genital bleeding in the genital tract. Meanwhile, the presence of other STDs increases human susceptibility to the virus by recruiting a large number of HIV target inflammatory cells to the site of infection and inducing mucosal disruption.

1.1.2 Early events of HIV-1 infection in the female reproductive tract

Previous studies, using a rhesus macaque nonhuman primate model, have shown that once the macaque's vagina was exposed to simian immunodeficiency virus (SIV), the virus penetrated through the mucosal epithelia within hours (Figure 1) [14]. The potential mechanisms for viral entry include direct epithelial infection, transcytosis, transmigration, internalization by

Langerhans cells, and the micro-trauma caused by sexual intercourse [15, 16]. The sites of viral entry are likely to be the endocervix and the transformation zone between the endo- and ectocervix since the epithelium in these two areas consists of a single layer epithelial cells in contrast to the multilayered vaginal epithelium. During the first week of infection, HIV mainly infects "resting" CD4 T cells in the cervicovaginal tissue [17]. These specific CD4 T cells do not express markers of activation on their surface but express some residue of co-receptors which facilitate viral replication and subsequent infection and work as a latent reservoir [18]. Other than the "resting" CD4 T cells, HIV also infects activated CD4 T cells, Langerhans cells, and macrophages [19]. The cells that are infected first, called the founder population, expand in the local tissue and are disseminated to the draining lymph nodes rapidly. During the second week, the self- propagating systemic infection is established in the secondary lymphoid organs such as the thoracic duct, spleen, lymph nodes, and Peyer's patches. After 4 weeks of HIV exposure, these infected lymphatic organs function as reservoirs for viral storage and production. In this regard, the most desirable window for HIV prevention would be the first week after HIV exposure as the infected founder populations are small and focal, and the self-propagating infection has not yet been established systemically.
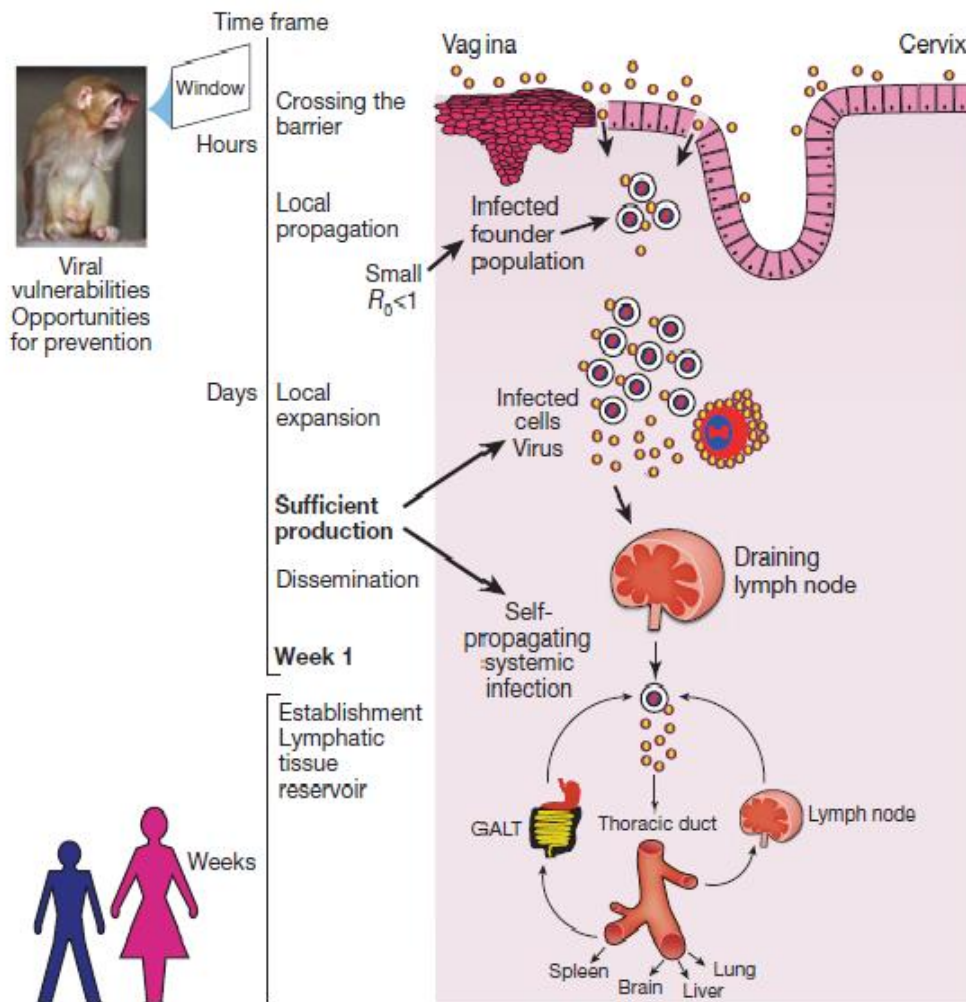
Figure 1 Early events in vaginal transmission of simian immunodeficiency virus.

Virus can penetrate in the cervicovaginal tissue within hours and infect a small group of susceptible target cells, founder population. The infected founder population expands locally and disseminated to the draining lymph nodes in the subsequent days. After the week 1, systemic infection will be established. The window for prevention is mainly in the stages of crossing the barriers, founder population and local expansion.

1.2   VAGINAL DRUG DELIVERY

1.2.1   Anatomy and physiology of vagina

The human vagina is a tubular and fibromuscular organ extending from vaginal vestibule to the cervix. The vagina is not a straight tube. When a woman is in a standing position, the axis of the lower vagina is more vertical and posterior, while the upper vagina from the pelvic diaphragm to the cervix curves horizontally forming a 130° angle [20]. This anatomical character provides the possibility for pharmaceutical products to stay in the vagina against gravitational forces.

Based on histological examination, the vagina is composed of four layers: stratified squamous epithelium, lamina propria, a muscular layer, and the tunica adventitia. The surface of the vagina is covered by a series of transverse muscular folds called "rugae" which dramatically increase the surface area of vagina [21]. The thickness of the epithelial cells varies during the different phases of menstrual cycle. The blood supply of vagina is received from a plexus of arteries including the internal iliac artery, uterine, middle rectal, and internal pudendal arteries. Afterward, blood enters the peripheral circulation through the surrounding venous plexus, and eventually drains to the internal iliac vein, avoiding the hepatic metabolism. Small blood and lymphatic vessels exist only in the lamina propria and the underneath muscular layer but not in the squamous epithelium [22, 23].

The human vagina is covered by a watery secretion called vaginal fluid. About 90% of the vaginal fluid is water, while salts, residual urine, cervical mucus, enzymes, enzyme inhibitors, lymphocytes, albumins, fatty acids, and epithelial debris account for the remaining 10% [21]. The volume of vaginal fluid secreted varies from 0.5 mL to 10 mL per day depending on blood flow, age, menstrual cycle, and presence of sexual intercourse [24]. In addition, the

amount and the physicochemical properties of the mucus will change with the menstrual cycle, which in turn will have significant effects on the viscosity and flow elasticity of the vaginal fluids [23]. Taken together, all these variations will substantially affect drug adhesion in the vaginal lumen, diffusion though the mucus barriers, and the extent of absorption.

Vaginal fluid is acidic with a pH about 3.5-4.5 [25]. The acidity is generated and maintained mainly by the commensal microorganism *Lactobacillus*. These bacteria convert the glycogen, synthesized by epithelial cells, to lactic acid which reduce the pH of the vaginal fluid [26]. The pH value changes during the menstrual cycle with the lowest pH detected during ovulation [27]. Some other physiological factors may also change the pH, such as the presence of semen (pH7.2-8.0), bacterial infections (pH 5.0-6.5), and menopause (6.0-7.5) [28]. Thus, a safe vaginal product must not affect the normal microflora and low pH milieu as they are essential for a healthy vaginal environment.

1.2.2 General features of vaginal drug delivery

Vaginal drug delivery has been commonly used in female-specific treatments. Because of its anatomical and physiological challenges, it is imperative to understand the advantages and limitations of this route of drug administration. Firstly, compared with oral administration, delivering drugs vaginally can avoid gastrointestinal (GI) absorption, the hepatic first pass metabolism and GI tract related side effects [29]. In addition, as the enzymatic category and activity in the vagina are different from that of GI tract, the vagina may be a favorable alternative site for the delivery of drugs that are susceptible for hepatic metabolism, especially proteins and peptides [21]. Given these factors decreases in drug dosing levels may achieve the same

biological effects. This may avoid some of the toxicities or side effects associated with higher dosing levels. Moreover, for the drugs that act topically in the vagina, intravaginal drug administration results in much higher drug concentrations in the reproductive tract tissues when compared to systemic administration, which in turn would lead to improved efficacy, especially for the antiretroviral drugs used as topical HIV prevention products. Additionally, it is important to note that vaginal delivery is not only a site for local acting drugs but also a potential route for systemic adsorption due to the large surface area and rich blood supply of the vagina [30]. These physiological characteristics allow for high drug permeation and bioavailability [31].

Vaginal drug delivery, however, has a few limitations. The major issue concerning this route of administration is its poor and variable drug absorption. Vaginal physiological factors, such as epithelial thickness, fluid volume and composition, presence of cervical mucus, and vaginal pH have significant effects on the rate and extent of drug absorption. Furthermore, the stages of the menstrual cycle, pregnancy, menopause, age, sexual activity, and hydrophobicity of the drugs can also change drug absorption profiles [21, 31]. In addition, vaginal products are commonly reported as having a low retention time in the lumen due to the shedding of fluids and epithelium in the vagina. Furthermore, some products have been associated with poor spreadability or messiness. These limitations need to be overcome in order to achieve efficacy and user adherence.

Taken as a whole, an ideal vaginal product should possess the following characteristics: (1) maintenance of the acidic microenvironment and the normal microbial flora in the female reproductive tract; (2) safe for vaginal use without causing irritation; (3) not likely to leak or become messy; (4) portable and allow for self-insertion; and (5) intercourse independent with no effects on sexual intercourses [29]. Additionally, it is worth noting that many factors, such as the

preference of the individuals and their partners, cultural norms, economic and sexual status, and age can affect women's choice on vaginal products. Since the decision to use vaginal products is very personal, multiple product types may be required in order to meet the needs of all women and improve user acceptability and adherence.

1.2.3 Vaginal delivery of PrEP agents for HIV-1 prevention

As the vagina is the initial site of HIV infection during male to female transmission, it would be beneficial to dose PrEP agents topically in vagina, which will allow for a higher drug concentration in the cervicovaginal tissue relative to the oral dosing. Previous clinical studies have shown that after intravaginal application of TFV 1% gel, drug concentrations in the vagina were substantially (~1000-fold) higher than that after oral Truvada dosing [32]. More importantly, the anti-HIV efficacy is directly associated with drug concentration in the vaginal tissue. When the concentration of TFV diphosphate, the active metabolites of TFV, was higher than 1000 ng/mL, HIV incidence rate was significantly lower than the placebo group and the group with lower drug concentrations in tissue [32]. A similar finding was described in a randomized pharmacokinetic cross-over study [33]. Compared to oral dosing, vaginal delivery of the anti-retroviral drug TFV increased drug concentrations in the cervicovaginal tissue and reached a greater PrEP efficacy. Meanwhile, a lower serum concentration was observed after vaginal administration, which would help to avoid many systemic side effects related to the drug use.

From the perspective of dosage form, vaginal applied microbicide products can be prepared as gels, creams, tablets, films, and rings. The gel dosage form was first chosen for

microbicide development since the drug candidates identified early in the field were themselves gel forming polymers [34]. Gel products are able to adhere to the surface of the vagina for a reasonable period of time before being removed. In addition, they are inexpensive and easy to make as well as familiar to women since many marketed vaginal products and lubricants are gels. However, several limitations related to the applications of gel dosage form should be considered [35]. The first concern is the stability issue associated with drugs that are unstable in water. Generally aqueous based hydrogels are used vaginally. These products contain a large volume of water so they would not be compatible with water liable drugs. In this scenario, solid dosage forms which contain minimal to no water would be highly recommended. Furthermore, the cost for packaging of gel products can be high due to the need for applicators. This may make such products costs prohibitive for use in developing counties. More importantly, gel leakage after vaginal application has been reported which may negatively impact patient adherence. As a consequence, solid dosage forms such as polymeric vaginal films have recently received increasing attention as alternatives for the vaginal application of antiretroviral drugs [36, 37]. Film products can be applied intravaginally without an applicator and dissolve rapidly in the vaginal fluid upon insertion. Because the amount of residual water in film formulations is very low, active pharmaceutical ingredients, especially the ones that are susceptible to degradation in aqueous medium, can be preserved well in this dosage form, and the drugs are less likely to leak [34, 38].

1.2.4   The use of nanotechnology for improved vaginal drug delivery

Recently, nanoparticle based formulations such as liposomes, nanoemulsions, micelles, dendrimers, and polymeric nanoparticles have been investigated for the vaginal drug delivery of PrEP agents [39-44]. Nanoparticles can help increase drug solubility, provide sustained drug release, and achieve rapid mucus penetration. Presently, over 40% of the new drugs identified through combinational screening programs exhibit poor water solubility. Similarly, in the field of topical PrEP, a substantial number of lead candidates being evaluated in the clinical pipelines are highly hydrophobic, especially the NNRTIs [45-47]. Poor drug solubility causes many issues: (1) uncontrolled drug precipitation after administration and poor ability for drug removal from the body during elimination, (2) use of excessive amounts of excipients or extreme pH conditions to enhance solubility, which may introduce toxicity concerns, (3) slow dissolution rate (dM/dt) due to the low drug concentration on the surface of the drug particles (C_s) as per the modified Noyes Whitney's dissolution equation described in the Equation 1, (4) limited and erratic bioavailability as a result of drug loss and poor absorption, and (5) lack of dose-response correlation resulting in a suboptimal dosing regimen [48]. Therefore, well designed pharmaceutical formulation approaches must be pursued to improve drug solubility.

$$\frac{dM}{dt} = \frac{AD(C_s - C_t)}{h}$$

(Equation 1)

Where,
M: mass of dissolved drug;   t: time;   dM/dt: dissolution rate
A: surface area of the dissolving drug particles
D: diffusion coefficient
h: thickness of the boundary layer of the dissolution medium at the surface of the dissolving drug particles
Cs: drug concentration on the surface of the drug particles
Cb: drug concentration in the bulk of the dissolution medium
(Cs-Cb): concentration gradient

Conventionally, many approaches have been applied to improve the solubility of hydrophobic drugs. The first is drug ionization by salt formation and pH adjustment [49, 50]. This method is most effective for acidic and basic drugs since ionization is easy to achieve and ionized products present higher aqueous solubility compared with neutral ones. However, as the ionized products are usually synthesized and isolated from organic solvents, they may be chemically unstable in aqueous environments and be converted to their original acid or base forms. As a consequence, the application of salt formation technology has been generally limited [49]. Another pharmaceutical approach to increase drug solubility is to use cosolvents such as propylene glycol, ethanol, and cremophor EL [51-53]. Cosolvents help to dissolve a sufficient amount of drugs. However, caution must be placed in the process of formulation development and clinical evaluation as excess amount of cosolvents could cause serious toxicities. Additionally, cyclodextrins and their derivatives have been applied to encapsulate hydrophobic drugs in order to improve drug solubility [54, 55]. Cyclodextrins are a group of molecules composed of sugar units. These sugar units are arranged in a circle and exist in a toroid shape with the hydroxyl groups protruding out. Due to this unique structure, the interior of cyclodextrins are more hydrophobic than the exterior so that hydrophobic drugs can be encapsulated to from inclusion complexes. This drug delivery system has been extensively investigated in the pharmaceutical field to formulate hydrophobic drug substances.

Recently, nanotechnologies have been commonly used to increase the solubility of poorly water soluble drugs [56, 57]. As per Ostwald-Freundlich equation (Equation 2), decreasing particle radius (γ) can increase saturation solubility of drug particles (S). The increased saturation solubility will result in a higher amount of dissolved drug, and lead to an improved bioavailability. This affect is substantial for particles below 1 μm, especially those under 200nm.

$$\ln\left(\frac{S}{S0}\right) = \frac{2v\gamma}{rRT}$$

(Equation 2)

Where,
S: solubility of fine drug particle at temperature T
S0: solubility of infinitely large particles (if r=∞)
v: molar volume
ϒ: interfacial surface tension of the solid
r: radius of the fine particle
R: gas constant
T: temperature

In addition to improved drug solubility, nano-formulations can be applied as a controlled release device to achieve sustained drug concentrations in local cervicovaginal tissue. A thermosensitive vaginal gel containing PLGA nanoparticles has been formulated to deliver antiretroviral drugs raltegravir and efavirenz for HIV prevention [58]. Sustained drug concentrations in HeLa cells could be detected for two weeks after the nanoparticle treatment. Similarly, antibiotic loaded liposome gels have been prepared to treat bacterial vaginosis [59, 60]. *In vitro* release studies showed that approximately 30-50% of the drugs were retained in the gels after 24h. The ability of these systems to release actives in a sustained profile may allow for the development of coitally independent products, which have the potential to help increase user adherence and product efficacy.

Moreover, mucus penetrating properties can be achieved through modulation of nanoparticle size and surface charge. This property is of paramount importance for HIV prevention since the viscous cervicovaginal mucus can have a significant impact on the drug penetration, distribution, and elimination after vaginal administration [61, 62]. Rapid mucus penetration will reduce the amount of drug loss during mucus turnover and result in increased drug accumulation in the cervicovaginal tissue.

1.3   LYMPHATIC TARGETING

1.3.1   Anatomy and physiology of the lymphatic system in female reproductive tract

The lymphatic system is composed of lymph, lymphatic capillaries/vessels, and lymphatic organs including lymph nodes, spleen and thymus. As a unique system parallelized to the cardiovascular system, it plays important physiological roles. Firstly, the lymphatic system helps maintain protein and fluid balance in the body. Vital plasma proteins existing in the interstitial fluid are collected in the lymphatic vessels and returned to the blood circulation. Excess fluid can also be drained from the interstitial spaces, and most of the fluid will be recycled. Meanwhile, the lymphatic system removes the dead cells, waste, debris, and toxins from the body before the lymph is returned to the blood. In the case of infection, lymphatic capillaries which are scattered throughout the tissue will collect antigens or antigen presenting cells in the interstitium and transport them to the draining lymph nodes. Afterwards, immune responses will be initiated via B cell and T cell priming. Moreover, the lymphatics also absorb lipids and fat-soluble vitamins

from the digestive system and subsequently transport these nutrients to the cells where they are needed.

In the female reproductive tract, the lymphatic drainage system is widely distributed in the pelvic area. The lower third of the vagina drains to the common iliac, superficial inguinal, and perirectal nodes, the middle third drains to the common and internal iliac node, and the upper third drains to the external iliac nodes [31]. In the cervix, lymph drains to the external or internal iliac and sacral nodes.

The mucosal immune system in the lower reproductive tract consists of a resident population of dendritic cells (DCs), macrophages, T cells, and B cells. In the vagina, the cell concentration of T cells is higher than the immature DCs, natural killer cells, and macrophages [63, 64]. $CD8^+$ T cells accounted for over 60% of the total T cells in the lamina propria, while a much smaller number of $CD4^+$ T cells were found [65]. In the cervix, cell availability in the endocervix is found to be significantly different from that in the ectocervix [66]. T cells and B cells are more prevalent in the ectocervix than the endocervix [63]. In the upper reproductive tract, mast cells and macrophages are the main subtypes of immune cells residing in the endometrium, while T cells only account for a small part of the population [67]. The density of leukocytes in the endometrial tissue is found to be the highest of the whole reproductive tract. In the fallopian tube, T cells are the major cell type among the leukocytes. Granulocytes including neutrophils and mast cells are the second largest constituent [64]. It is worth noting, however, that cell population in the female reproductive tract varies throughout the menstrual cycle which could be a result of the fluctuation of hormones [68].

1.3.2 Rationale for lymph node targeting in HIV

There is evidence showing that HIV infected DCs could be detected in the draining lymph nodes as early as 18 hours after viral inoculation [69]. By using the rhesus macaque vaginal transmission model, Hope et al. also shown that infection in the local draining lymph nodes could be detected at 48h when a high dose of SIV based particles was inoculated [70]. In addition, as adequate amount of HIV targeted T cells exist in the draining lymph nodes, HIV can replicate rapidly in these nodes during the first week of infection [19]. More importantly, previous studies have shown that exposing HIV intravaginally increased the expression of chemokine macrophage inflammatory protein-3α (MIP-3α) in the endocervical epithelium, which attracted plasmacytoid dendritic cells (pDCs) to submucosa, and subsequently induced the secretion of MIP-1β. As a consequence, large number of HIV target $CD4^+$ T cells were recruited from the draining lymph nodes to the cervicovaginal tissue which exacerbated the local expansion and infection [71]. Therefore, a more effective strategy would be one which suppresses the early infection in the draining lymph nodes in addition to the portal of viral entry. With the protection at the site of lymph nodes, the infiltrated target cells will be guarded by antiretroviral drug prior to HIV exposure.

Even from the standpoint of HIV treatment, antiretroviral drugs need to be delivered to lymphatic system as well for improved efficacy. Lymph nodes and other lymphatic tissues act as major reservoirs of HIV infection *in vivo* [73]. The detection of HIV in the blood, is coupled with high levels of HIV in the mononuclear cells located in the lymph nodes, mainly T cells, B cells, natural killer cells, and macrophages. In addition, the presence of a large number of HIV target cells in the lymph nodes increases the viral burden 5- 10 times in the lymph nodes compared to the blood. Similarly, viral replication in the nodes has been reported to be

approximately 10-100 times higher than that in the peripheral blood mononuclear cells [72]. Even if highly active antiretroviral therapy (HAART) can reduce plasma viral loads in HIV-infected patients by 90%, active virus can still be isolated from lymph nodes after 30 months of this therapy [72, 73]. With regard to these findings, delivery of anti-retroviral drugs to the lymph nodes will maximize therapeutic effects and might eradicate the established HIV infection.

1.3.3 Current strategies for lymph node drug delivery

Lymphatic targeting has been utilized for both therapeutic and diagnostic purposes. The major applications of lymphatic drug targeting include (1) delivery of anticancer agents to the regional lymph nodes in order to prevent tumor metastasis [74-76]; (2) localization of diagnostic agents, like Quantum dots and blue dyes, to sentinel lymph nodes before biopsy or dissection in cancer patients [77-79]; and (3) improvement of bioavailability of macromolecular drugs, such as peptides and proteins, via selective uptake by the Peyer's patch in the intestine [80-82].

Although drug delivery to the lymph nodes has been particularly difficult to achieve, increasing attention has been drawn to the development of nanoparticles. This is based on the recent understanding that colloidal particles in the interstitium can be recognized by lymphatic system and transported into the regional lymph nodes. By definition, colloid particles are insoluble substances that can be uniformly dispersed in a medium. Colloidal materials, such as liposomes, emulsions, dendrimers, and solid lipids nanoparticles, have been reported to transport drug agents to lymphatic tissues [83-87].

Currently, there are two approaches for lymphatic drug delivery, namely passive targeting and active targeting. Passive targeting mainly depends on simple diffusion or some

17

specific formulation properties such as particle size and surface charge. For instance, the size of nanoparticles has to be large enough to circumvent direct blood absorption before entering lymphatic vessels [73]. In some other scenarios, the fate of drug transport and localization in the lymphatic system cannot be modified unless different routes of administration are applied [80]. In comparison, active lymphatic targeting is ligand dependent. It relies on the attachment of targeting ligands on the surface of nanoparticles for specific receptor binding at the target site [88]. It has been suggested that phagocytosis by macrophages is one of the important mechanisms associated with nanoparticle uptake in lymph nodes [89, 90]. Therefore, surface modification of nanoparticles with ligands that can specifically bind to the receptors expressed on macrophages or other antigen presenting cells can significantly improve the efficiency of lymphatic targeting [75, 91, 92]. The targeting ligands that are commonly used include monoclonal antibodies (mAbs), antibody fragments, and peptides [80, 93].

Drug delivery to the lymph nodes can be achieved through different routes of administration. Generally, to attain therapeutic effects in the regional lymph nodes, the instilled colloid particles have to first drain from the site of administration and then preferentially migrate to the draining lymph nodes. Due to the existence of the physical barriers such as mucus, epithelium, or epidermis, traditional approaches all require needle injections so that drugs can be carried to the interstitial space directly. The most frequently used methods include intravenous (i.v) injection, subcutaneous (s.c) injection, intramuscular (i.m) injection, and intraperitoneal (i.p) injection [92, 94-96]. With i.v administration, the relative drug exposure in lymph versus blood could be determined by drug hydrophobicity, plasma protein composition, and lipoprotein binding. Instillation of highly hydrophobic drugs after high fat meals usually result in an increased drug concentration in the lymph [97]. Subcutaneous administration is another

18

commonly used approach for lymphatic delivery [96, 98, 99]. The major barrier associated with this route of administration is the poor drainage though the interstitium to the initial lymphatic vessels. Size of colloid nanoparticles has been reported as the principle factor on the rate of lymphatic drainage after subcutaneous injection [94]. Smaller colloids could lead to an easier and faster uptake.

Recently, non-invasive routes of administration (with no needle injections) as a new area of interest have started to be explored. The application of this new approach includes drug targeting to the pulmonary lymph nodes via nasal inhalation [100-103] and genital lymph node drug delivery via intravaginal administration. To date, there are three studies that investigated lymph node targeting via intravaginal instillation [104, 105]. One study investigated the migration of quantum dots to genital lymph nodes after vaginal instillation in mice. Another study explored T cell priming in the genital lymph nodes after intravaginal immunization. Notably, the vaginal epithelium in both studies, however, was pretreated with the permeation enhancer N-9. This pre-exposure disrupts the epithelium which most likely allowed drug exposure in the interstitium. This disruption is not applicable for HIV prevention since it will allow direct access for infectious HIV-1 to the target cells in the tissue. Only the third study has shown the migration of nanoparticles (20-40nm) to draining lymphatic ducts and regional lymph nodes at 1h without any treatment with sexual hormones, epithelial disruptors (N-9), or adjuvants [106]. The goal of the present dissertation was to investigate whether this non-invasive approach (without using N-9) could be applied to deliver microbicide drug candidates to draining lymph nodes after intravaginal administration.

1.3.4 Physicochemical properties of lymphatic targeting

Physicochemical properties can change biodistribution of nanoparticles *in vivo* and have significant effects on the efficiency of lymphatic drug delivery. The major properties that play a role include particle size, surface charge, hydrophobicity, molecular weight, concentration, and volume [107].

Particle size is one of the most important factors for lymphatic drug delivery. Particles that are smaller than a few nanometers (< 10 nm) can exchange freely through the blood capillaries and directly drain in the blood circulation at the site of administration. In contrast, particles with diameter around 100 nm can be absorbed in the lymphatic capillaries quickly and pass through the lymph nodes rapidly as well. As for larger particles (a few hundred nanometers), even though they could be trapped in the interstitium for a longer period of time before entering the lymphatic vessels, they retain well in the lymph nodes [88, 108]. In light of these findings, if lymph node retention is required for a diagnostic or therapeutic effect in the lymph nodes, larger particle sizes will be beneficial since they can stay longer in the nodes [80, 98].

The effect of surface charge on lymphatic uptake has been investigated using liposomes. Results indicated that negatively charged liposomes showed faster lymphatic drainage when compared to positively charged liposomes after i.p administration [91, 109]. Generally, for lymphatic drug delivery, a particular order was followed: negatively charged nanoparticles are better than positively charged, followed by the neutral ones [110].

Hydrophobicity of the nanoparticles is another important factor since it is closely associated with phagocytic responses. Hydrophobic materials are more likely to be opsonized and transported to the draining lymph nodes than the hydrophilic ones [111]. Surface modification with polymers such as polyethylene glycols can modify the hydrophobicity of nanoparticles, which will in turn change the rate and extent of lymphatic uptake.

1.4   MICROBICIDE CANDIDATE FOR HIV-1 PREVENTION

1.4.1   Non-specific microbicide candidate

Topical PrEP was originally termed as microbicide. The first generation of drugs evaluated as vaginal microbicides did not specifically target the HIV life cycle. They were detergents, surfactants, acidifying agents and anionic polyanions. One surfactant product nonoxyol-9 (N-9) was evaluated in a phase 2/3 clinical trial. Results showed that the use of N-9 did not reduce, but instead increased the rate of male-to-female HIV transmission because N-9 induced epithelial disruption and genital mucosal inflammation [112-114].

Acidifying agents BufferGel and Acidform were developed as bioadhesive vaginal gels. These products were designed to maintain the acidic microenvironment in the female reproductive tract. Clinical studies have shown that both BufferGel and Acidform were safe for vaginal application, however, not effective for the prevention of vaginal HIV transmission [115, 116].

Anionic polyanions such as Carraguard gel, cellulose sulfate gel, cellulose acetate phthalate (CAP) gel, and PRO2000 were also evaluated as microbicides. These gels are negatively charged which facilitate their interactions with the envelope proteins presenting on the surface of the virus. Ideally, this interaction interferes with viral attachment to the CD4$^+$ T cells, and subsequently compromises HIV infection. A phase 3 study has shown that Carraguard was safe but not effective against the vaginal transmission of HIV [117]. The investigation of cellulose sulfate gel effectiveness was terminated early due to the increased HIV infection rate at an interim analysis [118]. In addition, CAP gel was evaluated in a phase 1 trial, and this trial was stopped due to gel leakage and user complaints [119]. The efficacy of PRO2000 gel was examined in two large-scale effectiveness trials [115, 120]. The phase 2b trial found that 0.5% PRO2000 gel was safe for use, however, it only reduced the risk of HIV infection by 30%, which was not statistically significant [115]. To further understand the effectiveness of PRO2000 gel, a gel product containing a higher concentration of PRO2000 (2%) was assessed in a phase 3 trial, and results of which showed that no efficacy was found after 2% PRO2000 gel intervention [120].

1.4.2   Current microbicide candidates

As the first generation of non-specific microbicide candidates did not provide desirable efficacy *in vivo*, attention has shifted to compounds that have specific targets in the process of HIV replication. In the HIV life cycle (Figure 2), HIV first binds to a CD4 receptor and a co-receptor, CCR5 or CXCR4, on the surface of a CD4$^+$ T lymphocyte [121]. The virus then fuses with the T cells and release its RNA into the host immune cells. After that, single-stranded HIV RNA is

converted into double-stranded HIV DNA via reverse transcriptase (RT). Once the reverse transcription is complete, HIV DNA penetrates into cell nucleus and inserts itself to the DNA sequence of the host cells with the assistance of another viral enzyme, integrase. Afterwards, double stranded HIV DNA is unwound and the complementary messenger RNA is synthesized to build new long chain viral proteins. The new proteins were then cut into smaller proteins by enzyme protease and these smaller proteins are recombined for maturation and released out from the host cells.

Currently, inhibitors that can specifically stop viral fusion, reverse transcription, integration, and maturation are being investigated as microbicide candidates. Griffithsin, PSC-RANTES, and maraviroc are fusion/entry inhibitors which interfere with viral fusion [122-124]. The inhibitors blocking the activity of reverse transcriptase include NtRTIs and NNRTIs. TFV is an NtRTI which has to be activated prior to being pharmacologically active *in vivo* by two steps of phosphorylation. The CAPRISA 004 trial performed in South Africa has shown that TFV 1% vaginal gel was safe to use [121]. This coitally dependent application was found to be effective with a 39% reduction in the HIV acquisition. Especially among women with high adherence, HIV incidence in the TFV gel arm was 54% lower than the placebo gel arm. This study proved the possibility of utilizing vaginal microbicides for HIV prevention. In comparison to the NtRTIs, NNRTIs do not need to be converted to active forms *in vivo* and they are generally very potent with activity in the nanomolar concentration. The issue, however, associated with NNRTIs is that many are very hydrophobic in nature. Pharmaceutical strategies have to be applied to increase their solubility in order to obtain efficacy. DPV is an NNRTI which has been intensively investigated. A DPV containing intravaginal ring has been developed for extended use and this product is currently under investigation in a phase 3B open-label follow-on trial

(MTN-025). Integrase inhibitors are another category of inhibitor which impedes HIV DNA incorporation into host DNA. The integrase inhibitor MK-2048 is in development for phase 1 clinical study. Currently, many protease inhibitor products such as indinavir and saquinavir have been approved by FDA for HIV treatment, and some of these are under investigation as microbicide candidates [125, 126].
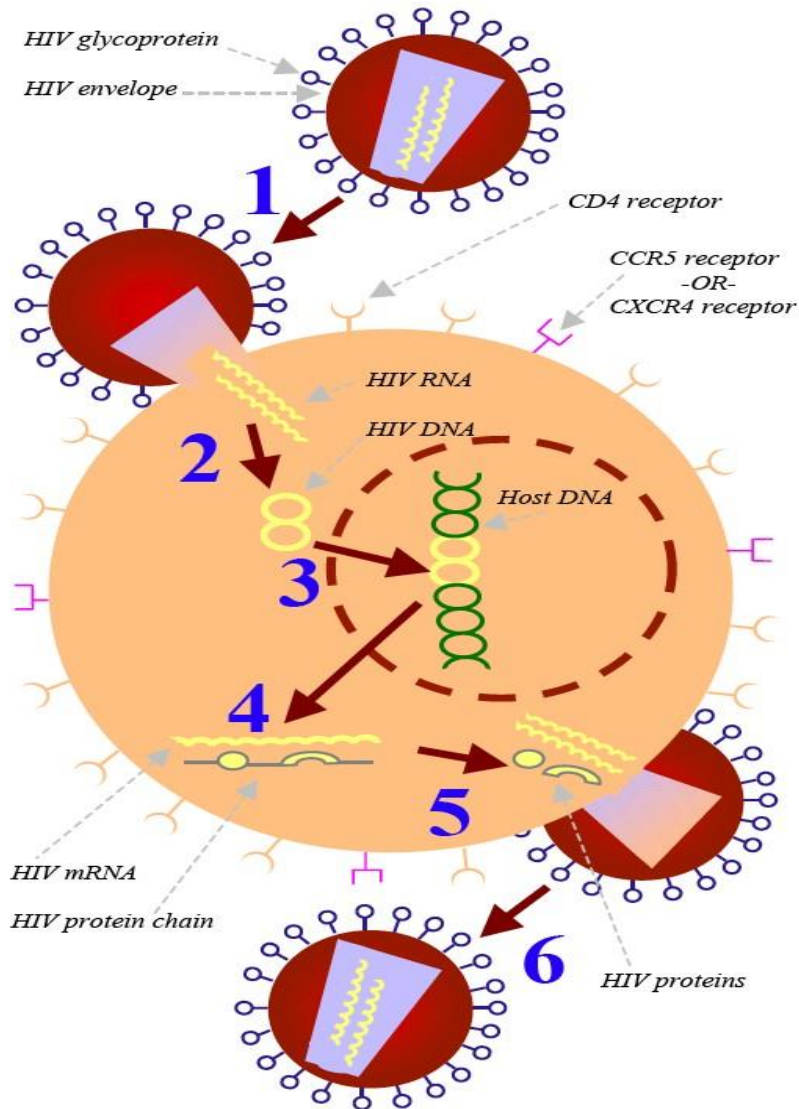
Figure 2 HIV life cycle.

1.Binding and fusion: HIV binds to a CD4 receptor and a co-receptor, CCR5 or CXCR4, on the surface of a host cell and release its RNA into the host immune cells. 2. Reverse transcription: HIV RNA is converted into a double-stranded HIV DNA via reverse transcriptase (RT). 3. Integration: HIV DNA penetrates into cell nucleus and inserts itself to the DNA sequence of the host cells. 4. Transcription: Double stranded HIV DNA is unwound and its complementary messenger RNA is synthesized to build new viral proteins. 5. Assembly: HIV proteins is then cut into smaller proteins by enzyme protease and these smaller proteins are recombined for maturation. 6. Budding: The newly assembled HIV will be released from the host cells.

1.4.3 CSIC as a microbicide candidate for HIV prevention
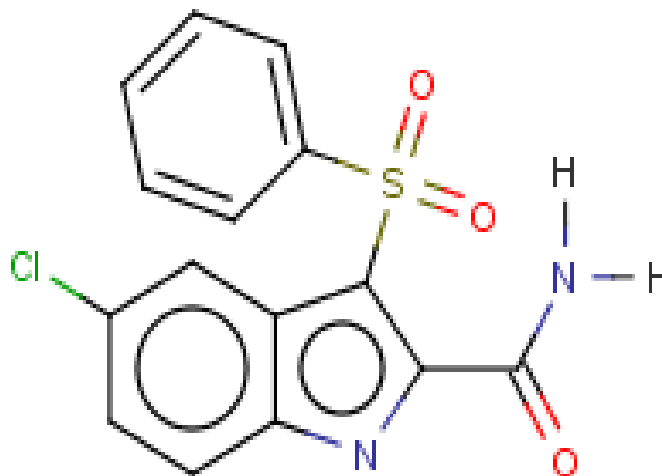
Figure 3 Chemical structure of microbicide drug candidate CSIC

5-chloro-3-(phenylsulfonyl) indole-2-carboxamide (CSIC) is another highly potent NNRTI with an half maximal effective concentration (EC_{50}) value about 1nM [127]. The chemical structure of CSIC is shown in Figure 3. CSIC has been shown to inhibit the activity of HIV reverse transcriptase in a tight binding mode [128]. The binding pocket for CSIC is directly below the polymerization site of the RT. This type of binding allows for a butterfly conformation and strong interactions (Figure 4) [129, 130]. The high affinity binding between CSIC and RT leads to a prolonged enzyme inhibition, thus allowing extended antiretroviral bioactivity even after drug has been removed (memory effects). A previous study has shown that pretreating

26

uninfected cells with CSIC protected the cells from subsequent HIV challenge [128]. Also, pre-exposing CSIC to the infected cells eliminated the infectivity of nascent virus and prevented cell-to-cell HIV transmission.
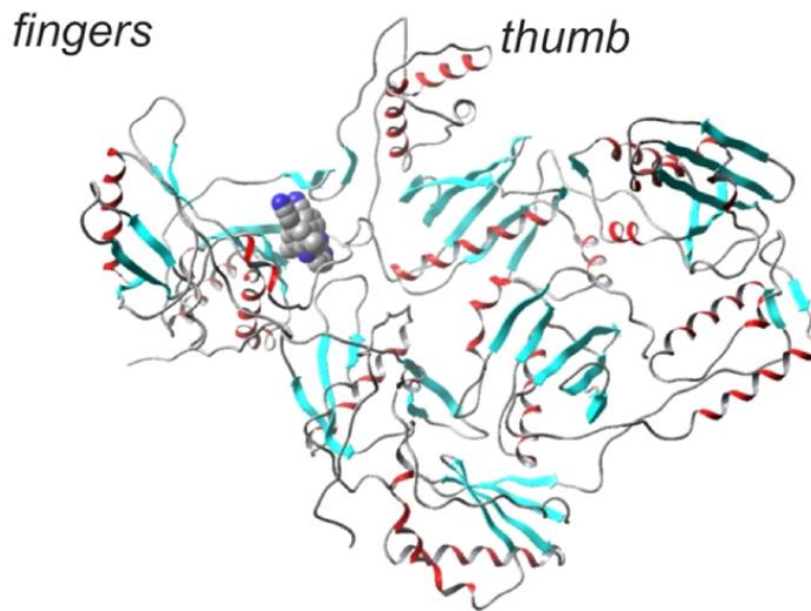
Figure 4 Model of HIV reverse transcriptase (Copyright (2008) National Academy of Sciences, U.S.A.)

Rilpivirine, a close analog of dapivirine, is located in the NNRTI binding site. The polymerization site is represented by the fingers and thumb domains.

In addition to its high potency and memory effects, CSIC exhibits superior resistance properties. Firstly, CSIC was found to possess improved bioactivity to the mutant reverse transcriptase K103N and Y181C [131]. More importantly, CSIC presented limited systemic exposure after topical exposure, which might reduce the chance of HIV tolerance and circumvent retrovirus evolution through drug treatments [128, 132].

Despite these promising characteristics of CSIC, the major challenge associated with vaginal delivery of CSIC is its hydrophobicity. Because of the aqueous environment in the vaginal lumen, CSIC must be formulated using effective pharmaceutical drug delivery strategies which enhance its aqueous solubility.

1.5   HYPOTHESIS AND SPECIFIC AIMS

CSIC is a highly potent anti-HIV agent with a promising resistance profile. It prevents HIV infection by interfering with the activity of viral reverse transcriptase and blocking the conversion of HIV RNA to HIV DNA in the host immune cells. As the HIV target cells are mainly located in the cervicovaginal tissue and the draining lymph, it is essential to deliver CSIC or other antiretroviral drugs to both sites of action. The hydrophobicity of CSIC is favorable for tissue penetration and lymphatic drug delivery; however, before it gets into the tissue, the drug has to remain stable in the acidic aqueous vaginal lumen, release from formulations, and filter through the cervicovaginal mucus. Therefore, a series of preformulation studies are warranted to investigate the physicochemical and biological characteristics of CSIC. Pharmaceutical strategies that can increase the drug aqueous solubility were utilized to design formulations for vaginal

application. The first part of this dissertation was focused on the development and evaluation of a water-soluble polymeric film product containing co-solvents for increased encapsulation of CSIC. As polymeric films have been successfully used to load hydrophobic NNRTI DPV [36], it was worthwhile to develop a polymeric film formulation containing co-solvents in order to deliver a high amount of CSIC to cervicovaginal tissue.

In the second part of this dissertation work, CSIC nanocrystals were prepared to investigate its potential application for improved tissue penetration and lymph node drug delivery. Nanocrystals are pure drug particles with a particle size controlled by the surrounding stabilizers. Since drug particles are not encapsulated in any carrier system, the hydrophobicity of the drug can be preserved, which can facilitate tissue penetration. Additionally, rational choice of stabilizers can allow nanocrystals to rapidly penetrate the mucus barrier, making lymph node drug delivery possible after intravaginal administration.

In this dissertation, we hypothesized that the hydrophobic microbicide candidate CSIC can be formulated in a polymeric vaginal film and a nanocrystal formulation with high loading capacities using multiple formulation strategies. We further hypothesized that the nano-delivery strategy can improve cervicovaginal tissue drug penetration and achieve lymphatic drug delivery.

This hypothesis was addressed through the following specific aims.

Specific aim 1: Formulation of a polymeric film containing hydrophobic NNRTI CSIC. Preformulation studies were conducted under this aim to investigate the physicochemical

properties of the drug. A compatibility study was performed to identify the polymers and solvents that can be used in combination with CSIC. This data was used to manufacture a stable film formulation with sufficient drug loading. (Chapter 2 and 3)

Specific aim 2: Formulation and evaluation of CSIC nanocrystals. The physicochemical properties of the nanocrystal, such as size, charge, and crystallinity were evaluated. Intracellular uptake profile of the nanocrystal and its mechanism of uptake were also investigated. We expected to have a formulation with enhanced saturation solubility, increased drug loading capacity, and rapid intracellular uptake. (Chapter 4)

Specific aim 3: Investigation of cervicovaginal tissue permeation *ex vivo* and genital lymph node targeting of CSIC nanocrystals. A tissue permeability study was carried out using excised human cervicovaginal tissue. *In vivo* drug distribution in the cervicovaginal tissue and the draining lymph nodes were also investigated over time using a mouse model. We expected to observe improved tissue penetration and lymph node drug delivery in mice. (Chapter 5)

2.0   PREFORMULATION EVALUATION OF CSIC

2.1   INTRODUCTION

As described in chapter 1, CSIC is a potent non-nucleoside reserve transcriptase inhibitor (NNRTI). It tightly binds to reverse transcriptase which leads to enhanced antiretroviral activity. Given these properties, CSIC is a promising new microbicide candidate. Before formulating CSIC into any specific dosage form, detailed preformulation studies are required to obtain critical information about the drug substance for the development of safe and effective formulations.

Studies in a preformulation investigation include: (1) assessment of drug solubility in various solvents such as water, polyethylene glycols, glycerin, Tweens, ethyl alcohol, methanol, etc.; (2) determination of drug partition coefficient; (3) evaluation of crystal properties including the crystal habit, crystallinity, and polymorphism; (4) chemical stability in solution and in the solid state under conditions typical for formulation, long term storage and administration. Factors that could impact a drug's stability include elevated temperature, high humidity, variable pH, and the presence of oxidants or light. When the test drug is a New Chemical Entity, typically a stability study will be conducted to evaluate its long term stability under specific temperature/ humidity conditions including accelerated conditions. In addition, in some cases, drug stability is investigated in the presence of other excipients to evaluate any potential incompatibilities.

In the current work, a series of CSIC preformulation evaluations were conducted to provide the information required for the development of desirable vaginal microbicide products. Firstly, the hydrophobicity of CSIC was determined based on its solubility in multiple solvents and partition coefficient. Solid state properties of CSIC were also assessed by its size, shape, surface morphology, and melting point. Furthermore, the stability of drug under variable pH, temperature, oxidation, and photolysis conditions were investigated as per international conference on harmonization (ICH) Q1A (R2) guidelines [133]. Lastly, cytotoxicity of CSIC in epithelial cell line HEC 1A and murine macrophage cell line J774A.1 was performed to evaluate the compatibility between test substance and HIV target cell types.

The majority of the studies conducted as part of the preformulation evaluation of CSIC explored its intrinsic properties. Studies also included various conditions that can be encountered in vaginal environment under physiological and pathophysiological settings. For example, it is well known that the normal pH of vaginal fluid is in the 3.5-4.5 range, however, elevated vaginal pH can be observed under various conditions, such as on the days prior to and during menstruation (6.6) [25], after bacterial infection (5-0-6.5), menopause (6.0-7.5) [28], and in the presence of semen (7.0-8.0) [134]. Therefore, a wide range of pH was utilized to assess CSIC stability. Consideration of these biological factors will permit a rational design for robust vaginal products.

2.2   MATERIAL AND METHODS

2.2.1   Materials

CSIC was obtained from Dr. Parniak from School of Medicine, University of Pittsburgh. It was originally synthesized by Dalton Laboratories (Toronto, ON, Canada) with a purity of >98%. The molecular weight of CSIC is 334 g/mol. Thiazolyl blue tetrazolium bromide was obtained from Sigma-Aldrich (St. Louis, MO, US). Polyethylene glycol 400 (PEG 400), propylene glycol, and glycerin were obtained from Spectrum (Gardena, CA, US). Polyethylene glycol 4000 (PEG 4000) was obtained from Dow Chemical Company (Midland, MI, US). Bovine serum albumin (BSA) was obtained from Spectrum (New Brunswick, NJ, US). Acetonitrile and trifluoroacetic acid were purchased from Spectrum and Thermo Scientific respectively (HPLC grade). All other chemicals were analytical grade. The human epithelial cell line, HEC-1A, was purchased from American Type Culture Collection (ATCC). The mouse macrophage cell line, J774A.1, was generously provided by Dr. Kerry Empey from the School of Pharmacy, University of Pittsburgh.

2.2.2   Methods

2.2.2.1 High performance liquid chromatography (HPLC) analysis

CSIC (and possible degradants) were quantified using reverse phase HPLC with a Gemini C18 column 4.6x150mm (Phenomenex, Florence, CA), with UV detection at 302 nm. The mobile phase comprised a gradient of 0.08% TFA in water (A) and 0.05% TFA in

acetonitrile (B), starting with 30% B and a linear increase to 50% B for 15 minutes, followed by a hold at this composition for 1 minute, then return to 30% B for equilibration over a period of 4 minutes. Flow rate was 1.4 ml/min. The limit of detection (LOD) and limit of quantification (LOQ) were determined based on Signal-to-noise approach according to ICH Q2(R1) guideline[135]. The signal measured from CSIC samples with known low concentrations were compared with those of black samples. The signal-to-noise ratios set for the detection limit and quantification limit were 3:1 and 10:1, respectively.

2.2.2.2 Solubility

CSIC solubility was determined in water, vaginal fluid simulant, 40% and 100% acetonitrile, PEG 400, propylene glycol, glycerin, 1%, 2.5%, 5% and 10% BSA, and 0.1%, 0.5%, and 1% cremophor. 5mg drug was added in 1.5 mL of each solvent. The mixtures were rotated using a rotator (Rotator-Gene™, Scientific Industries, speed 2) at room temperature for five days. The excess amount of drug was removed by centrifuge at 14,500 rpm (14,100 xg) for 5 minutes using a eppendorf MiniSpin® plus centrifuge. Samples were filtered through 0.22 µm PTFE filters before HPLC analysis.

2.2.2.3 Octanol/water partition coefficient (Log $P_{oct/wat}$) determination

The octanol/water partition coefficient is defined as the ratio of drug solubility in non-polar octanol phase to its solubility in aqueous water at equilibrium. In the current study, octanol and water were mixed at three different ratios, 1:1, 2:1, and 1:2 (v/v), in order to assure that the

partition coefficient is a constant. The mixtures were rotated vigorously overnight at room temperature to reach equilibration. After excess amount of CSIC was added, the samples were placed on a transverse rotator at 24 rpm for 6 minutes, and then centrifuged at 6000 rpm for 3 minutes.

The octanol/water partition coefficient was calculated using the following equation:

$$\log P_{oct/wat} = \log([solute]_{oct} / [solute]_{deionized\ water}).$$ (Equation 3)

Where $[solute]_{oct}$ indicates CSIC concentration in octanol phase, and $[solute]_{deionized\ water}$ denotes drug concentration in the water phase. CSIC dissolved in the octanol phase was extracted using acetonitrile at a ratio of 1:100 (v/v). Drug concentrations in the aqueous phase were analyzed directly by HPLC. The determined partition coefficient reveals the hydrophobicity of CSIC. A value larger than 1 indicate that CSIC is a hydrophobic compound because it has higher solubility in octanol phase. In contrast, a value smaller than 1 indicate that the test drug is hydrophilic presenting a higher solubility in water.

2.2.2.4 Size, shape and surface morphology of drug substance

Polarized light microscope

CSIC was first dissolved in acetonitrile and placed on a glass slide to allow it to air dry. Afterward, sample was fixed with Cytoseal^{TM} 60. The particle size, shape and surface morphology of CSIC were observed using a Zeiss Axioskop 40 inverted phase contrast microscope equipped with a polarized light filter, an AxioCam MRc5 color video camera, and analyzed by AxioVision Rel 4.7 software.

Scanning electron microscope (SEM)

The physical properties of CSIC were also studied using SEM (Philips XL30 FEG) with a 10kV accelerating voltage. Before scanning, CSIC powder was mounted on an aluminum holder by carbon conductive glue and coated with platinum using a platinum sputter coater.

2.2.2.5 Thermal behavior by differential scanning calorimetry (DSC)

DSC (DSC 1 with STAR^e DB V11.00 software, Mettler Toledo) was performed to investigate the melting behavior of the drug substance. Pure drug was placed in aluminum crucibles and sealed by a crucible sealing press. The thermograph was obtained by heating samples from 25 to 350°C at a rate of 10°C/min with a constant nitrogen purge at 50 mL/min.

2.2.2.6 Stability studies

For stability studies, buffer solutions were mixed with acetonitrile, which allowed for complete drug solubilization. Any drug loss detected over time would thus be a result of drug degradation. Drug concentration utilized for this series of studies was determined based on CSIC solubility in 40% acetonitrile.

pH stability

Standard buffer solutions with pH values of 1.2, 4, 5, 7, 9, and 10 were prepared according to United States Pharmacopeia (USP) 26. CSIC was first dissolved in acetonitrile, and then mixed with the buffer solution individually to achieve a final concentration of 100μg/mL.

Sample solutions were sonicated in a water bath until the drug was completely dissolved. Samples were then covered with aluminum foil and stored at room temperature for later analysis. Aliquots were taken daily for 10 days, and the drug content was analyzed by HPLC. Individual studies were performed in triplicate.

Thermal stability

CSIC was dissolved in 40% aqueous acetonitrile at a concentration of 100μg/mL. Samples were incubated at 25°C and 65°C. At various times aliquots were taken for analysis of drug content by HPLC as described above.

Oxidation

CSIC was dissolved in 40% aqueous acetonitrile containing 3% H_2O_2 (100μg/mL CSIC) and then stored at room temperature. At various times aliquots were taken for analysis of drug content by HPLC as described above.

Photolysis

CSIC solutions (100 μg/mL) were prepared in 40% aqueous acetonitrile and in 40% acetonitrile in phosphate buffer (pH 7.0). One half of each sample set was covered in aluminum foil, and the samples were all incubated at 30°C/ 65% relative humidity under a fluorescent light source (2x 20 watts). At various times aliquots were taken for analysis of drug content by HPLC as described above.

2.2.2.7 Cytotoxicity

Cytotoxicity was assessed using HEC-1A human endometrial epithelial cells and J774A.1 mouse macrophage cells. Cells were seeded into 96 well plates at a density of 2.5×10^4 cells per well for HEC-1A, and 8×10^4 cells per well for J774A.1. Cells were then treated with serially diluted CSIC with drug concentrations ranging from 10μg/mL to 1ng/mL. It was worth noting that 0.1% DMSO was added in the samples to facilitate drug solubilization and suspension in the aqueous medium. After 24h drug exposure, methylthiazolyldiphenyl-tetrazolium bromide (MTT) assay was performed to determine cell viability. Briefly, medium in each well was replaced by 180μL cell culture medium and 20 μL MTT solution (5 mg/mL). MTT was reduced to formazan in purple. After incubation at 37°C for another 3h, media was removed, and 200μL of solubilization solution DMSO was added in each well. DMSO dissolved the insoluble formazan product into a colored solution. The color of the solution was determined by the amount of MTT being reduced. The plates were then covered with aluminum foil and agitated on an orbital shaker for 20 minutes. The absorbance was measured at 595 nm using a microplate reader (Beckman Coulter DTX 880, USA).

2.2.2.8 Statistical analysis

All results were presented as the mean ± standard deviation (SD). Pairwise differences were determined by Student's t test. In the stability studies, drug concentration determined over time is reported as CSIC recovery (% of time zero) ± SD. The differences among groups were tested by a repeated measures mixed model with pairwise comparisons using STATA version 13. A p value <0.05 was considered statistically significant. By using the mixed models, post hoc tests could be conducted and the time could be treated as a continuous variable.

2.3   RESULTS

2.3.1   HPLC method

As part of the preformulation studies, an HPLC analytical method was developed and validated. Under the conditions used (as described in Methods (2.2.2.1), the retention time of CSIC was at 10.9 minutes. The LOD was determined to be 0.01 µg/mL, and the LOQ was 0.033 µg/mL. A linear standard curve was obtained over a range of 0.5-200 µg/mL(Figure 5). No CSIC degradation products were noted via HPLC chromatogram during the analysis. The overlay among the ten CSIC chromatograms illustrated the repeatability of samples at the lowest standard level (0.5 µg/mL) (RSD< 1%). This developed HPLC method was applied to quantify the solubility of CSIC throughout the dissertation work.
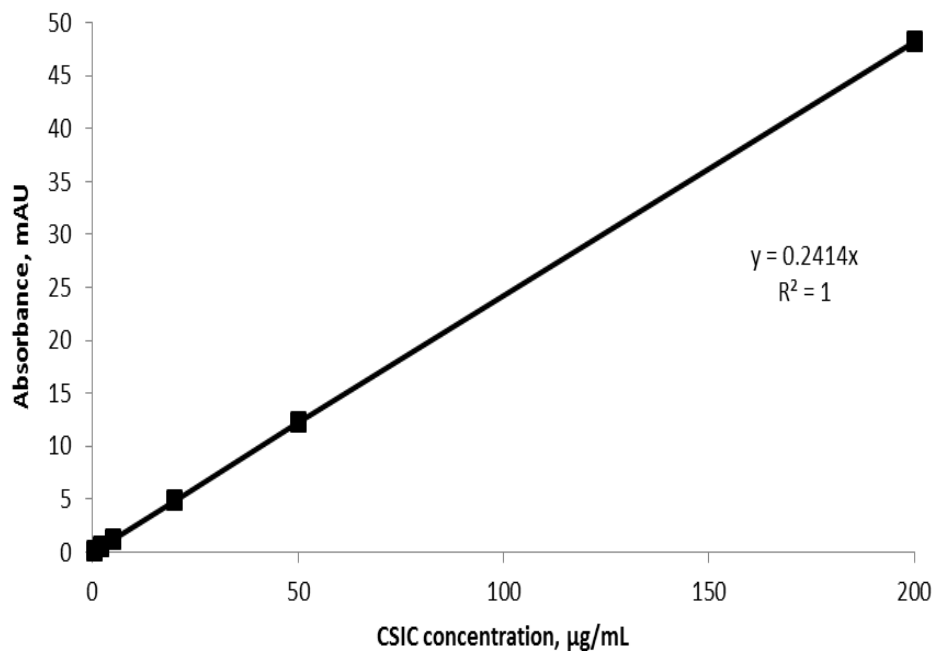
Figure 5 Linearity rage of CSIC (0.5-200 µg/mL) determined by HPLC. Drug was detected by a diode array detector, and the wavelength was set at 302 nm. Data were represented by mean ± standard deviation (n=4). The standard deviations all were within the symbols.

2.3.2 Solubility

The validated HPLC method was used to determine the solubility of CSIC in various solvents presented in Table 1a. Solubility criteria provided in Table 1b were defined according to the USP and the British Pharmacopeia (BP) [136, 137]. Specifically, solubility was classified in seven different categories in terms of the parts of solvents required to dissolve one part of solute

regardless of the solvent chosen. CSIC is practically insoluble in water, vaginal fluid simulant, propylene glycol, glycerin, all the BSA solutions, 0.1% cremophor and 0.5% cremophor; very slightly soluble in PEG 400, 40% acetonitrile and 1% cremophor; and slightly soluble in 100% acetonitrile.

Table 1 CSIC solubility.

(a) **CSIC solubility in commonly used solvents. (b) USP and BP solubility criteria**

(a)

Solvents	Solubility		Ratio with antiviral activity (EC$_{50}$=1nM)
	µg/mL	µM	
MilliQ water	1.44	4.31	4311.38
Vaginal fluid simulant	30.5	91.32	91317.37
40% acetonitrile	360	1077.84	1077844.31
100% acetonitrile	1700	5089.82	5089820.36
PEG 400	129	386.23	386227.54
Propylene glycol	53	158.68	158682.63
glycerin	10.2	30.54	30538.92
1% BSA	14.21	42.54	42544.91
2.5% BSA	21.60	64.67	64670.66
5% BSA	36.05	107.93	107934.13
10% BSA	55.87	167.28	167275.45
0.1% Cremophor	18.89	56.56	56556.89
0.5% Cremophor	48.83	146.20	146197.60
1% Cremophor	136.65	409.13	409131.74

Table 1 (continued)

(b)

Descriptive terms	Parts of solvent needed for 1 part solute	Solubility
Very soluble	< 1	>1g/mL
Freely soluble	1-10	0.1-1g/mL
Soluble	10-30	0.03-0.1g/mL
Sparingly soluble	30-100	0.01-0.03g/mL
Slightly soluble	100-1000	1-10mg/mL
Very slightly soluble	1000-10,000	0.1-1mg/mL
Practically insoluble	> 10,000	< 0.1mg/mL

2.3.3 Octanol/water partition coefficient (Log $P_{oct/wat}$) determination

The hydrophobicity of CSIC was also determined by the partition coefficient (Log P) which was calculated by the logarithm of drug solubility in hydrophobic solvent octanol and hydrophilic solvent water (Equation 3). The Log P values of CSIC in the 1:1, 2:1 and 1:2 (v/v) octanol:water mixtures were found to be 3.72, 3.69, and 3.72 respectively. The consistent values among the various ratios of octanol/water demonstrate that the partition coefficient is a constant. The observed partition coefficient greater than 1 demonstrates that CSIC is hydrophobic. Compared with the Log P value of DPV (mean predicted log P = 4.73 ± 0.64)[46], CSIC is less hydrophobic.

2.3.4 Size, shape and morphology

The physicochemical properties of CSIC such as surface morphology, particle size and shape were investigated by polarized light microscope and SEM. Hexagonal prism-shaped crystals were observed under light microscope (Figure 6a). The size of the CSIC crystal was not uniform, varying from less than 1 μm to over 100 μm. SEM imaging showed that CSIC exists in a prismatic form and aggregated in a needle/long rod shape (Figure 6b).

(a)   (b)
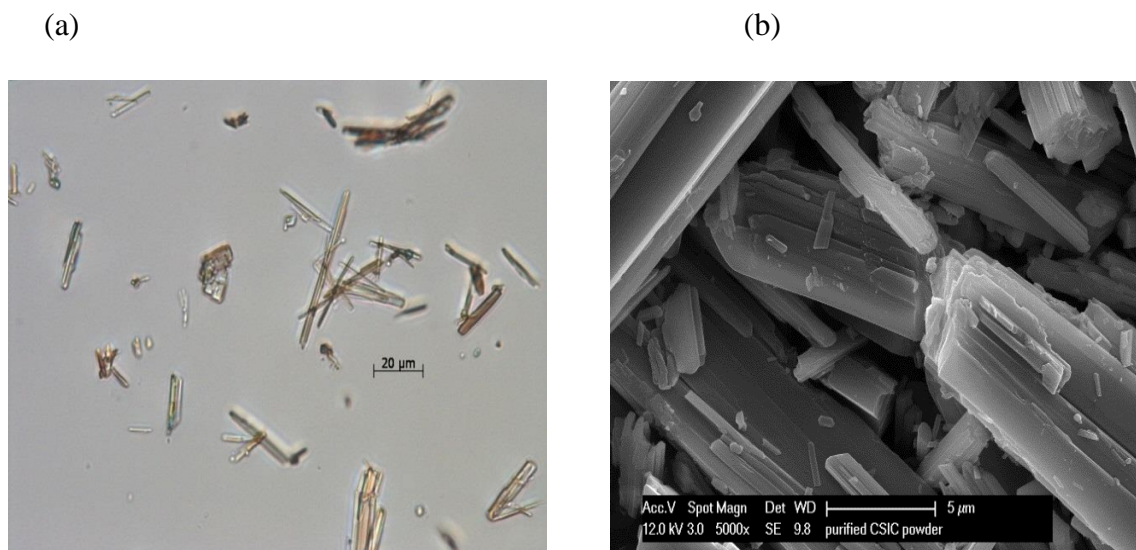
Figure 6 Physicochemical characterization of CSIC.

(a) Polarized light microscopic image of CSIC (scale bar=20μm) (b) Field emission scanning electron microscopy image of CSIC (scale bar=5μm)

2.3.5 Thermal behaviors of CSIC

DSC thermograms showed a downward endothermic peak at 257°C which indicates the transition of CSIC powder from a crystal form to a liquid form. The peak temperature reveals its melting point (Figure 7). The presence of one sharp peak suggests that CSIC exists as a single crystal arrangement with no polymorphism.
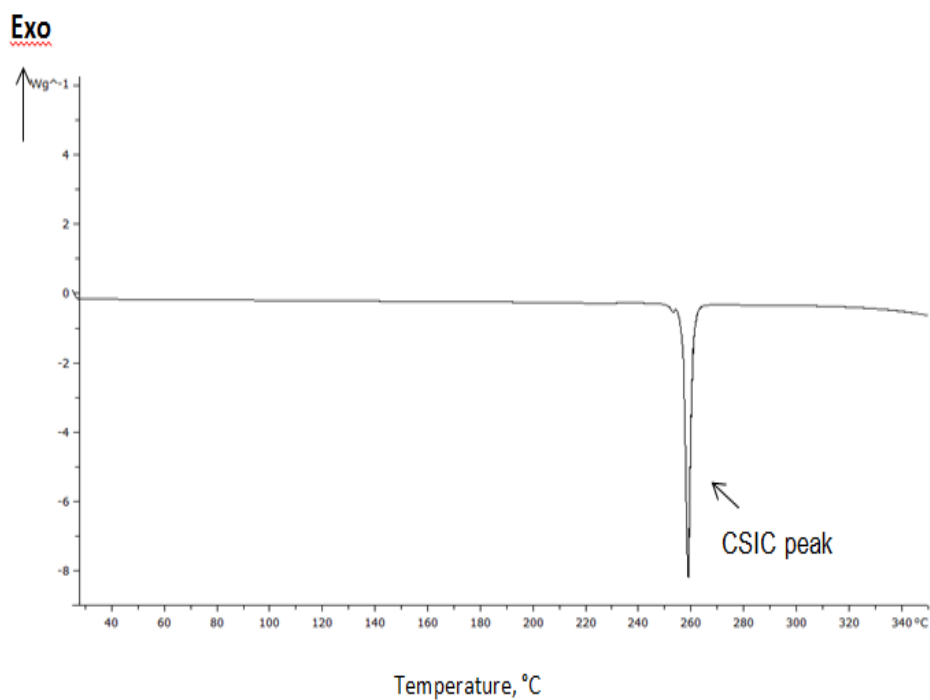
Figure 7 DSC thermograph of CSIC.

Melting point of CSIC was observed at 257°C.

2.3.6   Stability studies

The susceptibility of drug across a wide range of pH was investigated for potential hydrolytic degradation (Figure 8a). CSIC was found to be stable under all pH conditions for at least 10 days (<5% of drug loss). At each time point, more than 95% of the drug was detected compared to the drug concentration at time zero.

In the thermal stability study, the concentration versus time profiles for CSIC exposed to 25°C/60% RH and 65°C were plotted. Results showed that CSIC was stable under both thermal conditions and drug concentrations remained unchanged for more than 10 days (Figure 8b).

Upon H_2O_2 exposure in the oxidation study, a trend of drug loss was observed over time, however, no statistical difference could be found at the end of 10 days in comparison to Time 0 (Figure 8c).

For the photolysis stability study, CSIC stored in the dark was found to be stable for at least 12 days. In comparison, drug concentration declined over time in samples that were exposed to light. After 144 hours, a significant difference in drug content was confirmed between samples stored in light and samples stored in dark (Figure 8d). The indole moiety of CSIC may contribute to the photosensitivity of this drug. The susceptibility of CSIC to light, however, is not a significant problem in the final solid film formulation of CSIC.

(a)

(b)

(c)

(d)
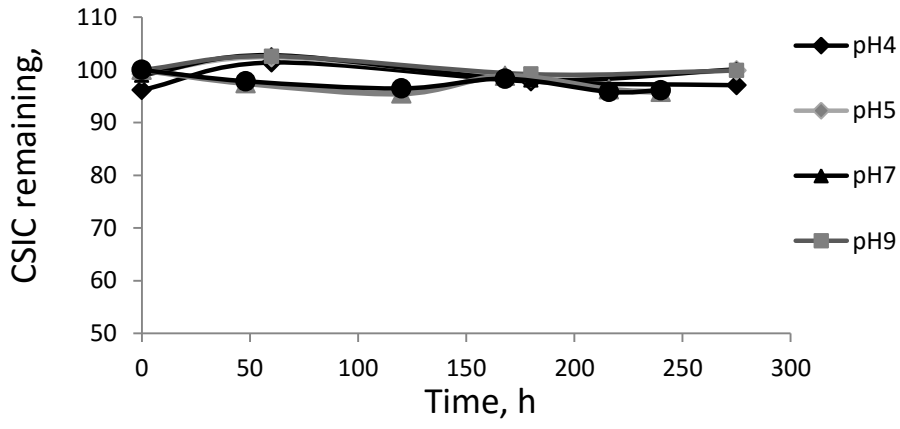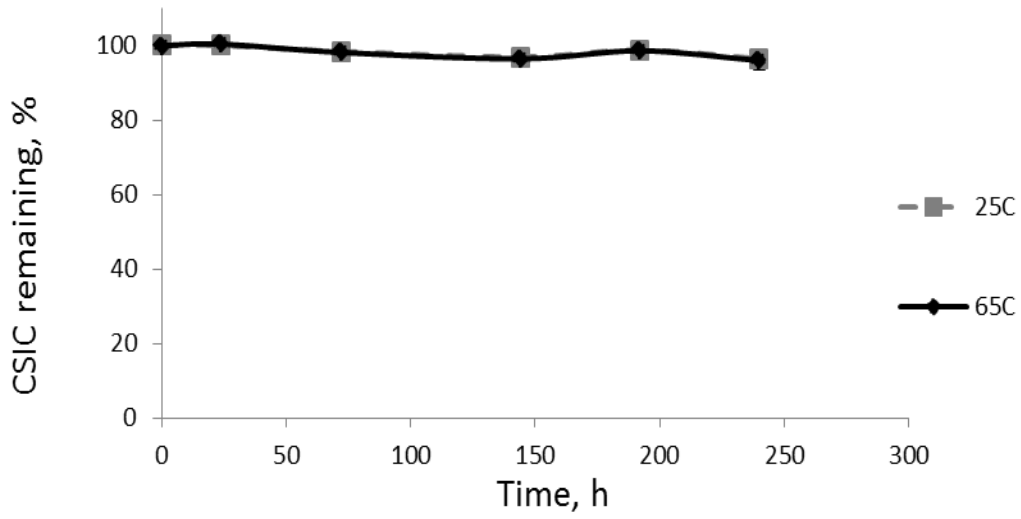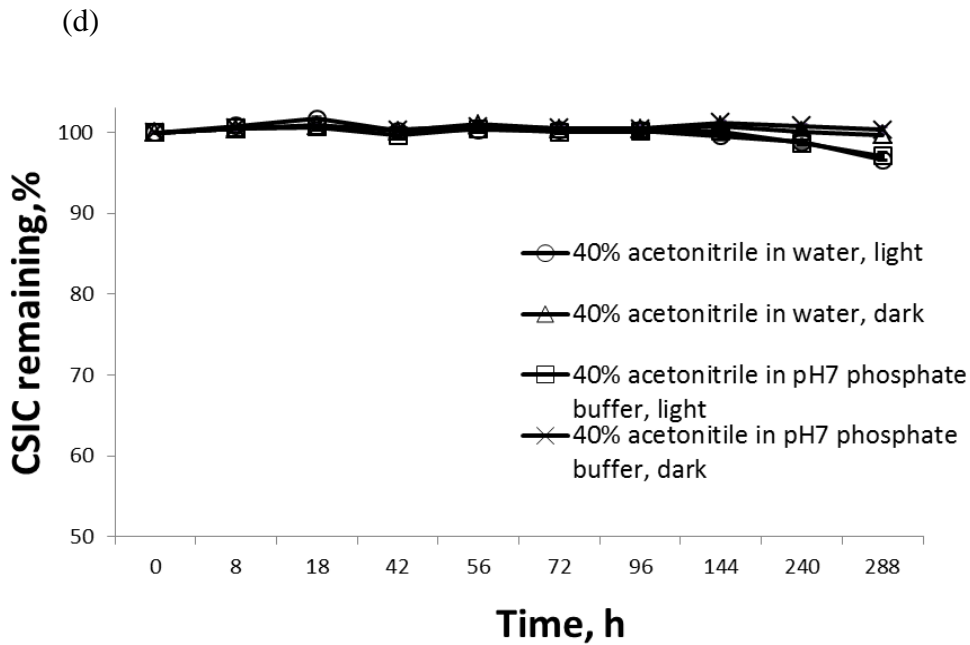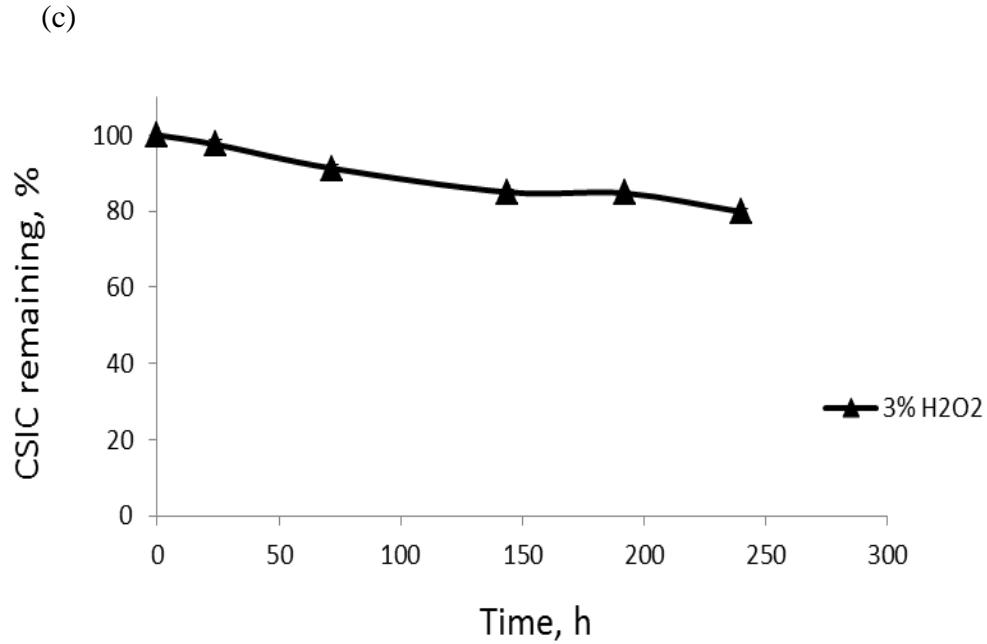
Figure 8 CSIC stability profiles.

CSIC stability (a) at various pHs, (b) in 25°C/60%RH and 65°C environmental chambers, (c) in 3% H₂O₂ solution at 25°C, and (d) with or without fluorescent illumination (2 x 20 watts) exposure in water or pH7 phosphate buffer solution respectively . Each point represents mean ± SD (n=3)

2.3.7 Cytotoxicity

Some degree of dose-dependent cytotoxicity was noted in both HEC-1A and J774A.1 cell lines exposed to CSIC, with the 50% cytotoxic concentration (CC_{50}) of CSIC for both cell lines greater than 5μg/mL (Figure 9). This CC_{50} value is several orders of magnitude higher than the antiviral EC_{50} of CSIC (15μM vs. 1nM), providing an *in vitro* selectivity index of 15,000. This suggests that CSIC is a reasonably safe candidate for pre-exposure prophylaxis use.
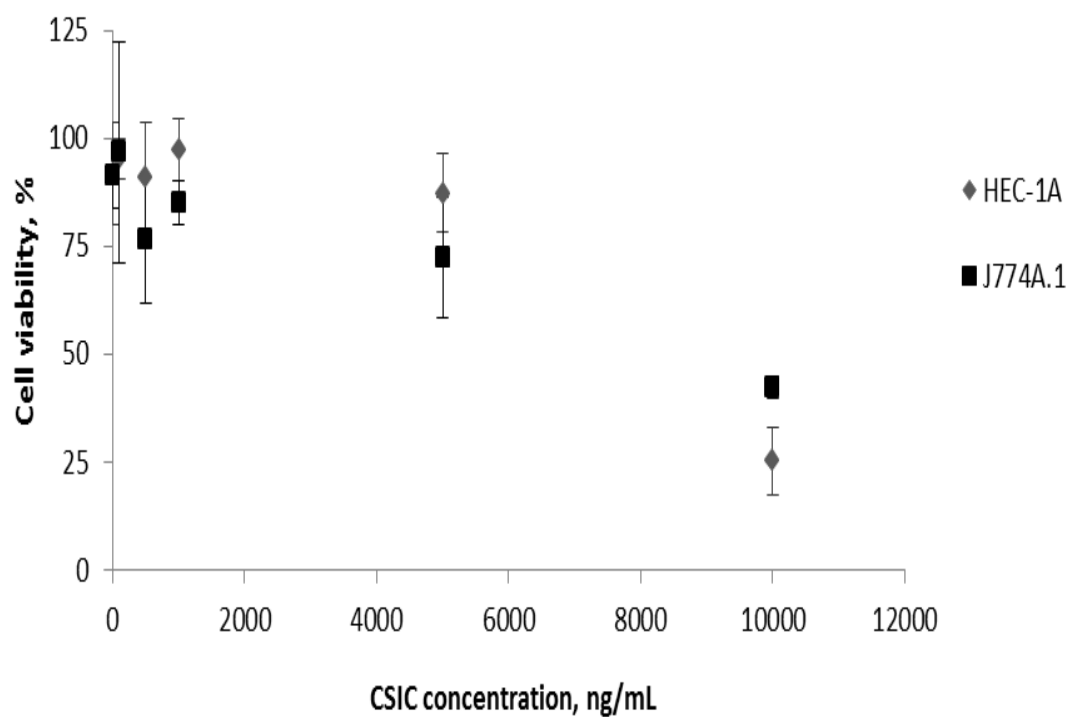
Figure 9 *In vitro* **cytotoxicity of CSIC against cell line HEC-1A and J774.A1.**

The cytotoxicity of CSIC was measured at concentrations ranging from 10μg/mL to 1ng/mL. 0.1% DMSO was added in the samples to facilitate drug solubilization and suspension in the aqueous medium. Following 24h drug treatment, cell viability was determined by MTT assay. The absorbance was measured at 595 nm using a microplate reader (Beckman Coulter DTX 880, USA).Each point represents mean ± SD (n=6)

2.4   DISCUSSION AND CONCLUSION

The overall goal of the preformulation studies conducted in this chapter was to evaluate the physicochemical and biological properties of the active pharmaceutical ingredient (API) and its stability profile under various conditions to identify factors that could potentially lead to formulation problems. The test article CSIC is found to be highly hydrophobic according to its poor solubility in various solvents and the determined partition coefficient (LogP >1). As a consequence, the hydrophobic nature of CSIC will significantly impact its dissolution rate in the aqueous vaginal fluid [24]. In addition, the drug's bioavailability *in vivo* will be compromised as well since the drug molecules have to be dissolved first to be absorbed [138]. Therefore, formulating CSIC in vaginal products would be very challenging and the majority of work will be focused on solubility improvement.

In addition to the drug solubility study, crystal properties of CSIC were evaluated. As observed under polarized light microscope and SEM, CSIC possessed a needle shape crystal structure which indicated that the growth of CSIC crystals was faster in one dimension. In addition, the experiment carried out by DSC identified the melting point of the raw drug. As pharmaceutical companies prefer to market drugs that are stable at ambient temperature (25°C), the melting point of CSIC at 273°C approved its suitability as a promising drug candidate. This information will be compared with the nanocrystal formulation described in the Chapter 4 to confirm the successful preparation of the nano-sized CSIC crystals.

Chemical stability of API is of great importance since it affects the safety and efficacy of the drug substance. The stability studies were designed according to the ICH guidelines [133]. The goal of the stability evaluation is to monitor the quality and quantity of CSIC under stress conditions over time. The resulting data can help identify the potential degradation

product/pathway, validate the power of the developed analytical procedures, select appropriate formulation and dosage form, and determine appropriate package requirement and storage conditions.

As part of the stability study, the susceptibility of drug across a wide range of pH was investigated for potential hydrolytic degradation. Hydrolysis is a chemical reaction, which decompose drug substance under acidic and basic conditions via reaction with water. CSIC was found to be stable under all pH conditions for at least 10 days (<5% of drug loss). No degradation peaks could be detected by HPLC. The desirable stability profile of CSIC will make it suitable for vaginal drug delivery.

In the thermal stability study, two storage conditions were chosen: 25°C/60% RH and 65°C. The 65°C was introduced as stress, which may increase the rate of degradation if it exists. Data showed that the API was very stable under both temperatures for at least 10 days which was a positive finding indicating the drug might have a long shelf life.

During the process of formulation, storage, handling and application *in vivo*, there are many resources that could oxidize the drug, such as the use of organic solvents and excipients in formulations, and, biologically, the hydrogen peroxide produced by Lactobacillus in the female reproductive tract. In the current study, 3% hydrogen peroxide was utilized to test CSIC's oxidative stability. This concentration was chosen since it has been commonly used in the pharmaceutical field to identify the relevant degradation products [139, 140]. It was found that no significant drug loss or apparent degradants were observed by the end of 10 days. To note, the lactobacillus *in vivo* only secretes 0.02% of hydrogen peroxide, which is much lower than the 3% used in the current study. Therefore, the result suggests that CSIC could be stable under oxidative environment.

Photolysis was also investigated for CSIC in the current preformulation study. As shown in the result section, CSIC is photosensitive and has potential for photodegradation. Further studies may need to be conducted to investigate the corresponding degradation products. This finding has an influence on sample handling, manufacturing, packaging and product labeling, which is elaborated in the following studies.

To assess the safety profile of the API in cells, the cytotoxicity profiles of this drug were evaluated in epithelial cell line HEC 1A and mouse macrophage cell line J774A.1. It is well known that epithelial cells in the female reproductive tract are the primary site of sexually transmitted HIV infection and act as a physical barrier against the initial HIV acquisition [16, 141]. Any damage to the epithelium will result in an increased risk of infection. It is critical to maintain the integrity/ viability of epithelia when developing vaginal delivery products, especially for HIV prevention [112, 142]. In addition, HIV also targets macrophages in the female reproductive tract. These cells are actively involved in the phagocytosis of exogenous components and the transport the virus to the draining lymph nodes which facilitates the establishment of systemic infection [16]. Therefore, the cytotoxic information of the drug to both the epithelium and macrophages are essential for future biological evaluations. Based on the results generated from the cytotoxicity study, a dose-dependent reduction in cell viability was observed. A non-toxic concentration, 5 µg/mL, was chosen for the cell based study described in Chapter 4. This concentration should be able to provide sufficient anti-HIV activity since it is several orders of magnitude higher than the EC_{50} of CSIC (~0.3 ng/mL) [128, 143].

In conclusion, the preformulation evaluation preformed in this chapter proved CSIC as a promising drug candidate for vaginal drug delivery since it is stable under many stressed conditions. The studies in this chapter also identified the major challenge for CSIC formulation

development and bioavailability, which is its hydrophobicity. The use of pharmaceutical strategies is highly recommended to improve CSIC aqueous solubility. To date, numerous pharmaceutical strategies have been developed and applied to improve aqueous solubility of hydrophobic drug candidates, such as crystal modification, amorphization, particle size reduction, solid dispersion, co-solvents, cyclodextrin complexations, self-emulsification [50, 51, 144]. In this dissertation work, co-solvent and solid dispersion strategies were applied in combination to improve the aqueous solubility of CSIC in a vaginal film formulation (Chapter 3). Moreover, a nanocrystal formulation was developed utilizing the particle size reduction approach to enhance CSIC solubility (Chapter 4).

3.0 FORMULATING CSIC IN WATER SOLUBLE POLYMERIC FILM USING COSOLVENT AND SOLID DISPERSION STRATEGIES

3.1 INTRODUCTION

As discussed in Chapter 2, CSIC is a highly potent non-nucleoside reverse transcriptase inhibitor (NNRTI). The major challenge for the vaginal delivery of CSIC, however, is its hydrophobicity. Research on strategies to improve drug's aqueous solubility is, therefore, warranted. In this chapter, cosolvent and solid dispersion strategies were utilized as means to increase CSIC solubility. These approaches helped loading a high dose of drug in a water soluble polymeric thin film.

Cosolvents are defined as water miscible organic solvents that can be used in liquid drug formulations to increase the solubility and chemical stability of hydrophobic agents [145]. They work by reducing the interfacial tension between the aqueous solution and hydrophobic API and disrupting the self-association network among water molecules [146]. The technique of using cosolvents, cosolvency, has been commonly employed throughout the history of drug formulation. Cosolvent system is favorable due to its safety profile, high loading efficiency, and ease of manufacturing [144]. Cremophor EL, one of the most investigated cosolvents, has been used to improve the solubility of anticancer drug paclitaxel (Taxol) [147]. Recently, a cosolvent system comprising N-methyl pyrrolidinone, ethanol, and Tween 80 was developed to enhance the solubility and bioavailability of a hydrophobic drug curcumin [51].

Solid dispersions refer to the dispersions of active pharmaceutical ingredients (API) in inert matrix at solid state. Usually, they are composed of hydrophobic drugs and hydrophilic matrixes[148, 149]. When the hydrophilic matrix dissolves in the aqueous medium, the dispersed API will be released as very fine, colloidal particles with reduced particle size ($<1\mu m$), which in turn increase the solubility, dissolution rate and bioavailability of drug [150]. Recently, solid dispersion strategy has been applied in the development of a bioadhesive vaginal film for the delivery of a hydrophobic drug itraconazole against vaginitis [151]. During the process of manufacturing, itraconazole was dispersed uniformly in film-forming polymers in water, and the film product was then prepared by solvent evaporation method. Additionally, in the field of PrEP, a solid dispersion of a hydrophobic NNRTI, dapivirine (DPV), was utilized in a vaginal film formulation [152]. The results have shown that DPV containing vaginal film provided rapid drug release and effective protection against HIV-1 infection both *in vitro* and *ex vivo*.

Polymeric thin films are an emerging dosage form for vaginal delivery. In addition to itraconazole and DPV, vaginal films have been utilized to deliver drug substances such as the contraceptive antimicrobial agent sodium polystyrene sulfonate [153], the first generation of microbicide cellulose acetate phthalate [154], and second generation microbicide tenofovir [155]. The development of vaginal films has provided women with more dosage form options and leads to an improved user adherence [156, 157]. In comparison to other vaginal products, vaginal film presents negligible vaginal leakage, easy application using fingers, discreet use, and low cost [37, 152, 158]. Therefore, vaginal film dosage form was chosen for the delivery of CSIC in the current work.

In this chapter, the cosolvent and solid dispersion approaches were both utilized within the film formulation for the delivery of CSIC to the vagina. A compatibility study was first conducted to identify the polymers, surfactants and cosolvents that could be used with CSIC. A ternary phase diagram was developed to optimize the cosolvent system, which facilitated the drug dispersion in the film formulation. Once the film products were developed and manufactured, a series of evaluations were carried out including drug content, water content, tensile strength, disintegration, dissolution, anti-HIV bioactivity, and biocompatibility. These properties were monitored over 12 months under different storage conditions to assess drug product stability.

3.2   MATERIAL AND METHODS

3.2.1   Materials

Polyvinyl alcohol (PVA) was obtained from Spectrum (Gardena, CA, US). HPMC 4000 (HPMC K4M) was purchased from Colorcon (West Point, US). Polyethylene glycol 4000 (PEG 4000) was obtained from Dow Chemical Company (Midland, MI, US). For information about drug CSIC and other excipients, please refer to Chapter 2.

3.2.2   Methods

3.2.2.1 CSIC-excipient compatibility study

The goal of the compatibility study was to preclude excipients that might induce stability issue over time. Test excipients included polyvinyl alcohol, HPMC K4M, PEG4000, PEG400, propylene glycol, and glycerin. These were mixed with CSIC individually at a ratio of 1:1 (w/w) to assess any potential interactions [159]. Physical compatibility of CSIC with the excipients was determined by DSC and compared to that of CSIC alone [159, 160]. Samples were heated from 25 to 280˚C at a heating rate of 10°C/min with a constant nitrogen purge at 50.0 mL/min.

3.2.2.2 Co-solvent system to increase CSIC solubility

PEG 400, propylene glycol, and glycerin were selected as cosolvents for CSIC. Identification of the optimal ratio of these solvents was carried out by mixing them at different

percentages according to the ternary phase diagram shown in Figure 10. Excess CSIC was added in each solvent matrix. Samples were then placed on a rotating mixer for 5 days at room temperature to allow solubilization. To determine CSIC solubility, samples were centrifuged to remove the undissolved drug particles, and the supernatant was used for drug extraction and quantification by HPLC as described above.
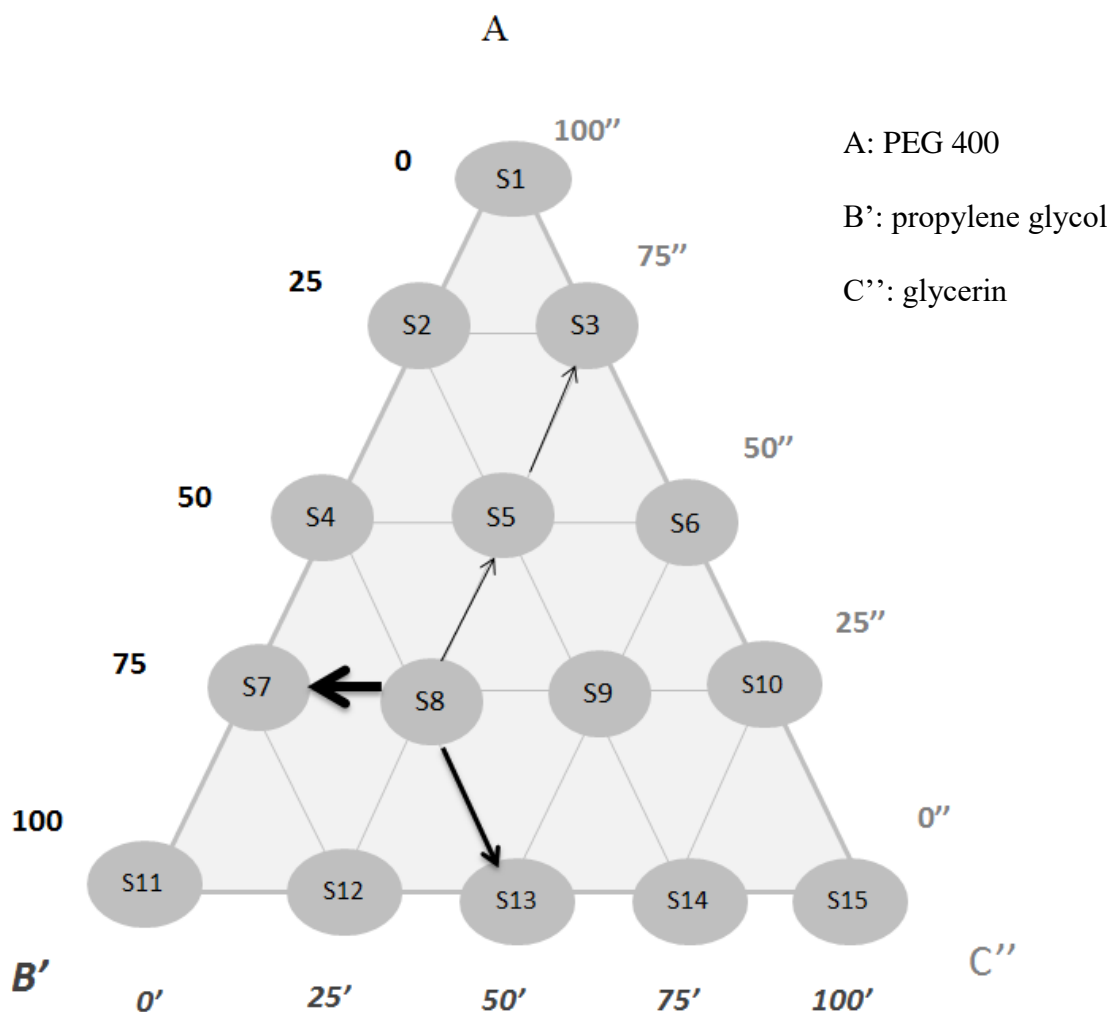
Figure 10 Ternary phase diagram.

The distance AB', B'C'' and C''A indicate the parts of PEG 400, propylene glycol, and glycerin respectively. Outward arrows from each solvent matrix are drawn parallel to the sides of the triangle. Any point within the triangle represents a given composition. For example, in the case of solvent matrix (S8), the matrix was composed of 75 parts of A, 50' parts of *B'* and 75'' parts of C''. The ratio among A, *B'* and C'' was 75:50:75, or 3:2:3.

3.2.2.3 Preparation of CSIC vaginal film

CSIC film was manufactured using a solvent casting technique as reported previously with minor modifications [36]. Briefly, film forming polymer PVA was first dissolved in MilliQ water upon heating at 90°C in a water bath. Polymer HPMC K4M and PEG 4000 were then added into the PVA solution at room temperature. The polymer solution was stirred overnight using an overhead stirrer (Erostar Power Control –Visc, IKA Works, Inc) with a stirring rate at 50 rpm. CSIC was dissolved in the optimized cosolvent system according to the ternary phase diagram, and then added to the pre-prepared polymer solution with stirring over 15 minutes to ensure uniform distribution of CSIC. The mixture was then cast onto a preheated film applicator (70˚C) to evaporate the excess amount of water (within 15 minutes). Film sheets were removed and cut into 1"x2" pieces and then stored in foil packages.

3.2.2.4 Physicochemical characterization of CSIC film

Standard measurements of the film formulations included weight, thickness, film appearance, water content, tensile strength, disintegration time, drug content, content uniformity and dissolution. Film appearance was evaluated subjectively by texture and color. Film surface morphology was observed by SEM. Water content was determined using the Karl Fisher approach (Model 890 Metrohm Titrando and 832 KF Thermoprep). Film tensile strength was measured using a texture analyzer (TA-XT.Plus) in combination with a TA 96B probe, and calculated using the equation: Tensile strength= Force (kg) / cross-sectional area of film (m^2) (Equation 4). Film disintegration analysis was performed by submerging films into 3 mL MilliQ water followed by rotation on an orbital shaker with constant observation. The disintegration time was determined when separation of the first piece was observed. To determine the drug

content, film matrix was first dissolved in MilliQ water, and CSIC was extracted by mixing with 70% acetonitrile solution before HPLC analysis. Film drug content uniformity was evaluated by cutting a film into six small pieces, and then quantifying the CSIC content in each sample. The dissolution profile of CSIC films was tested using a USP class IV method coupled with a SOTAX CE7 smart apparatus. 80 mL of 1% cremophor solution with a flow rate of 16mL/min used to maintain sink conditions. At predetermined time points, 1 mL samples were collected for analysis of CSIC content by HPLC as described in Chapter 2.

3.2.2.5 Film compatibility with *Lactobacilli*

Compatibility of CSIC film with seven different *Lactobacillus* strain were conducted by standard microbicide safety techniques [113]. Briefly, *Lactobacillus*-containing suspension and film dissolving solution were incubated together at a ratio of 1:1 (w/w) for 30 minutes at 37°C. Colony forming units determined after film exposure were counted and compared with the units before film treatment.

3.2.2.6 *In vitro* anti-HIV bioactivity test

Two types of bioactivity assays were conducted in this study [156], both using single replication cycle analysis with P4R5 cells. Direct antiviral activity was assessed by simultaneously exposing cells with HIV and various concentrations of CSIC film solutions for 48h. The protective effect (memory effect) of film-formulated CSIC was assessed by pre-exposing cells to various concentrations of CSIC film solutions for 2 hours, followed by removal of the drug prior to exposure to HIV. In both studies, a single replication cycle assay was used to evaluate HIV replication. As a control, similar studies were completed for CSIC substance only. CSIC was dispersed in the cell culture medium with the presence of DMSO.

3.2.2.7 CSIC film stability

Stability studies were carried out according to the Guidance for Industry (Q1A (R2) stability testing of new drug substances and products)[161]. Films were individually sealed in foil packages and stored in 30˚C/ 65% Relative Humidity (RH) for 12 month as a long term study and 40˚C/ 75% RH for 6 months as an accelerated study. At time zero, 15 day, 1 month, 3 month, 6 month, 9 month, and 12 month, film samples were taken for evaluation.

3.2.2.8 Statistical analysis

All results were provided as the mean ± standard deviation (SD). Pairwise differences were determined by Student's t test. A *p* value <0.05 was considered statistically significant.

3.3   RESULTS

3.3.1   CSIC-excipient compatibility study

Prior to CSIC film formulation development and optimization, the compatibility of CSIC with each individual excipient was investigated by monitoring the impact of the excipient on the melting point of CSIC. No shifts for the melting point of CSIC were observed when the drug was mixed with PVA, HPMC K4M, and propylene glycol separately (Figure 11a-c). When CSIC was exposed to PEG 400, its melting peak disappeared indicating the solubilization of CSIC in this excipient (Figure 11d). Similar finding was also observed for CSIC/ PEG 4000 mixture. The majority of CSIC dissolved in PEG 4000, while the small endothermic peak detected at 253°C may arise from a small fraction of undissolved drug (Figure 11e). In contrast, the melting peak of CSIC has shifted to a lower temperature at 217°C (Figure 11f) in the presence of glycerin. Hydrogen bonding between CSIC and glycerin may result in the decrease of melting temperature. Overall, among all the excipients, glycerin was the only one that might cause incompatibility issues. It would be very important to reduce the percentage of glycerin use.

(a)

(b)

(c)

(d)

(e)

(f)
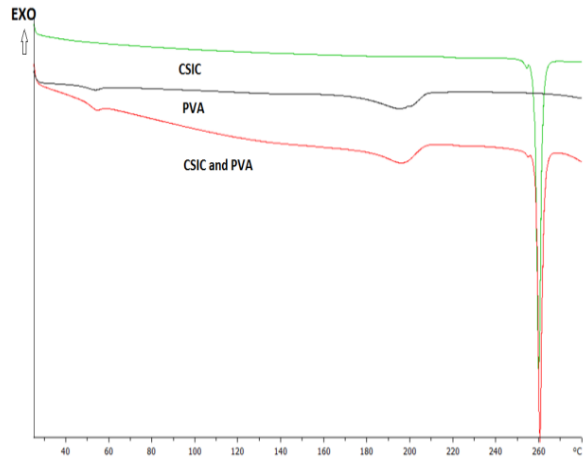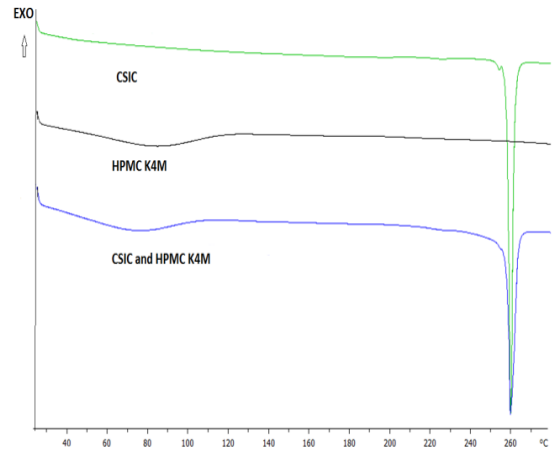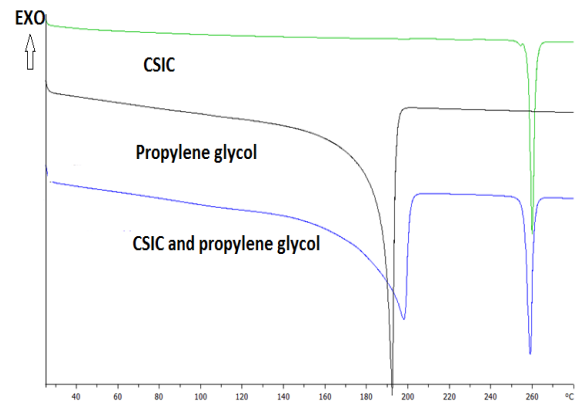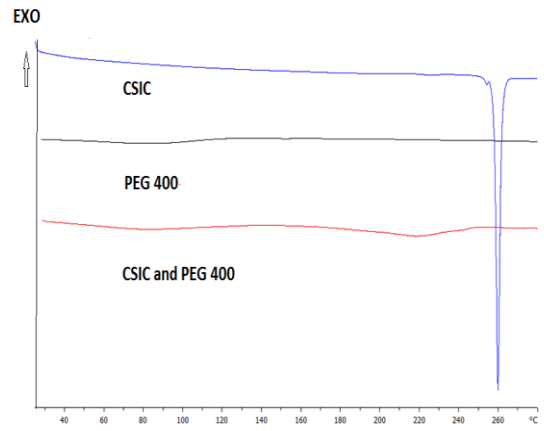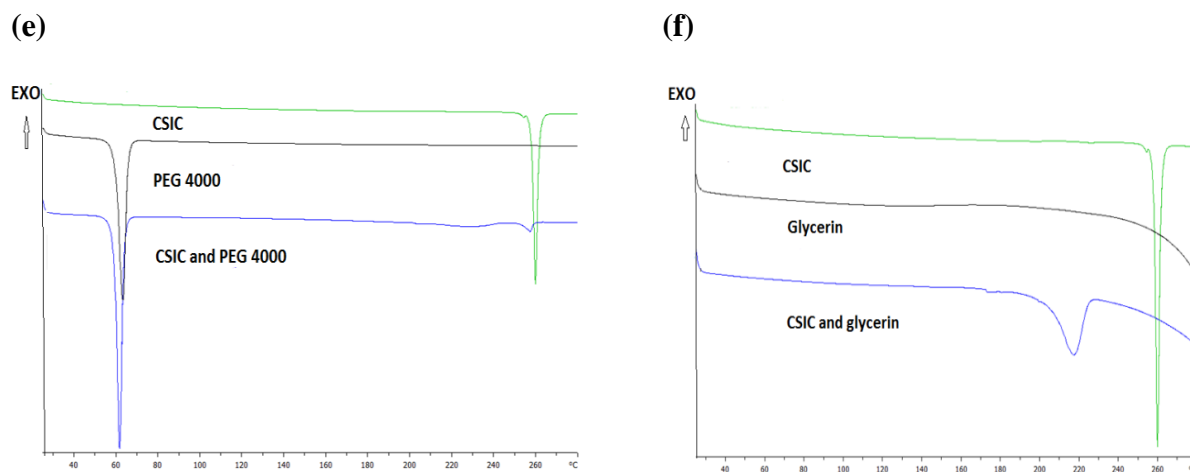
Figure 11 The compatibility between CSIC and each individual excipient evaluated by differential scanning calorimetry.
The melting peak of CSIC did not change when drug was mixed with PVA (a), HPMC K4M (b), and propylene glycol (c) separately. Drug dissolved in PEG 400 (d) and PEG 4000 (e). While the small endothermic peak detected at 253°C in the CSIC-PEG4000 may arise from a small fraction of undissolved drug. In contrast, the melting peak of CSIC has shifted to a lower temperature at 217°C (f) in the presence of glycerin which might indicate some incompatibility issues.

3.3.2   Co-solvent system to increase CSIC solubility

To improve the solubility of CSIC in the film formulation, a co-solvent system including PEG 400, propylene glycol and glycerin was designed. The three cosolvents were chosen due to their favorable safety properties for vaginal application and the ability to improve drug solubility. A ternary phase diagram was utilized to optimize the ratio among these three solvents (Figure 10). Data showed that the utilization of PEG 400 significantly enhanced the solubility of CSIC followed by propylene glycol (Table 2a). Among all the solvent matrixes illustrated in Figure 10,

solvent matrix No.15 (S15), which is composed of 50% PEG 400 and 50% propylene glycol, presented the maximum solubility of CSIC at 28.64 mg/mL. To further optimize the co-solvent system, solvent matrixes containing higher percentages of PEG 400 such as 67.5% and 75% were prepared (Table 2b) to achieve even high drug solubilization. Maximum CSIC solubility was obtained at 30.2 mg/mL for the solvent matrix No.18 (S18, Figure 10) when the ratio among PEG 400, propylene glycol, and glycerin was set at 10: 4: 2 (5:2:1).

Table 2 CSIC solubility in different solvent matrixes.

CSIC solubility in (a) solvent matrixes prepared according to the ternary phase diagram and (b) CSIC solubility in solvent matrixes with even higher proportion of PEG 400. The percentage of PEG 400 used in each sample is noted in the parenthesis. Solvent matrix 18 represented the highest drug solubility.

(a)

Sample No.	PEG 400 %	PG %	G%	Solubility mg/mL
S1	0	50	50	5.23
S2	12.5	37.5	50	10.60
S3	12.5	50	37.5	12.85
S4	25	25	50	12.85
S5	25	37.5	37.5	17.08
S6	25	50	25	19.99
S7	37.5	12.5	50	20.46
S8	37.5	25	37.5	21.81
S9	37.5	37.5	25	24.63
S10	37.5	50	12.5	22.59
S11	50	0	50	22.86
S12	50	12.5	37.5	23.67
S13	50	25	25	24.31
S14	50	37.5	12.5	28.21
S15	50	50	0	28.64

(b)

Sample No. / Component	S16	S17	S18	S19	S20
PEG 400, %	10 (62.5%)	10 (62.5%)	10 (62.5%)	6 (75%)	3 (75%)
PG, %	2	3	4	1	1
G,%	4	3	2	1	0
Solubility, mg/mL	22.7	20.7	30.2	29.1	28.8

3.3.3 CSIC film formulation development and characterization

Polymeric vaginal films comprising PVA, HPMC K4M, PEG 4000, PEG 400, propylene glycol, glycerin, and drug CSIC at a ratio of 50:20:20:25:10:5:1 were manufactured using a solvent cast technique. CSIC films were soft, flexible, smooth and translucent (Figure 12). No precipitation of either drug particles or dehydrated polymers was observed on the film surface. The result indicates sufficient water content remaining in the film product to allow for polymer hydration. In addition, the percentage of the co-solvents and polymers applied in the current formulation were adequate for drug solubilization and dispersion.

Figure 12 Picture of a CSIC vaginal film (1″ x 2″)

Numerous physicochemical properties of the CSIC films were characterized in the current investigations. The average weight and thickness of the films were recorded to be 137 ± 11.5 mg and 133 ± 0.013 μm, respectively. This thickness was adjusted to load sufficient amount of drug in each $1''$ x $2''$ film product. Drug content in CSIC films was quantified to be 1.19 ± 0.1 mg, and drug substance was distributed uniformly across the film sheet as well as within each individual film (relative standard deviation <5%). The dosing level for CSIC was designed based on the dosing regimens used for DPV vaginal film, which is 1.25 mg DPV per film [36]. In addition, the residual water in the films was determined to be less than 10% ($6.8 \pm 0.49\%$). The limited amount of water (<10%) remained in the films will help maintain long term stability of the drug substance and film properties. To understand the mechanical property of CSIC films, tensile strength was measured. The tensile strength was found to be in the range of 1000-1400 kg/m^2 which was relatively lower than that of the vaginal contraceptive films VCF$^®$ (1400-2200 kg/m^2). Moreover, in the disintegration study, once the films were exposed to water, the separation of the first piece was observed within 3 minutes indicating the fast disintegrating nature of the films. Also, drug release from the film formulation was evaluated in a class IV USP dissolution apparatus. Within three minutes, drug concentrations were detected at 3 μg/mL, which is 3 orders of magnitude higher than the EC_{50} of CSIC (Figure 13).An estimated 50% of loaded drug released from the formulation within 10 minutes, and over 85% of drug released in 60 minutes. The results generated from the dissolution study confirmed the fast dissolving property of the vaginal film which was similar to the DPV containing vaginal film [36].
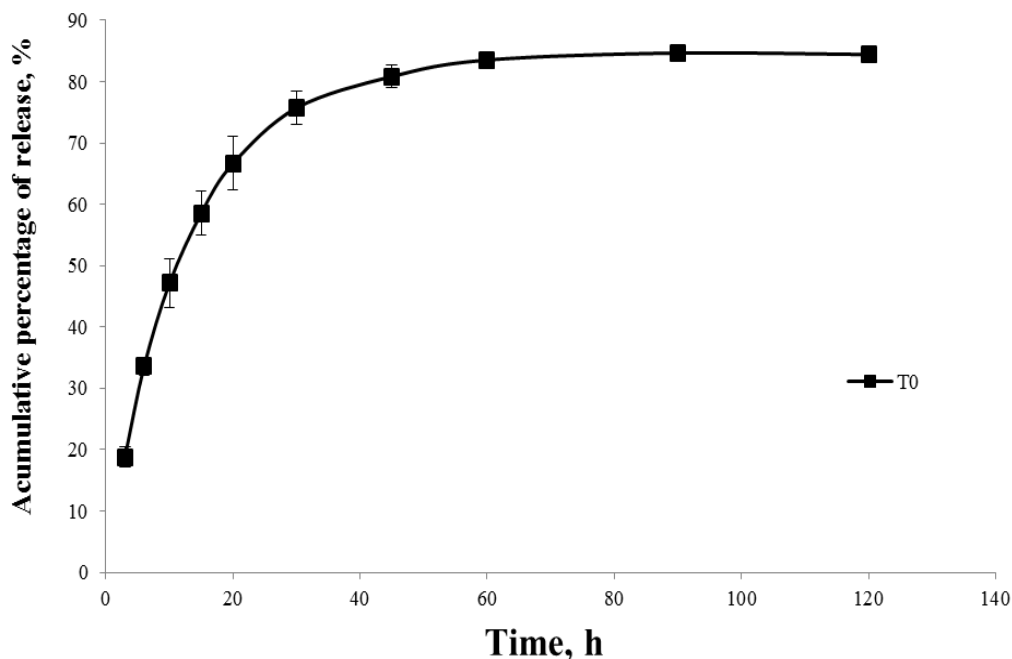
Figure 13 Dissolution profile of CSIC film at time zero

The dissolution profile of CSIC films was tested using a USP class IV method coupled with a SOTAX CE7 smart apparatus. 80 mL of 1% cremophor solution with a flow rate of 16mL/min used to maintain sink conditions. CSIC was released from the film formulation with a burst effect. Over 80% of drug could be detected in the dissolution medium in 60 minutes, (n=3).

In addition, bioactivity of the film formulated CSIC, including direct antiviral activity ($EC_{50\text{-antiviral}}$) and protective effect ($EC_{50\text{-protection}}$), was investigated in P4R5 indicator cells. Drug's antiviral activity was evaluated when the cells were simultaneously incubated with HIV and serially diluted CSIC films. Whereas, the protective effect was determined when the cells were pretreated with film formulated CSIC and then removed from the cells. According to the current study, $EC_{50\text{-antiviral}}$ and $EC_{50\text{-protecction}}$ of CSIC in the film dosage form were found to be <1

71

nM and <20 nM, respectively (Figure 14). The antiviral activity of film formulated CSIC was similar to that of the API (1.2-5 nM) [128, 132]. Formulating CSIC in a polymeric vaginal film thus had no substantial effect on its anti-HIV bioactivity. A comparable finding was also reported by Ayman et al showing that formulating DPV in a polymeric vaginal film could maintain the drug's bioactivity [36]. The $EC_{50\text{-antiviral}}$ of DPV API and DPV film were determined to be 7.9 nM and 8.7 nM respectively using a TZM-bl indicator cell assay [152].
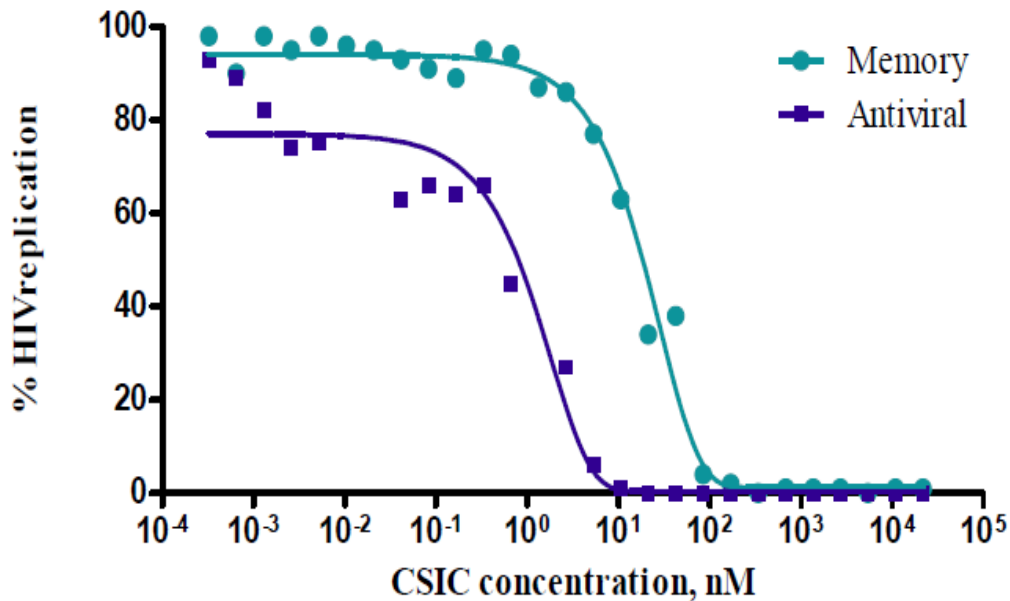
Figure 14 Bioactivity of film formulated CSIC at time zero.

The bioactivity of film formulated CSIC was investigated in P4R5 HIV infection indicator cells. Both direct antiviral activity (with the presence of drug) and protective effect (without the presence of drug) were tested.

Since *Lactobacillus* play an important role against viral infection in the vagina by maintaining acidic pH and producing hydrogen peroxide, it is important to assess the compatibility between CSIC film products and *Lactobacillus* for safety purpose using the Standard Microbicide Safety Test. As shown in Table 3, the seven major strains of Lactobacillus were unaffected by exposure to the CSIC film formulation.

Table 3 Evaluation of CSIC film compatibility with Lactobacillus.

The positive value indicates increased cell viability. In contrast, negative values illustrate decreased cell viability. The loss of viability has to be < 1 log10 to meet the safety requirement.

Lactobacillus strain tested	Log Difference (T30 minute Plate Count – T_0 minute Plate Count)
L.crisp ATCC 33197	0.113
L.jen LBP 28Ab	-0.154
L.jen ATCC 25258	-0.068
L.crisp ATCC 20225	-0.082
L.crisp LBP 90Aa	-0.143
L.crisp 6099	-0.100
L.crisp 2116V	-0.023

3.3.4 CSIC film stability

CSIC film stability studies were carried out by storing films in 30°C / 65% RH and 40°C / 75% RH environmental chambers. Based on the physicochemical evaluation performed, CSIC films were found to be stable at 30°C/65% RH for a period of 12 months, and at least 6 months under stressed condition (40°C/75% RH). Figure 15 and Table 4 show drug content in the films and drug dissolution detected at 10 minutes respectively. The drug content obtained at each time point was unchanged ($\pm$ 10%) relative to the drug content at time zero. Additionally, film disintegration was observed within 3 minutes, and the residual water contents in the film products were found be to lower than 10% at all the time points. Moreover, bioactivity of CSIC could be maintained in the film formulation throughout the stability assessment period. No loss of *Lactobacillus* viability was observed over time, which again confirmed the compatibility between CSIC film and the vaginal Lactobacillus.
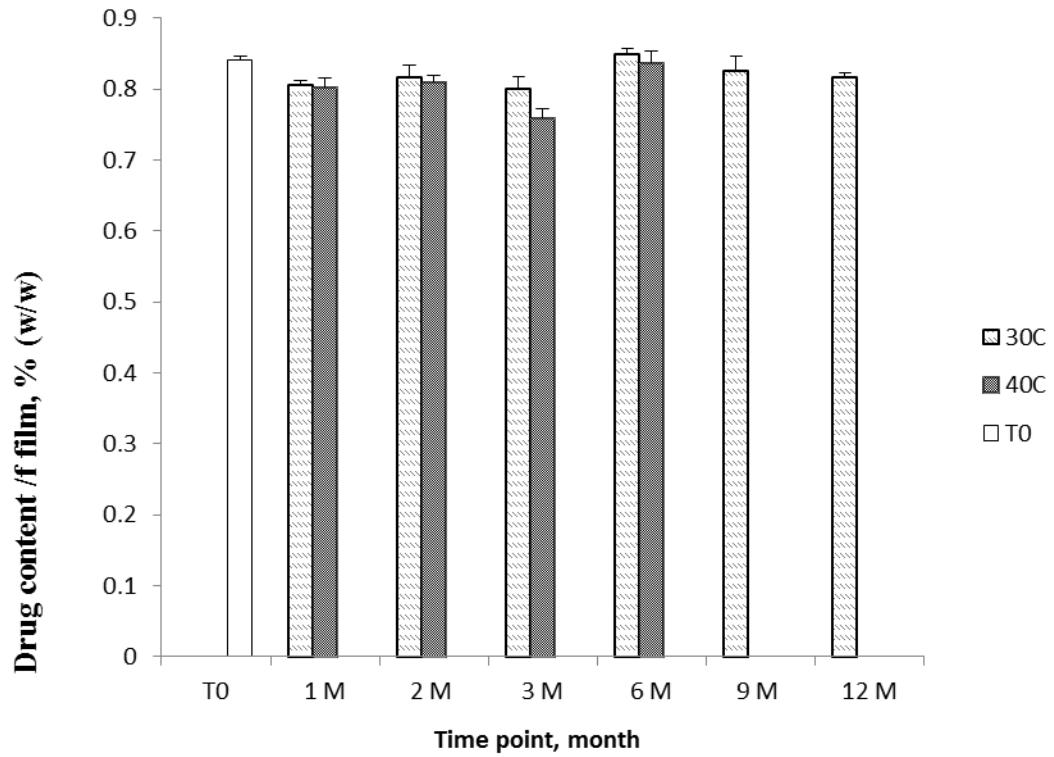
Figure 15 CSIC drug contents results from the stability study.

CSIC films were stored for 12 months in 30°C/65% RH and 6 months in 40°C/75% RH as per ICH guidelines. Data presented as Mean ± SD (n>3)

Table 4 Dissolution of CSIC film over the time frame of stability study.

No change in terms of cumulative drug release at 10 minutes was observed compared with time zero. Data presented as mean ± SD (n=3).

	30°C/65%	40°C/75%
1 M	53.7±5.0	55.5±2.0
2 M	51.9±0.5	44.1±5.4
3 M	52.9±4.5	57.9±4.4
6 M	50.1±5.9	53.7±14.4
9 M	45.1±2.1	
12 M	52.5±8.7	

Taken together, these results have demonstrated the safety property of the film product. The stability study showed that CSIC film should have a minimal shelf life of 12 months. The stressed temperature/humidity condition had negligible effects on film properties over a period of 6 months.

3.4 DISCUSSION AND CONCLUSION

Vaginal film formulation is a mixture of drug substances and excipients that are safe for vaginal application. In general, the key components in film products include film forming polymers as base platforms and plasticizers for improved flexibility. In addition, other excipients could be used to achieve different objectives. For instance, in some cases, cosolvents can be utilized to improve drug solubility; enhanced film softness could be attained with humectants; and disintegrant can be employed to facilitate film disintegration. Polymers with variable mucosal adhesion properties might also be used to modulate film residence time on the surface of the vaginal mucosa.

In terms of film forming polymers, numerous polymers can be used, which include hydroxyethyl cellulose (HEC), polyvinyl alcohol (PVA), hydroxypropylmethyl cellulose (HPMC), poly(vinyl pyrrolidone) (PVP), and Carbopol® [162]. In the current CSIC film formulation, PVA and HPMC were selected. PVA was chosen since it is safe for vaginal preparations and is the base polymer used in the VCF product. In addition to the film forming characteristics, PVA can also be used as a lubricant and a viscosity-increasing agent with moderate mucoadhesive properties [162]. The lubrication effect might help improve user adherence since it can boost sexual pleasure. The increased viscosity and mucoadhesive function will allow the film to stay longer in the vagina which in turn may increase drug concentration in the cervicovaginal tissue and lead to an improved efficacy. Other than PVA, another film forming polymer HPMC was included. Previous *in vitro* release studies have shown that the utilization of HPMC resulted in an initial burst release of APIs from film formulations [36, 163]. The fast drug release, over half of the loaded drug detected in the dissolution medium within one hour, could be essential for the development of coitus-dependent regimens. Lastly, these two

film-forming polymers provide a hydrophilic matrix, in which drug particles can be uniformly distributed.

Another category of component involved in the CSIC film formulation is the co-solvent. Although the lipids, bile salts and BSA are present in the vaginal fluid, which can help dissolve CSIC, the majority of the fluid is water which will substantially restrict the amount of drug being dissolved [24]. Limited drug solubilization will impact the dissolution rate of CSIC in the vagina. Also, drug remaining in the vaginal lumen could be removed rapidly by mucus shedding and menses before drug permeation in the tissue. In this regard, co-solvents can be used in the formulation to increase drug solubility. In this chapter, a co-solvent system consisting of PEG 400, propylene glycol, and glycerin was employed for vaginal application. The three cosolvents enhanced water miscibility of CSIC. This increased miscibility could be due to the hydrogen bonding by their hydrophilic regions, and, simultaneously, disruption of water self-association by their hydrophobic groups [164]. In addition to the solubilization properties, these three agents also improved the flexibility and the manufacturability of the film as plasticizers. Without the presence of propylene glycol and glycerin, film products were found to be rigid and curly in early stages of investigation. Furthermore, glycerin also acted as a humectant, which absorbed moisture and enhanced film softness. Importantly, in addition to these physicochemical advantages, the three cosolvents are included in the FDA Inactive Ingredients Database and generally considered as safe for vaginal exposure.

Once all the excipients were chosen, drug-excipient compatibility studies were performed prior to film preparation. As film formulation is a solid dosage form, a compatibility study was conducted in solid state by monitoring the thermal events of CSIC using DSC. Even though a shift of CSIC's melting point to a lower temperature was observed for the CSIC-glycerin mixture

(Figure 11), the drug's bioactivity study has confirmed that the pharmacological properties of CSIC remained unchanged in the presence of glycerin (Figure 14). In conclusion, the results confirmed the compatibility between drug substance and the excipients investigated.

The dosing level of CSIC in the film formulation was determined based on the antiviral activity of CSIC ($EC_{50\text{-antiviral}}$ of 1 nM) and the dosing level used in DPV vaginal films (1.25 mg). Previous studies have shown that the EC_{50} of CSIC was about 1 nM (0.3 ng/mL). To achieve anti-HIV efficacy, it is assumed that the drug concentration in the local cervicovaginal tissue has to be 1000 time higher than its EC_{50}. Therefore, approximately 0.3 μg/mL CSIC was required for each dose. As the volume of vaginal fluid secreted every day in vaginal lumen is about 1 mL, at least 0.3 μg of CSIC has to be formulated in each unit of film. In case of DPV, 1.25 mg DPV was originally loaded in a vaginal gel formulation. The gel product was assessed in clinical trials and approved to be safe and well tolerated [165, 166]. The same dosing level was later applied in a vaginal film formulation (1.25 mg/film), which showed potent anti-HIV bioactivity in TZM-bl model and no toxicity to the innate microflora lactobacilli [36]. In light of these considerations, approximately 1mg CSIC per film was chosen as the target dose. It is however important to note that with the co-solvent system chosen, the current film formulation allow for a much higher dose of CSIC if needed [167]. Previous work conducted in our labratory has shown that up to 10 mg of CSIC can be dissolved and dispersed uniformly in each film unit using the current formulation platform.

To further optimize the film formulation, the amounts of glycerin and propylene glycol that could be applied were adjusted according to the characteristics of film products, manufacturability, and safety regulations. In terms of safety, previous studies have reported that the application of high doses of glycerin and propylene glycol in vagina or rectum resulted in

some adverse effects, such as epithelial damage, excessive mucosal fluid secretion and increased HIV infection risk [168, 169]. These side effects are mainly caused by the dehydration effect of the excipients. When glycerin and propylene glycol are used in high concentrations, the product becomes hyperosmotic and tends to absorb solvents from the surrounding tissues. For example, in the TFV gel study, when 20% of glycerin was used in the formulation, this high percentage of glycerin caused a high product osmolality (3111 ± 10 mmol/kg), which induced epithelial stripping [170]. In contrast, when the percentage of glycerin was reduced to 5%, gel's osmolality was reduced to 836 ± 11 mmol/kg and the adverse reaction of epithelial damage was absent. Therefore, for safety purposes, the percentages applied for propylene glycol and glycerin in any vaginal preparations have to remain low. In the optimized film formulation, the percentages of solvent PEG 400, propylene glycol and glycerin were set at 2.5%, 1%, and 0.5% respectively in order to avoid potential adverse effects.

In addition, osmolality of all the products needs to be monitored. Despite osmolality applies only to liquid or semi-solid dosage forms, in a biological environment, films will become a gel-like product upon contact with vaginal fluid and posse an osmolality. In the worst case scenario *in vivo*, if the gel-like product cannot be distributed rapidly in the vaginal lumen, local solute concentration will increase, which may create a hyperosmotic condition and cause toxicity. In order to avoid these potential adverse effects, the percentages of solvent PEG 400, propylene glycol, and glycerin in the optimized film formulation were kept low, and set at 2.5%, 1%, and 0.5% respectively. To confirm the safety properties, film induced osmolality was assessed. CSIC film was dissolved in 3 mL vaginal fluid simulant, and tested for osmolality using an osmometer. The volume was chosen since it was the minimal volume required to completely dissolve a 1" x 2" vaginal film. The resulting data showed that the osmolality of

CSIC film was slightly hyperosmotic (334±4.04 mOsm/kg) compared with normal vaginal secretions (260-290 mOsm/kg). Nonetheless, compared with the osmolality determined for the reduced glycerin TFV gel (<836±11 mmol/kg), CSIC film product was still considered as a safe vaginal product [170] .

After the film product was prepared, the physicochemical and biological properties of the CSIC film were thoroughly investigated. Fast drug release from film formulation was confirmed by rapid film disintegration (< 3 minutes) and drug dissolution (< 1h) (Figure 13). About 50% of drug being detected in the dissolution medium 10 minutes after film administration indicate a burst effect. The burst drug release could be contributed to the presence of detergent PEG 4000 because it has been reported to accelerate the disintegration and subsequent drug dissolution in a fast-release tablets due to its high molecular weight [171].

Water content retained in the CSIC film product was determined to be less than 10%. This amount of water ensured film softness and flexibility, on the other hand, warranted drug stability and film attributes over time. In addition, the bioactivity of film formulated CSIC was found to be comparable to CSIC API. This result suggests that the presence of target excipients and manufacturing procedures such as physical mixing and heating will not have any effect on the anti-HIV activity of the drug substance. Once all the favorable film characteristics were established, the stability study was carried out at 30°C/65%RH for 12 months and at 40°C/75%RH for 6 months. The physicochemical characterization performed at different time points during the stability study indicates that CSIC film remains stable with insignificant changes in its drug content, dissolution, bioactivity, and biocompatibility.

In conclusion, a co-solvent system consisting of PEG400, propylene glycol and glycerin was utilized to disperse CSIC uniformly in a water-soluble film dosage form. Using a solvent

cast technique, a thin, soft and flexible CSIC film was manufactured. The film formulation was found to be stable physicochemically and biologically for at least 12 months. The developed film formulation has potential for use with other hydrophobic drugs.

4.0   DEVELOPMENT OF CSIC NANOCRYSTAL FORMULATION FOR HIV PREVENTION

4.1   INTRODUCTION

Currently, 40% of the new chemical entities (NCEs) generated through drug discovery programs are poorly water soluble [48]. Poor solubility usually results in a low dissolution rate and erratic absorption at the desired site of action. One approach emerging to overcome these issues is the preparation of nanocrystal formulations. Drug nanocrystals are nano-sized pure drug particles stabilized by stabilizing agents [162]. When the drug nanocrystals are suspended in liquid dispersion media, they are termed as nanosuspensions. Unlike the well-known polymeric nanoparticles, the stabilizing agents in nanosuspensions cannot form any carrier structure. Therefore, the pure drug particles are not encapsulated in carrier systems.

Drug nanocrystal formulation presents numerous advantages compared to other nanosystems. First of all, this formulation strategy can be applied as a universal approach to address formulation issues associated with poorly water soluble drugs. Additionally, nanocrystal formulations have been administrated via different routes, such as orally, intravenously, and topically for hydrophobic drugs [172-174]. Furthermore, nanocrystal formulations can be prepared by manufacturing processes currently used in the pharmaceutical industry. The cost of manufacturing is low and it can be easily scaled up.

Bottom-up precipitation methods and top-down technologies are the two standard approaches used for the production of drug nanocrystals in laboratory and pharmaceutical industry settings [175]. Bottom up technologies involve methods of assembly. They all start by dissolving drugs in solution, allowing the drug molecules to aggregate into particles with sizes in the nano-scale range. Specific technology under this category include micro- or nano-precipitation/solvent replacement, pharmaceutical hydrosol, and high-gravity controlled precipitation [176].

In comparison, top-down technologies can be classified as disintegrating methods, which generate nanosized materials by wet bead/pearl milling (NanoCrystal® techonology) or high pressure homogenization (HPH) [177]. These processes have been applied to successfully formulate poorly water soluble drugs and bring them to the market, for example, Rapamune® (sirolimus), Emed® (aprepitant), Tricor® (fenofibrate), and Megace ES® (megestrol acetate).

Recently, a combination of the bottom-up and the top-down approaches have been developed to further improve the technology [178]. For instance, the NANOEDGE™ technology by Baxter relies on the combination of a micro-precipitation step with a subsequent annealing step. This annealing step converts thermodynamically unstable materials into a more stable, well oriented lattice structure, and prevent the growth of the precipitated nanocrystals [179]. Another example of the combination technology is the smartCrystal® technology owned by Abbott, which is a series of combination processes tailor-designed for each specific drug and application [180, 181]. Examples of the smartCrystal® technology include H 42 (spray-drying and HPH), H 69 (cavitation-precipitation and HPH), and H 96 (freeze-drying and HPH) [177, 182]. Using this technology, the particle size of the drug crystals can be reduced to smaller than 100nm. This reduction in particle size will lead to a significant increase in saturation solubility and extremely fast dissolution [182].

Previously, nanocrystal formulation has been used to prepare a long-acting injectable product containing hydrophobic NNRTI rilpivirine (TMC278)[183]. TMC278 nanocrystals with a particle sized of 200nm were manufactured by wet milling. After a single injection (intramuscularly or subcutaneously), drug released sustainably from the formulation over 3 months in dogs and 3 weeks in mice.

In studies described in this chapter, a bottom up technology, nanoprecipitation, was applied to prepare a CSIC nanocrystal in order to improve its saturation solubility. Physicochemical properties, bioactivity, and stability of the CSIC nanocrystal were thoroughly evaluated. In addition, macrophages, as one of the most important target cells for HIV infection, have been utilized in the present work to assess the rate of cellular uptake. The mechanism of nanocrystal uptake was also studied using a series of pharmacological inhibitors.

In this dissertation, CSIC nanocrystals were not intended for active lymph node targeting. Instead, the desirable physicochemical properties of the nanocrystals were designed for sufficient tissue penetration and drug exposure in the interstitium. Therefore, the migration of the nanocrystals from interstitium to the draining lymph nodes was a result of passive delivery. If CSIC nanocrystals can get into the lymph nodes, theoretically, they can be internalized by all types of antigen presenting cells including macrophages, dendritic cells, langerhans cells, and B lymphocytes. Studies using macrophages were first conducted since macrophages are the key cells in recognizing micro/nanoparticles, and efficient uptake by macrophages would ensure desirable drug delivery outcome [184-186]. Even though macrophage was the only cell line being investigated in the present work, further studies using other antigen presenting cell lines, especially the dendritic cells (langerhans cells) will be warranted.

4.2   MATERIALS AND METHODS

4.2.1   Materials

CSIC was synthesized by Dalton Laboratories (Toronto, ON, Canada) with a purity of >98%. CSIC existed in fine powder with molecular weight of 334 g/mol. Hydroxypropyl methylcellulose E5 (HPMC E5) was obtained from Dow Chemical Company. Pluronic® F98 Prill was purchased from BASF. 3mL Thermo Scientific™ Slide-A-Lyzer™ dialysis cassette with a molecular weight cut off (MWCO) at 3.5K was purchased from Fisher Scientific for in vitro release study. Mouse macrophage cell line J774A.1 was generously provided by Dr. Kerry

Empey from the School of Pharmacy, University of Pittsburgh. Lisamine[TM] Rhodamine B 1,2-Dihexacanoly-sn-Glycero-3-phosphoethanolamine, Triethylammonium salt (rDHPE) and Vybrant® DiO cell labeling solution were purchased from Invitrogen. Pharmaceutical inhibitor mannan, filipin, and chlorpromazine were purchased from Sigma-Aldrich. Pharmaceutical inhibitor cytochalasin D, nocodazole, amiloride, and amiloride were obtained from Fisher Scientific. Sucrose was purchased from Spectrum.

4.2.2 Methods

4.2.2.1 CSIC nanosuspension and nanocrystal preparation

CSIC nanosuspension was manufactured using a nanoprecipitation method named three phase nanoparticle engineering technology [30, 187]. 12 mg CSIC was physically mixed with 4.5 mg surfactant Pluronic® F98 and 75 mg polymer HPMC E5. The mixture was then completely dissolved in organic solution methylene chloride (16mL) and ethanol (8mL). By applying nitrogen gas on the top of the solution, the drug and stabilizers (F98 and HPMC E5) were co-precipitated while solvent evaporation. The sample was then placed in a vacuum oven overnight to remove the residual organic solvents. The precipitate was re-hydrated in 15 mL 5% sucrose solution (w/v) for 0.5h followed by 1h sonication using probe sonicator. The liquid nanosuspension obtained was then lyophilized to obtain solid CSIC nanocrystals.

4.2.2.2 LC/MS analytical methods

For the quantification of CSIC, samples were injected into an ultra-high performance liquid chromatography (UHPLC) which equipped with a triple quad mass spectrometer and an atmospheric pressure chemical ionization probe. CSIC was separated from excipients by Thermo Scientific BDS hypersil C8 150x4.6mm column. Mobile phases consisting of A: 5mM ammonium formate buffer in 60% acetonitrile and B: 5mM ammonium formate buffer in 80% acetonitrile was used at a flow rate of 1mL/minute. A gradient method was programmed to start with 100% mobile phase A, and gradually switched to 100% mobile phase B by the end of 1.5 minutes, maintained at B for 2 minutes, and returned back to mobile phase A for the rest of the run till 6 minutes. 20uL of each drug-containing sample was injected, and a negative single reaction monitoring (SRM) scan was applied to monitor the ionization pathway of CSIC from 330 to 290 Dalton. A standard curve was obtained in the rage of 0.1-500 ng/mL.

4.2.2.3 Physicochemical characterization

Particle size and surface charge

Hydrodynamic particle size (Z-average) of CSIC nanocrystals were measured using a Malvern Zetasizer Nano ZS (Malvern Instruments, Massachusetts) equipped with a back scattering. Nanosuspension or reconstituted nanocrystals were diluted 10 times in deionized water for optimal measurements. The diluted samples were loaded in the standard disposable "polystyrene" cuvettes for dynamic light scattering (DLS) measurement. All the samples were analyzed in triplicate at 20°C.

Same instrument was used to determine the surface charge (zeta potential) of CSIC nanocrystals. Samples prepared for the DLS measurement were transferred to folded capillary cells for charge analysis. At least three measurements were made for each sample.

Drug Content

The CSIC in the nanosuspension was extracted by 40% acetonitrile. Samples were vortexed for 10 minutes, followed by centrifugation at 14,500 rpm (14,100 xg) for 5 minutes using a eppendorf MiniSpin® plus centrifuge. Drug presented in the supernatant was determined by LC/MS method as described above.

Nanocrystal Morphology by Transmission Electron Microscopy (TEM)

CSIC nanosuspensions with different concentrations were freshly prepared by logarithmic dilution in deionized water. Samples were then placed onto 200-mesh formvar carbon-coated copper grids, and negatively stained with 1% uranyl acetate. All images were acquired by JEM-1011 TEM (JEOL, Ltd, UK).

Crystalline properties of CSIC nanocrystals by differential scanning calorimetry (DSC)

To confirm the crystalline properties of CSIC in the nanocrystal formulation, DSC analysis was performed for CSIC nanocrystals, as well as physical mixture and the co-precipitates in comparison with free drug CSIC, Pluronic® F98, HPMC E5, and lyophilized

cryoprotectant sucrose. As melting points can only be observed for crystalline materials, any change to the melting endotherm indicated a transformation of drug CSIC. The thermography was obtained using DSC 1 STAR[e] system (METTLER TOLEDO) by heating samples form 25-350°C at a rate of 10°C per min with a constant nitrogen purge at 50.0 mL/ minute.

In vitro release

Drug dissolution studies were performed using Distek dissolution system 2100c equipped with Distek syringe pump, Disteck TCS 0200C water bath system and Evolution 4300 dissolution auto-sampler. Nanosuspension was injected into a Slide-A-Lyzer dialysis cassette with a 3.5K MWCO. Phosphate-buffered saline (PBS) at both pH 7.4 and pH 4.2 were prepared as dissolution medium in order to investigate drug release profiles at different pHs. Further, as vaginal fluid simulant (VFS) is more biorelevant compared to buffered solutions. In vitro drug release in VFS was also investigated. In detain, VFS was prepared as previously reported: 3.51 g/LNaCl, 1.40 g/L KOH, 0.222 g/L $Ca(OH)_2$, 0.018 g/L bovine serum albumin (BSA), 2 g/L lactic acid, 1 g/L CH3COOH, 0.16 g/L glycerol, 0.4 g/L urea and 5 g/L glucose [24]. The pH of PBS and VFS solutions were adjusted to either 7 or 4.2 by adding 0.1N NaOH or HCL. Cremophor® RH 40 was added to the dissolution media at a final concentration of 0.1% to increase the solubility of CSIC. Additionally, a volume of 500 mL dissolution medium was used to maintain a sink condition. Samples were collected at 0.5, 1, 2, 4, 8, 12, 24, 36, 48, 72, 96, and 120 h. Drug contents in each sample were determined by the developed LC/MS method.

4.2.2.4 *In vitro* bioactivity

    Direct antiviral activity was carried out using P4R5 indicator cells. P4R5 cells express the gene sequence of receptor CD4, co-receptors CCR5 and CXCR4, and β-galactosidase reporter. To test the direct anti-HIV activity of CSIC nanocrystals, P4R5 cells were incubated simultaneously with HIV-1 p24 and serially diluted CSIC nanosuspension for 48h. Afterward, the extent of HIV infection was determined using a single replication cycle assay as previously described [188].

4.2.2.5 Stability studies

    Stability studies of CSIC nanocrystal in terms of particle size were performed in both liquid and solid forms. In the liquid state, freshly prepared nanosuspension was stored at ambient temperature for 7 days. Prior to size analysis, the nanosuspension was vortexed for 5 seconds to re-suspend the contents. To test its stability in the solid state, the nanosuspension was immediately lyophilized following preparation to remove water. At the end of 1 month, 2 months, and 5 months, the solid nanocrystals were reconstituted and diluted in water as described in section 4.2.2.3. Particle size was then determined by dynamic light scattering (DLS) using a Malvern Zetasizer Nano ZS.

4.2.2.6 Mechanism of cellular uptake of CSIC nanocrystals by macrophages

The involvement of energy dependent pathways

As the application of a much lower temperature (4°C) has been reported to block energy dependent processes such as endocytosis [189], an uptake study was performed at both 4°C and 37°C to investigate their involvement during the process of nanocrystal intracellular uptake. Mouse macrophage-like J774.A cells were seeded in 12 well plates at a density of 1.5×10^5 cell/mL. Cells were cultured overnight to achieve a 50% confluence. On day 2, macrophages were treated with CSIC nanosuspension (5μg/mL, 2ml) and placed in either a cell culture incubator (37°C) or a refrigerator (4°C). At 5, 15, 30, and 60 minutes, the drug containing solution was removed from cells. Cells were then lysed using 1% Triton in PBS, physically scraped from the plates, and stored at -20°C for future analysis. The CSIC that was internalized by macrophages was quantified by LC/MS. The amount of cellular protein presented in each well was determined by BCA protein assay in order to normalize the drug uptake. Similar studies were also conducted for the free drug. 0.1% DMSO was utilized to disperse the hydrophobic CSIC in aqueous cell culture medium.

Mechanism study using pharmacological inhibitors

The uptake mechanism for CSIC nanocrystals was investigated using various pharmacological inhibitors which include: phagocytosis pathway inhibitor mannan (200 μg/mL) and cytochalasin D (10 μg/mL); clathrin dependent pathway inhibitor sucrose (150 mg/mL), chlorpromazine HCL (10 μg/mL) and nocodazole (10 μg/mL); caveolae dependent pathway inhibitor filipin (1 μg/mL); and micropinocytosis pathway inhibitor amiloride (100 μg/mL).

Specifically, cells were pretreated with each inhibitor for 0.5-1h. Subsequently, the inhibitors were replaced by 5 μg/mL CSIC nanosuspension (200 μL) and cultured for 1h. Cells were then washed by PBS and lysed for drug content analysis. The amount of cellular protein in each well was also determined as described above in order to normalize the drug uptake. It is important to note that the concentration and incubation time applied for each inhibitor were pre-determined to assure ≥70% cell viability. Adjustments were made as needed.

4.2.2.7 Cell imaging

Transmission electron microscopy (TEM)

To confirm the internalization of drug nanocrystal by J774A.1 cells, cells were first incubated with CSIC nanosuspension (5μg/mL) for 1h. The cells were then washed by PBS and fixed in cold 2.5% glutaraldehyde in 0.1M PBS. After being rinsed, cells were fixed in 1% Osmium Tetroxide with 1% potassium ferricyanide. Subsequently, cells were rinsed again in PBS, dehydrated through a graded series of ethanol, and embedded in Epon. Semi-thin (300 nm) sections were cut on a Reichart Ultracut, stained with 0.5% Toluidine Blue and examined under light microscope. Then, ultrathin sections (65 nm) were cut, and stained with uranyl acetate and Reynold's lead citrate. Sections were examined on Jeol 1011 TEM.

Live cell imaging by confocal microscope

To visualize the cellular uptake of CSIC nanocrystals, this nanomaterial was labeled with a red fluorescent dye rDHPE, while, and the viable macrophages were labeled with a green

fluorescent probe Vybrant® Dio cell-labeling solution [150]. The CSIC/rDHPE hybrid nanocrystals were prepared by mixing the dye with the drug and the stabilizers prior to dissolving in the organic solvents. J774A.1 macrophages were incubated with Vybrant® Dio solution (0.5%, v/v) in DMEM for 20 minutes. Afterward, the staining medium was removed, and the cells were washed by fresh, warm DMEM three times (10 minutes for each wash). Then, specimen was placed under a confocal microscope. Images of planes at various depths within the cells (0.5 μm per step) were collected as baseline for 3-D reconstitution. Subsequently, CSIC/rDHPE hybrid nanocrystals were applied. More optical images of the cells were captured every 2 minutes for the first 1h, and every 5 minutes for the following 3h using a Nikon A1 confocal microscope, 488 nm (Vybrant® Dio) and 562 nm (rDHPE) laser excitations, and a 60x objective.

4.2.2.8 Statistical analysis

All results were presented as the mean ± standard deviation (SD). Pairwise differences were determined by Student's t test. A *p* value <0.05 was considered statistically significant. Two-way ANOVA with Bonferroni test was applied for *in vitro* release study since two independent variables time and dissolution medium were involved (GraphPad Prism 5).

4.3   RESULTS

4.3.1   Physicochemical characterization

The nanocrystal particle size (Z-average) weighted by intensity was determined to be 243 nm. The Polydispersity Index (PdI) of the sample was less than 0.3 (Figure 16), which indicates a narrow size distribution in the CSIC nanocrystal formulation. As shown in the graph, the sample was monomodal with only one peak. Additionally, CSIC nanocrystals were slightly charged at -7.8mV. Drug concentration in the CSIC nanosuspension sample was analyzed by LC/MS and quantified to be 0.8 mg/mL.

The crystal morphology of CSIC nanocrystals was also observed under TEM (Figure 17). CSIC nanocrystals resembled long rods with smooth edges, which were quite similar to that of free drug substance described in chapter 2 (Figure 6). Upon series dilution, no change was observed in the morphology of the nanocrystals.
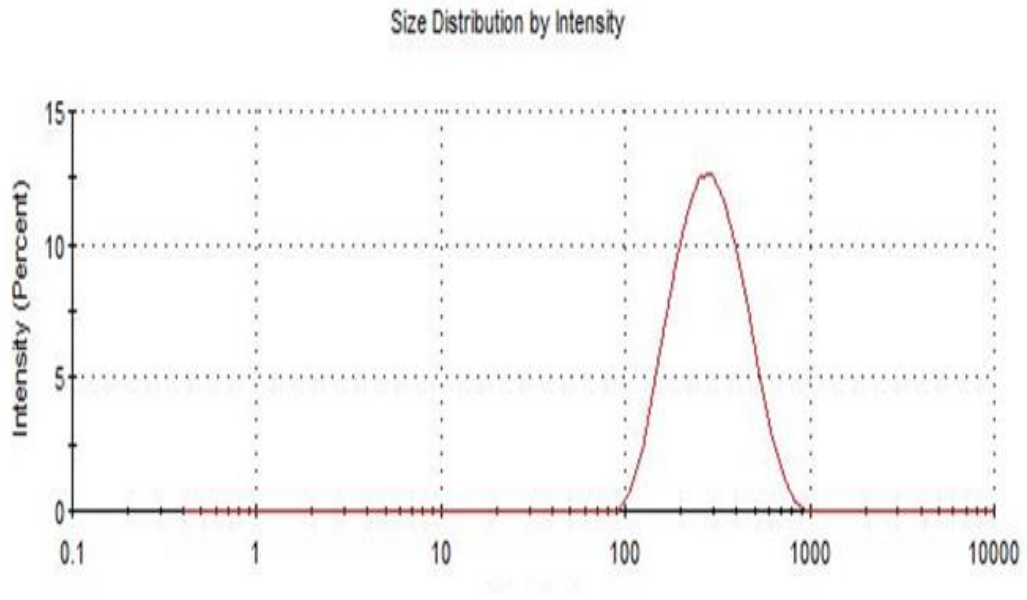
Figure 16 Particle size distribution of CSIC nanocrystals determined by dynamic light scattering. Particle size distribution was presented by intensity.
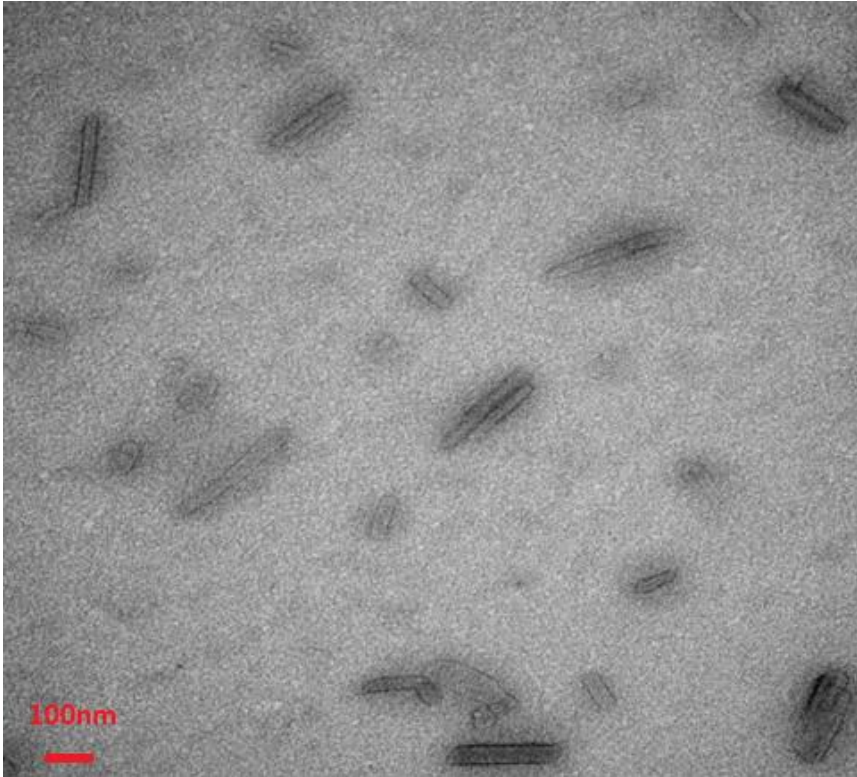
Figure 17 The morphology of CSIC nanocrystal observed under TEM.

CSIC nanocrystals resembled long rods with smooth edges. The morphology of the nanocrystals was quite similar to that of free drug substance. Upon series dilution, no change was observed in the morphology of the nanocrystals.

The crystalline property of CSIC within each stage of preparation was monitored by its thermal behavior (Figure 18). It was found that the melting point of CSIC was observed at 252 °C in the physical mixture, while, no endothermic peak for the drug substance was detected for the co-precipitate sample. This change indicated that CSIC formed amorphous precipitates with the stabilizers during the process of rapid solvent evaporation. More interestingly, the missing melting peak of CSIC re-emerged in the final nanocrystal products (278 °C) when the co-precipitates were hydrated in the aqueous solution which suggested the recrystallization of the drug during the process of probe sonication.
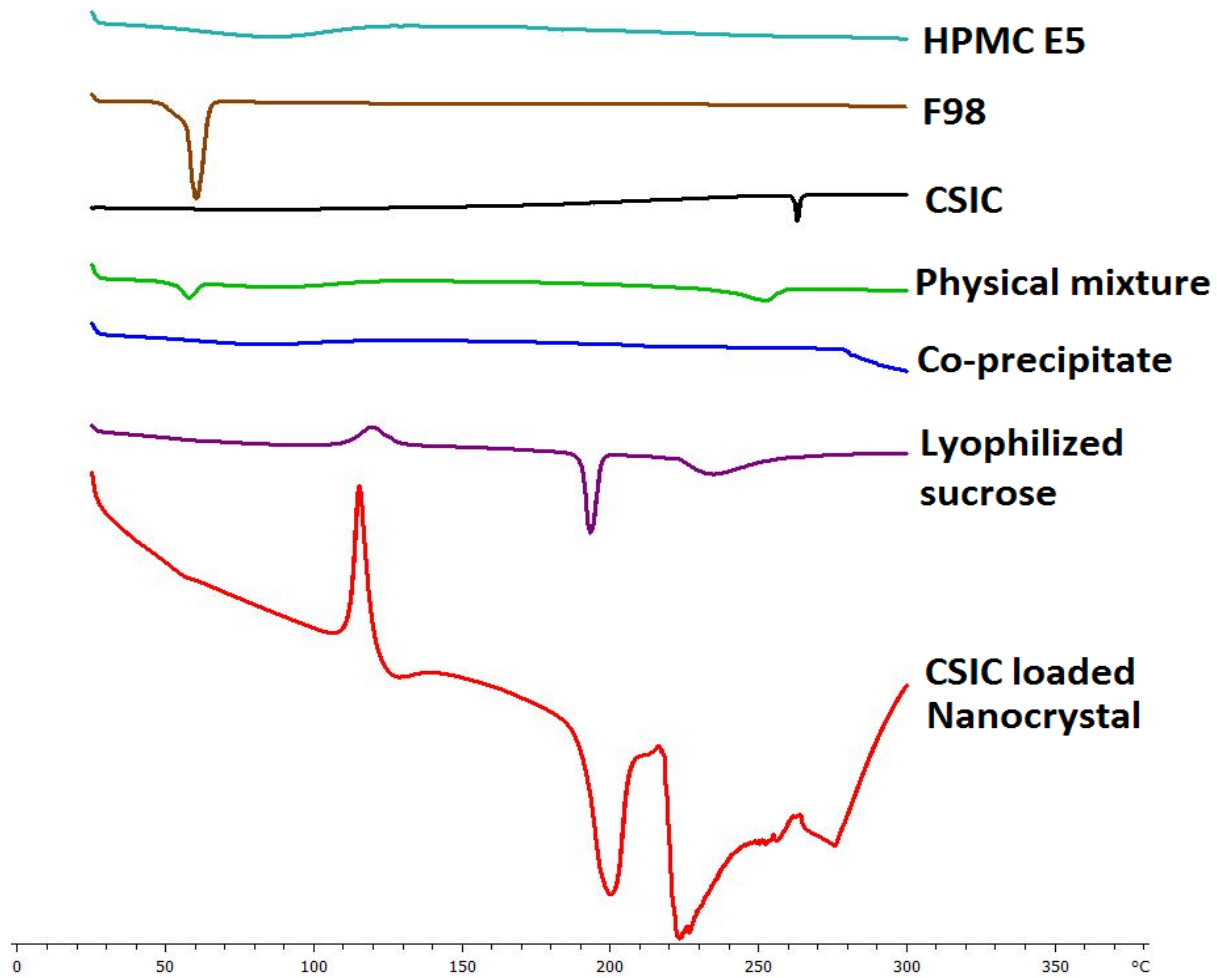
Figure 18 Thermal behaviors of each stabilizer, drug CSIC, drug/stabilizer physical mixture, drug/stabilizer co-precipitate, lyophilized sucrose and CSIC nanocrystals.
Thermal behaviors were assessed by DSC. Samples were heated from 25-350 °C at a rate of 10°C per min. The results have shown that the melting points of CSIC remained unchanged for the physical mixture, but disappeared for the co-precipitate sample. The missing melting peak of CSIC re-emerged in the final nanocrystal products (278 °C) when the co-precipitates were hydrated in the aqueous solution.

In vitro drug release studies were conducted in both PBS (pH 7.4) and VFS (pH 4.2) using a USP-I Distex instrument. CSIC was released continuously from the nanocrystal formulation in a linear fashion for 96 h (Figure 19). Approximately 90% of the drug was recovered by the end of the experiment. A zero order kinetics model can be used to describe this release profile with a dissolution rate of 0.11 µg/min ($R^2 > 0.97$). Even though the percentage of drug release from CSIC nanocrystals in PBS dissolution medium was found to be higher than the corresponding ones in the VFS dissolution medium at 36h and 72h ($p<0.05$), the overall trends of release in these two dissolution media are very similar.
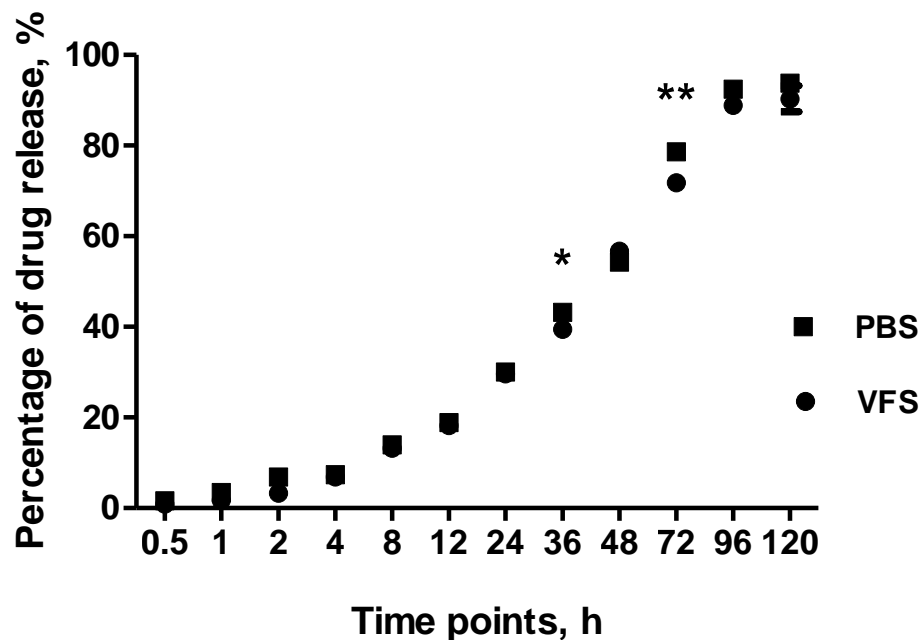
Figure 19 *In vitro* **release profiles of CSIC from CSIC nanocrystal formulation in vaginal fluid simulant (VFS, pH 4.2) and phosphage-buffered saline (PBS, pH 7.4) respectively. Dissolution study was conducted using Distek dissolution system 2100c equipped with Distek syringe pump, Disteck TCS 0200C water bath system and Evolution 4300 dissolution auto-sampler. Nanosuspension was injected into a Slide-A-Lyzer dialysis cassette with a 3.5K MWCO. At 36h and 72h, the percentage of drug release from CSIC nanocrystals in the PBS group was significantly higher than the VFS group (Two-way ANOVA, Bonferroni test, *p<0.05, **p< 0.001) (n=3).**

4.3.2 *In vitro* bioactivity study

In the bioactivity study, P4R5 HIV indicator cells were treated with CSIC nanosuspension or CSIC API at various concentrations. Drug concentration versus HIV survival percentage

profiles were plotted for both test articles. The bioactivity of CSIC nanocrystals was found to be

identical to that of the free drug substance (Figure 20) and caculated to be 1nM. This result

suggests a limited effect of the stabilizers and the nanotechnology on CSIC's bioactivity.
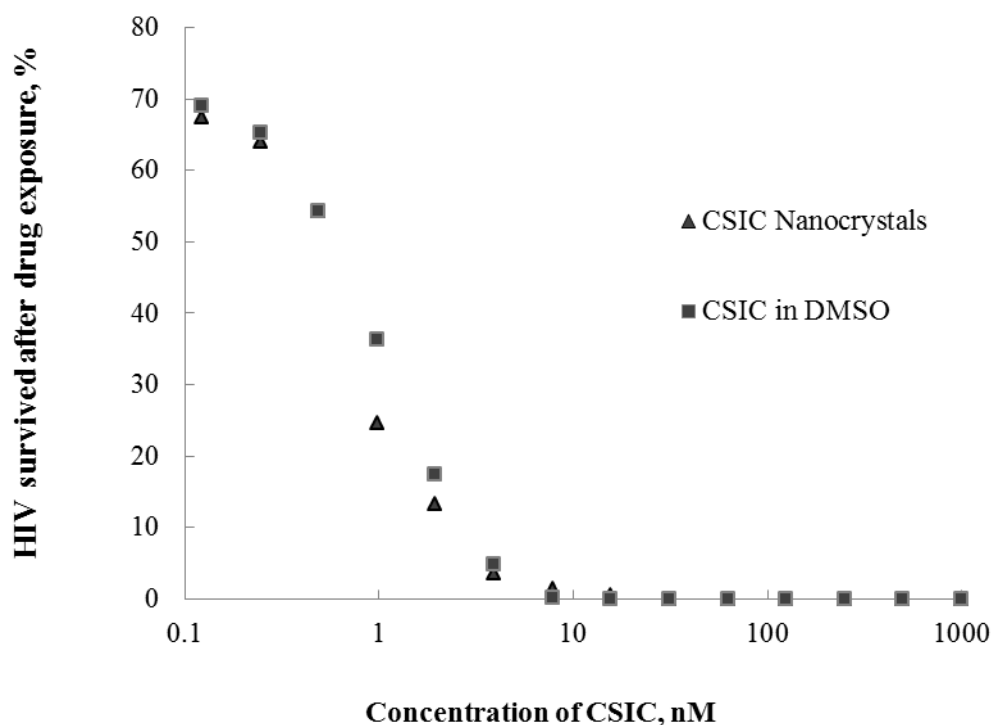
Figure 20 Antiviral activity of CSIC nanocrystals compared to the free drug substance.

HIV was incubated with CSIC free drug or CSIC nanocrystals at different concentrations. After 48h of incubation, the infectivity of HIV-1 was determined using a single replication cycle assay. The inhibition effect of CSIC nanocrystals was determined to be identical to that of free drug substance. (n=1)

4.3.3   Stability study

In the stability studies, particle size of the nanosuspension/ nanocrystals was monitored over time in both lipid and solid form. In the liquid state, the particle size was found to be stable for at least 7 days. After lyophilization, particle size of the solid CSIC nanocrystals is stable for a period of 5 months in a desiccator at room temperature. In all cases, particle sizes were maintained at 230 nm with a narrow size distribution (PdI <0.3) (Table 5).

Table 5 Stability of CSIC nanocrystals in both liquid and solid states.

The particle sizes of CSIC nanocrystals in liquid and solid states were monitored for 7 days and 5 months respectively. (n=3)

	Time points	Z-Average, nm	PdI
In liquid state	T0	217.0±6.9	0.24
	7 days	238.0±2.4	0.22
In solid state	T0	227.9±0.2	0.22
	1M	232.0±2.4	0.22
	2M	233.0±2.6	0.24
	5M	244.6±1.4	0.22

4.3.4 Intracellular uptake by macrophage cell line J774A.1

It is well known that low temperature (4˚C) can block the energy dependent pathways involved in endocytosis. By comparing the uptake profiles of test articles at 37°C and 4°C, the existence of energy dependent endocytosis during the process of intracellular uptake can be determined. In the case of CSIC nanocrystal, its cellular internalization uptake was significantly inhibited by the low temperature (4°C) compared with the physiological temperature (37°C), especially at earlier time points. Five minutes after drug exposure, the amount of CSIC nanocrystal internalized at 4°C was only 42.4% of that at 37°C (Figure 21a). In contrast, the amounts of free drug internalized at 4°C at 5 minutes accounted for about 80% of the drug internalized at 37°C ((Figure 21b). These results thus indicated the involvement of energy dependent pathways while the intracellular uptake of CSIC nanocrystals. As lower temperature could also decrease the diffusion coefficient, most likely the free drug molecules entered the macrophage via simple diffusion. The reduction in API's uptake was a result of a decreased diffusion coefficient at lower temperature.

(a)
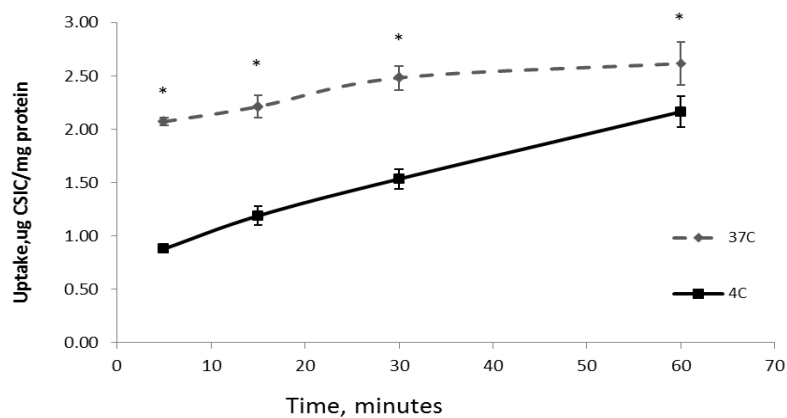
(b)
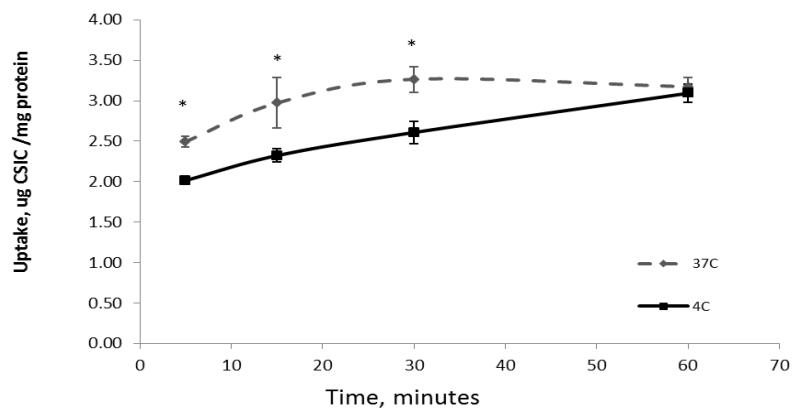
Figure 21 The intracellular uptake of nanocrystal and free drug substance at 37°C and 4°C for a period of 1h.
Intracellular uptake of (a) CSIC nanocrystals and (b) free drug. Uptake was reported as ug of CSIC per mg of total cell protein. The amount of cellular protein presented in each well was determined by BCA protein assay in order to normalize the drug uptake. Pairwise differences were determined by Student's t test. A *p* value <0.05 was considered statistically significant. * denotes significant difference (p<0.05) when comparing the amount of cell uptake at 37°C to 4°C. (n=6)

To further understand the mechanism of nanocrystal uptake by J774A.1 cells, seven pharmacological inhibitors were applied individually to block specific endocytosis pathways prior to drug exposure. Any diminution of nanocrystal internalization after certain treatment reflected the involvement of the typical pathway targeted by that inhibitor [190] .

Mannan and cytochalasin D are the inhibitors specific for phagocytosis pathway. Mannan competes with the test articles on mannose receptors expressed on the surface of antigen presenting cells such as macrophages and dendritic cells. Cytochalasin D disrupt the F-actin filaments necessary for phagocytosis [191]. As shown in Figure 22, the use of these two inhibitors did not reduce the uptake of nanocrystal. This result might suggest that the phagocytosis pathway is not involved in the process of nanocrystal internalization.

In addition, sucrose, chlorpromazine, and nocodazole, all clathrin mediated inhibitors, were also evaluated for uptake pathways. Sucrose induces hypertonicity, which prevents the assembly of clathrin-coated pits [192]. Chlorpromazine inhibits the formation and budding of clathrin-coated pits [193]. Nocodazole inhibits endosome-lysosome trafficking by interfering with the microtubule network causing microtubule depolymerization.

In the cellular uptake mechanism study, sucrose (150mg/mL), a pharmacological inhibitor for clathrin mediated endocytosis, was found to reduce the cellular uptake of CSIC nanocrystals substantially. Nonetheless, the inhibition effect of sucrose might be complicated by the fact that sucrose (50mg/mL) was used in the CSIC nanocrystal formulation as a cryoprotectant. Thus, other clathrin mediated inhibitors have to be investigated as well. The result has shown that the uptake of CSIC nanocrystals was also impeded by another two clathrin mediated inhibitors chlorpromazine and nocodazole. Taken together, we can conclude that clathrin-mediated endocytosis was actively involved in the process of cell uptake.

Moreover, filipin, which perturbs cholesterol functions, was also applied to inhibit the caveolae-mediated pathway [194]. However, after its treatment, no significant effect on nanocrystal uptake was observed, revealing a caveolae-independent process.

Furthermore, macropinocytosis inhibitor amiloride which impede the function of Na+/H+ exchange protein was tested [193]. The application of this inhibitor had no impact on the extent of internalization. Thus, macropinocytosis was not involved in the cellular uptake of nanocrystals either. Overall, these results indicated that the uptake of CSIC nanocrystal is mediated predominately by clathrin-mediated endocytosis, at least in the J774A.1 cells (Figure 22).
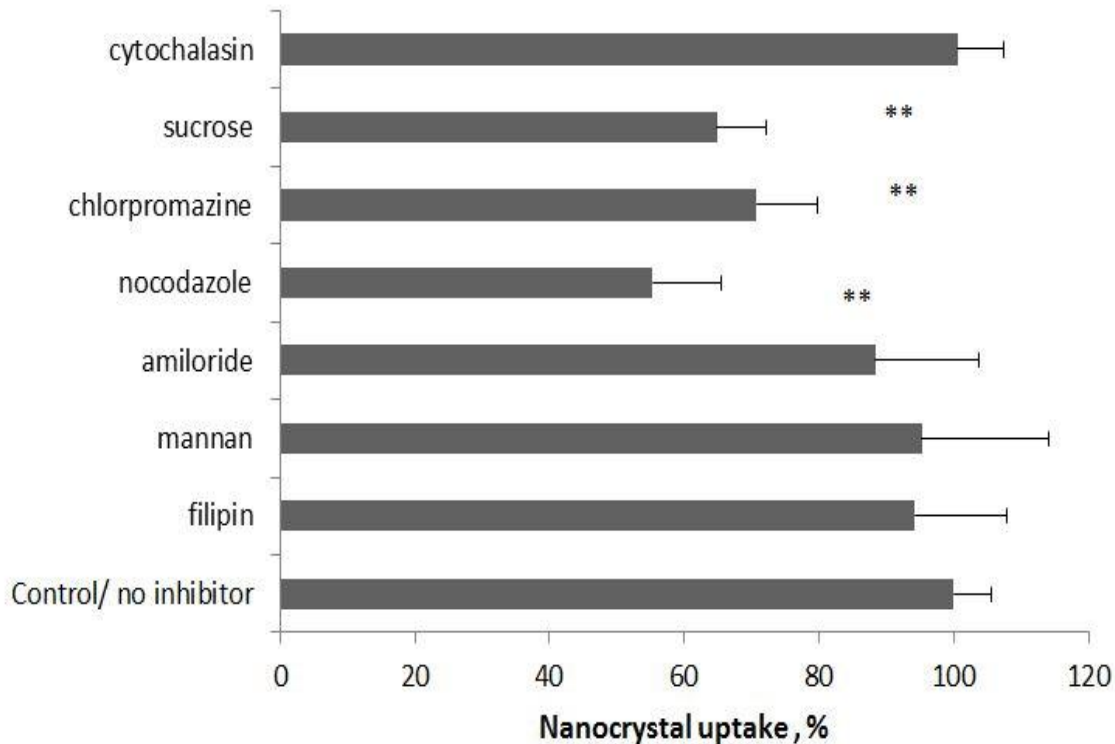
Figure 22 The impact of pharmaceutical inhibitors on cellular uptake of CSIC nanocrystals in macrophage cell line J774A.1.

Various pharmacological inhibitors were applied to investigate the mechanism of nanocrystal cellular uptake: phagocytosis pathway inhibitor mannan (200 µg/mL) and cytochalasin D (10 µg/mL); clathrin dependent pathway inhibitor sucrose (150 mg/mL), chlorpromazine HCL (10 µg/mL) and nocodazole (10 µg/mL); caveolae dependent pathway inhibitor filipin (1 µg/mL); and micropinocytosis pathway inhibitor amiloride (100 µg/mL). Macrophages were pretreated with each inhibitor for 0.5-1h. Subsequently, the inhibitors were replaced by 5 µg/mL CSIC nanosuspension (200 µL) and cultured for 1h. Cells were then washed by PBS and lysed for drug content analysis. The amount of cellular protein in each well was also determined as described above in order to normalize the drug uptake. Pretreatment with clathrin mediated inhibitors sucrose, chlorpromazine, and nocodazole inhibited the uptake of CSIC nanocrystals in J774A.1 cells compared with the control group with no inhibitor intervention.

4.3.5 Cell based imaging

In the imaging studies, both TEM and confocal microscopes were utilized to confirm the internalization of CSIC nanocrystal by macrophages. In Figure 23, CSIC nanocrystal determined by TEM was outlined in a red rectangle. Drug nanocrystal was present in the cytoplasm of the macrophage with a particle size of 250 nm. A similar finding was obtained by confocal microscopy in a real time fashion using rDHPE/CSIC hybrid nanocrystals. As shown in Figure 24, 15 minutes after drug exposure, nanocrystal uptake could be easily observed. CSIC nanocrystals first accumulated on the surface of the cell membranes presented as a round circle. Afterwards, drug nanocrystals penetrated the cytoplasm and merged with the cytoplasm marker Vybrant® Dio.
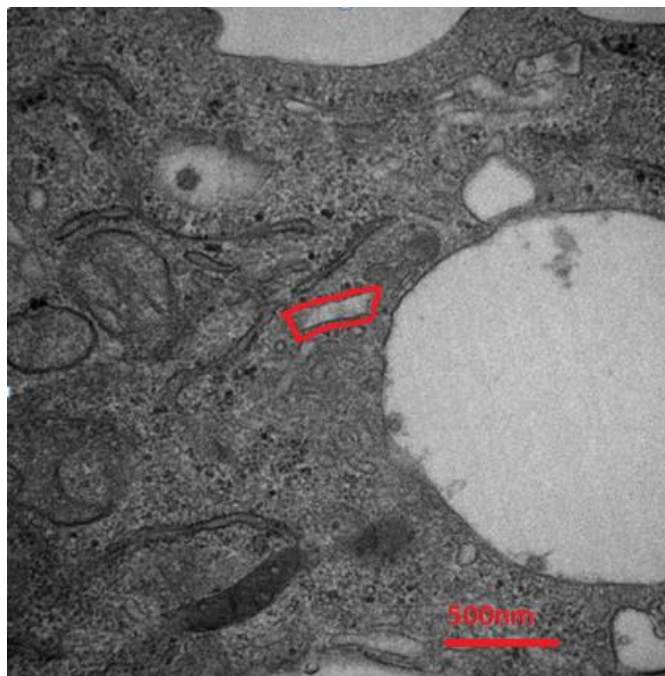
Figure 23 Cellular uptake of CSIC nanocrystals by TEM.

Drug nanocrystals could be readily identified by shape as outlined in red. Cell samples were embedded in Epon and cut into ultrathin sections (65 nm). Sections were then stained with uranyl acetate and Reynold's lead citrate, and examined on Jeol 1011 TEM.
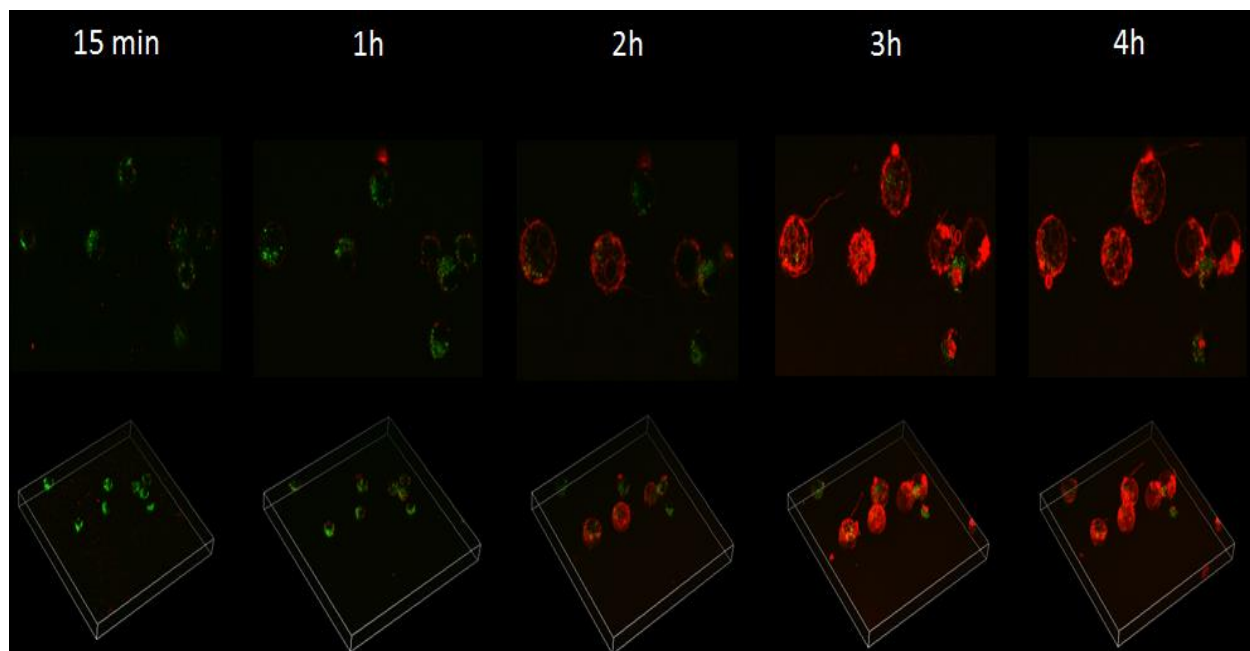
Figure 24 Cellular uptake of rDHPE/CSIC hybrid nanocrystals over a period of 4h.

Live cells were labled in green using a green fluorescent probe Vybrant® Dio cell-labeling solution and rDHPE/CSIC hybrid nanocrystals were presented in red.The images in the top panel were collected from one optical section at different time points, and the bottom ones were the reconstructed 3-D model from the Z-stacks. Images of the cells were captured every 2 minutes for the first 1h, and every 5 minutes for the following 3h using a Nikon A1 confocal microscope, 488 nm (Vybrant® Dio) and 562 nm (rDHPE) laser excitations, and a 60x objective.

4.4   DISCUSSION AND CONCLUSION

During the process of nanocrystal formulation development, the biggest challenges were the choice of the right stabilizers and the appropriate concentrations. In general, a desirable stabilizer needs to be amphiphilic. The hydrophobic segments can interact with hydrophobic drugs via hydrophobic interactions, while the hydrophilic segments can interact with the aqueous medium via hydrogen bonding. To date, stabilizers that have been successfully employed in nanocrystal formulations include the polymers HPMC, PVA, and HPC, and the surfactants Pluronics and sodium lauryl sulfate. In the current study, the class of Pluronics was chosen since it has been previously used to stabilize paclitaxel nanocrystals which was manufactured by the same method as CSIC nanocrystals [195]. In addition, as Pluronics are hydrophilic and neutral charged, these properties can help reduce their surface interactions with the hydrophobic or negatively charged segments in cervicovaginal mucin structures. As a consequence, the application of Pluronics could facilitate drug penetration through human cervicovaginal mucus [61, 196]. Furthermore, Pluronics are triblock copolymers composed of a hydrophobic poly(propylene oxide) (PPO) chain in the center and flanked by two uncharged hydrophilic PEG chains. When the molecular weight of the hydrophobic segment PPO is higher than 3 kDa [196], the large section of PPO will allow sufficient interactions with hydrophobic drug CSIC and stabilize the nanocrystal system sufficiently. In light of these findings, among many Pluronics, Pluronic F127, F108 and F98 were selected as candidates for the formulation development [196].

The concentrations of Pluronic were determined according to their critical micelle concentrations (CMCs). When the concentration goes beyond its CMC, the amount of surfactant monomers adsorbed on the surface of nanocrystals will be substantially reduced due to micelle formation. Thus, the concentration of the residual monomers that can physically separate the

nanocrystals will be much less than what we expect, making the nanocrystals prone to aggregation. According to the data provided by the manufacturer, the CMC of F127, F108 and F98 at 37°C are 0.011mg/mL, 0.012 mg/mL, and 0.36 mg/mL respectively. Therefore, Pluronic F98 at a concentration of ≤0.36 mg/mL was applied in this study.

Furthermore, from the stand point of lymph node drug delivery, the application of Pluronics can also reduce the non-specific interactions between the particle surface and the interstitium as shown by improved lymphatic uptake [197-199]. More importantly, this surface coating would not decrease drug retention in the lymph nodes [200].

To further stabilize CSIC nanocrystals and prevent them from agglomeration, another stabilizer was warranted. HPMC was selected in the current formulation since it is safe for vaginal drug application and it has been commonly used as a stabilizing agent or suspending agent. In addition, it has been reported that increased hydrophobicity of a stabilizer is correlated to a decreased tendency of nanoparticle aggregation [201]. Thus, among the HPMC family, HPMC E5 with a relatively high hydrophobicity (higher percentage hydrophobic methoxyl groups) was chosen to hinder the nanocrystal growth.

The size of the CSIC nanocrystal was set to be in the range between 200 and 500nm since it was ideal for vaginal drug delivery according to previous literatures [39, 202]. This size range would allow for sufficient drug loading even though much smaller nanoparticles (20-40 nm) could be internalized by the epithelial cells in the FRT efficiently and detected in the draining lymph nodes within one hour when administered vaginally [106]. Hanes et al. also reported that, compared with the 100nm nanoparticles, the larger ones (200nm and 500nm) with a dense surface coating by polyethylene glycol (PEG) could traverse the cervicovaginal mucus more efficiently [203]. In the current study, the target particle size of CSIC nanocrystals was achieved

by adjusting the time of probe sonication during the process of manufacturing. As confirmed by DLS (Figure 16) and TEM (Figure 17), it can be concluded that CSIC nanocrystals can be prepared with an optimal particle size using the current processing method. After preparation, sucrose was used as a cryopreservative to maintain the nanocrystal size during lyophilization. Based on the particle size determined by DLS (243 nm) and TEM, it can be concluded that CSIC nanocrystals can be prepared with an optimal particle size using the current processing method.

In addition, the prepared CSIC nanocrystals featured a slightly negative charge which may benefit vaginal drug delivery and lymphatic targeting. Since cervicovaginal mucus and interstitium are both negatively charged [204-206], the anionic nanocrystals might transport more rapidly in the mucus and drain well from the interstitial space due to electrostatic repulsion [94, 107].

The melting point of CSIC in the nanocrystal formulation was tested by DSC and was found to be similar to that of free drug (Figure 18). The preservation of drug crystal property could be beneficial since crystal structure is generally more stable compared to the amorphous forms.

The sustained release of CSIC from nanocrystals (Figure 19) suggests that drug nanocrystals act as a saturated drug reservoir, whereas, the stabilizers act as a semipermeable membrane maintaining a constant concentration gradient [207]. This finding is in line with a previous study in which a paclitaxel nanocrystal formulation was manufactured using the same preparation method as CSIC, and paclitaxel was released in a sustained manner from the nanocrystal formulation for over 72h [208].

To gain insights into whether nanocrystal technology can preserve or benefit the ability of CSIC to prevent HIV associated cell infection, the antiretroviral bioactivity of CSIC

115

nanocrystal was investigated. The result showed the high potency of CSIC in the nanocrystal formulation presenting an EC50 value at the same nanomolar level as free drug (1 nM, Figure 20). Formulating CSIC into a nanocrystal formulation did not hinder drug interaction with the cell membrane and its diffusion into the cells for enzyme binding.

Other than the physicochemical properties, intracellular uptake of the CSIC nanocrystal by macrophages was also explored and compared with CSIC API. Primary studies showed that both CSIC nanocrystals and the free drug could be readily internalized by macrophages. However, despite statistical analysis revealing that there is no significant difference between these two test articles, there was a trend for better uptake with free drug (Figure 21), which was unexpected. To better explain these results, comprehensive mechanism studies were conducted. By performing an uptake study at lower temperature (4°C), it was found that an energy dependent pathway was involved in the process of nanocrystal uptake but not for the free drug. The following study using the pharmacological inhibitors further proved that the clathrin-dependent endocytosis as the main pathway for the uptake of CSIC nanocrystals. In this regard, the application of cryoprotectant sucrose, a clathrin dependent inhibitor, might result in a reduced nanocrystal uptake even though the concentration of use (50mg/mL) in the formulation was only one third compared to that employed as an inhibitor (150mg/mL).

Another interpretation for the limited nanocrystal uptake could be described as orientation dependent particle recognition. A previous study has shown that the internalization of elliptical disk shaped particles (long 3-14μm, aspect ratio 2-4, thickness 400-1000nm) was highly dependent on the local particle shape at the point of initial contact on cells [209]. Specifically, when the cells approached along the major axis of the elliptical particles, the cell membrane showed marked progression on the particles. In contrast, if the cell contacted the flat/

116

long side of the particles initially, no engulfment would occur. In this regard, as CSIC nanocrystals possess a long rod shape that is similar to the elliptical dish, the reduced macrophage uptake could be explained by the undesirable angle of contact between nanocrystals and macrophages.

In addition, the utilization of Pluronic F98, a PEG containing stabilizer, might also impede the uptake of CSIC nanocrystals. To date, no study has investigated the effect of Pluronics as a stabilizer on nanocrystal uptake by macrophages. However, the presence of stabilizer (Pluronic®) on the surface of nanocrystals might play a similar role as the surface modifier Pluronic® employed in nanocarrier systems such as liposomes [210, 211]. In these nanocarrier systems, surface modification by PEG or Pluronics® has been utilized to prevent the polymeric nanoparticles from recognition and uptake by phagocytic cells [209]. Moreover, a higher PEG density would result in a less amount of cell uptake. Therefore, the application of Pluronic® in the CSIC nanocrystal formulation may also suppress nanocrystal recognition by macrophages and result in a decrease of drug uptake.

In the cellular uptake mechanism study, it was surprising that the application of phagocytosis pathway inhibitor mannan and cytochalasin D did not curb the intracellular uptake of CSIC nanocrystals. As the inhibitor concentrations and incubation times employed in the current investigation were determined according to previous literatures, these conditions might not be optimal for macrophage cell line J774A.1. Further experiments are warrant to rule out or confirm the involvement of phagocytosis pathway by using different experimental setting such as higher treating concentrations or longer incubation times.

To better visualize the localization of nanocrystals in cells, live cell imaging was conducted by confocal microscopy. Theoretically, Vybrant DiO solution is a cell membrane

marker which can be employed to outline the shape of the cell membrane. Once applied, however, the cell membrane marker entered into the macrophages rapidly prior to drug exposure and worked as a "cytoplasm marker". To overcome this barrier and confirm the intracellular uptake of CSIC nanocrystal, optical sections from cell specimens at specific plane of focus were collected. Nanocrystals were found to accumulate on the surface of the cell membrane presented as a round circle at the earlier time points, whereas the drug nanocrystals internalized were merged with the "cytoplasm marker" as shown at the later time points in Figure 24.

In the same imaging study, fluorescent dye phospholipid rDHPE was applied to trace the movement of CSIC nanocrystal. Because of its hydrophobicity, it was assumed that this dye is entangled with the hydrophobic segments of the stabilizers and, therefore, was in close contact with the CSIC nanocrystals. As the amount of tracer added was quite low, the use of rDHPE should have limited impact on the particle size, polydispersity, surface charge, and morphology of the CSIC nanocrystals. In addition, Kabanov's group has reported that the application of rDHPE as a tracer in nanocrystal formulation had no effect on drug uptake and *in vitro* drug release [212]. Overall, this is a promising approach to investigate the cellular uptake of CSIC nanocrystals.

In conclusion, a CSIC nanocrystal formulation was prepared by a nanoprecipitation method for vaginal administration. Drug nanocrystals were stabilized in aqueous solution using the surfactant Pluronic F98 and the polymer HPMC E5 with a particle size of 240nm and a near neutral surface charge. Drug released from the nanocrystals occurred in a controlled manner with no burst effect. Even though the CSIC nanocrystal formulation did not seem to increase the extent of drug uptake compared with free drug, it has been confirmed that CSIC nanocrystal might be rapidly internalized by macrophages via clathrin mediated endocytosis.

Acknowledgement

120

5.0 VAGINAL DRUG PERMEATION AND LYMPH NODE DRUG DELIVERY OF CSIC NANOCRYSTALS

5.1 INTRODUCTION

As discussed in Chapter 1, drug concentration in the cervicovaginal tissue is directly associated with anti-HIV efficacy after intravaginal administration. Therefore, it is critical to increase the drug exposure in the target tissue. In the last decade, nanocrystal technology has attracted great attention and has been applied in the field of transdermal and mucosal drug delivery since it has been reported to improve tissue penetration and retention [174, 177, 213, 214]. These favorable properties of nanocrystals are achieved through increased saturation solubility and larger concentration gradients at the site of biological barriers and membranes. In addition, nanocrystals exhibit increased bio-adhesiveness due to their large surface area [215].

Recently, hydrophobic antioxidants rutin and hesperidin were formulated as nanocrystals for dermal applications [213, 216]. The antioxidative capacity of the rutin nanocrystal formulation was investigated *in vivo* and compared to that of a water soluble rutin derivative, rutin-glucoside [217]. Interestingly, although the concentration of the dissolved rutin in the rutin-glucoside formulation (5%, w/w) was 500 times higher than that of the rutin nanocrystals (0.01%, w/w), drug bioactivity of the rutin nanocrystals was two times as much as the rutin-glucoside formulation, 59% versus 27%. This finding could be explained by the hydrophobicity

of the drug rutin, since hydrophobic molecules generally exhibit better penetration properties than hydrophilic molecules. Although glucosidation improved the drug's water solubility, it compromised its ability to penetrate tissue. In comparison, the rutin nanocrystals provided a supersaturated solution and an increased concentration gradient on the surface of tissue. The hydrophobicity of the drug molecule was also preserved in the form of a nano-sized pure drug particle, allowing sufficient drug permeation. Furthermore, the hydrophobic rutin has a higher affinity to the binding site in cells than the hydrophilic glucoside (Figure 25).
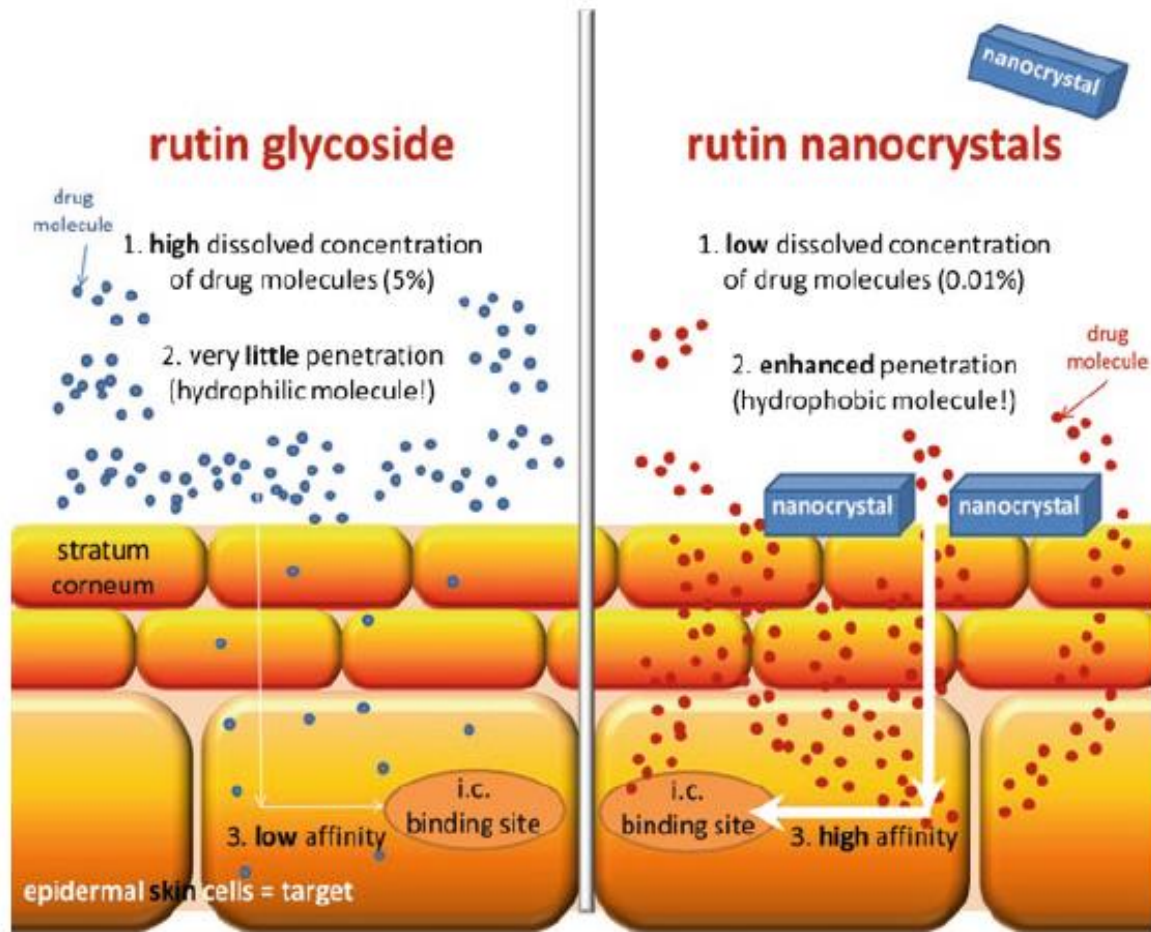
Figure 25 Mechanism of action for the enhanced dermal bioactivity of rutin nanocrystals.

Compared with rutin glycoside, rutin nanocrystals possess enhanced penetration properties because rutin is a hydrophobic molecule with high affinity to the binding site, even though its dissolved concentration is 500 times lower than that of the hydrophilic rutin glycoside.

In light of these findings, the CSIC nanocrystal formulation prepared in the Chapter 4 should display a favorable drug permeation property in the cervicovaginal tissue. This chapter will describe *ex vivo* tissue permeability studies and an *in vivo* pharmacokinetic study in mice that were performed to confirm this hypothesis. Tissue permeability studies were conducted with excised human cervical tissue. Excised human tissue features complete cell structures including epithelial, connective and immune cells [218, 219]. Human cervicovaginal tissue is commonly used in the field of microbicide to evaluate the permeation properties of antiretroviral drugs after vaginal administration [39, 155, 220]. In the current study, a flow-through diffusion system, in-line cell, was employed to study permeation of the hydrophobic drug CSIC (Figure 26). This diffusion system uses a perfusion fluid below the tissue surface to collect the permeating substance in the receptor chamber, which in turn helps maintain sink conditions throughout the experiment.
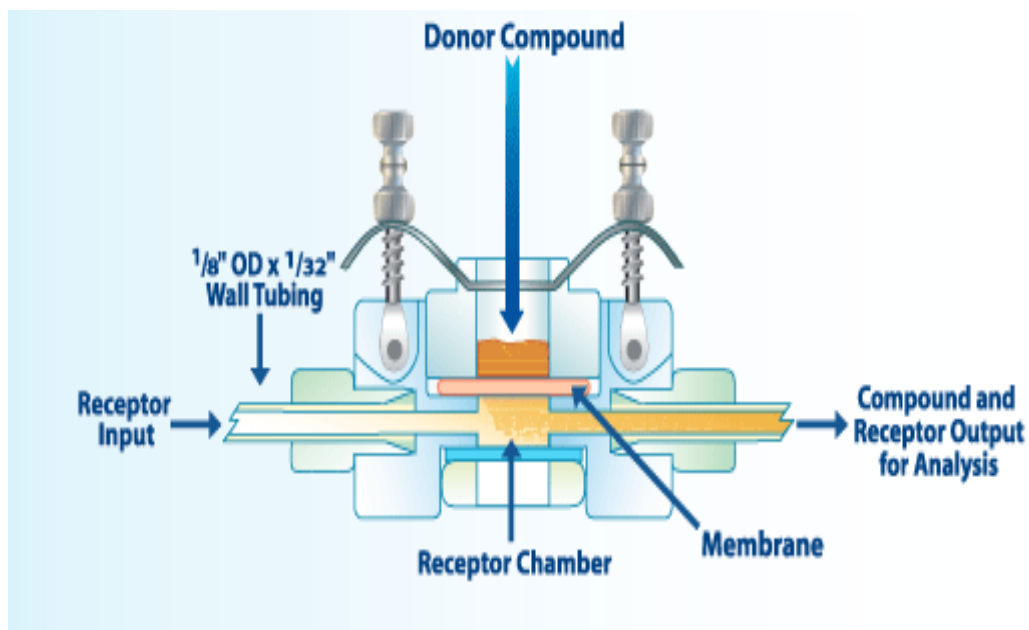
Figure 26 In-line cell for tissue permeability study.

In the current study, membrane was replaced by the explanted human cervicovaginal epithelium. CSIC nanocrystals or free drug were dispersed in DMEM and loaded in the donor chamber. Receptor medium was infused from the receptor input and collected from the receptor output by an autosampler.

An *in vivo* animal study was performed to gain insight into the permeation and biodistribution of CSIC nanocrystals after intravaginal instillation, especially their migration to genital lymph nodes. Genital lymph nodes play a critical role in the early stages of HIV-1 acquisition. Thus, it is beneficial to deliver drugs to both lymph nodes and cervicovaginal tissue in order to achieve improved drug efficacy. Through evaluation of drug distribution *in vivo*, evidence can be generated to confirm our hypothesis that improved tissue penetration can facilitate lymphatic trafficking. Previously, Dr. Byron Ballou's laboratory demonstrated the

migration of quantum dots (Qdots) from vaginal lumen to lumbar lymph nodes [105]. The same animal model which was used in that study was applied in this dissertation to investigate the pharmacokinetic profile of CSIC nanocrystals.

Prior to drug permeation in the tissue, cervicovaginal mucus is the first barrier following intravaginal administration. To target the underlying mucosal tissue, drug particles, either pure drug aggregates or drug containing nanoparticles, must first diffuse through the unstirred adherent layer of mucus. Previous study has points that drug nanocrystal with specific composition could facilitate drug particle transport in mucus [221]. Two mechanisms can contribute to the inhibition of particle diffusion across this mucus layer [222, 223]. The first is the interaction between particles and mucin induced by electrostatic and/or hydrophobic forces. Mucin is a group of highly glycosylated proteins. It is negatively charged because of the high content of sialic acid and sulfate [224]. The negative charge of mucin can attract positively charged nanoparticles via electrostatic force. In addition, mucins that exist in the ectocervical and vaginal epithelia contain some hydrophobic domains (lipid-coated, nonglycosylated, cysteine-rich domains), which can anchor lipophilic drug particles [225-227]. This hydrophobic interaction will hinder the movement of drug particles in mucus. The second mechanism is the size filtering effect due to the limited mesh spacing between the mucin fibers (340±70 nm) [227]. In Chapter 4, a CSIC nanocrystal formulation with particle size about 243nm and negatively charged surface was designed and prepared for rapid mucus penetration. The goal for this chapter was to verify this mucus penetration property by investigating the interaction between mucin and CSIC nanocrystals.

Plasma protein adsorption is commonly investigated for intravenously injected drugs. Although for this study CSIC nanocrystals were instilled intravaginally instead of intravenously,

it is still imperative to evaluate their plasma protein binding. Generally, plasma proteins tend to exhibit strong interactions with free drugs, especially those of hydrophobic nature, once they enter the blood circulation. In the case of nanoparticles, the different particle sizes and surface properties will have a significant impact on the extent of protein adsorption. As described by the Vroman effect, plasma proteins are competitive for a finite number of surface binding sites. The process of plasma protein adsorption and dissociation with nanoparticles are kinetic in nature. In this regard, varying incubation times will result in different adsorption profiles [210]. In this chapter, to investigate the effect of incubation time on the extent of protein adsorption, different time points were explored.

The overall goal of this chapter is to describe studies undertaken to investigate the penetration and distribution of CSIC nanocrystals by evaluating mucin-nanocrystal interactions, nanocrystal associated plasma protein absorption, drug permeation in human cervicovaginal tissues, and pharmacokinetics in a mouse model. As CSIC nanocrystals possessed the physicochemical properties desirable for mucus penetration, and nanocrystal formulations in general show enhanced tissue permeation, we expected to observe limited interaction between mucin and the CSIC nanocrystals, and an increased drug concentration in the cervicovaginal tissue compared with CSIC free drug. Genital lymph node drug targeting after nanocrystal treatment was therefore be anticipated.

5.2   MATERIALS AND METHODS

5.2.1   Materials

Bovine serum albumin (BSA) was purchased from Spectrum. Dulbecco's Modification of Eagle's Medium (DMEM) was obtained from Corning. Normal human plasma containing the anticoagulant citrate phosphate dextrose was obtained from Lee Biosolutions, Inc. Other chemical and reagents were of analytic grade or equivalent.

5.2.2   Methods

5.2.2.1 Nanocrystal-mucin interaction

Vaginal fluid simulant (VFS) was prepared as described above (section 4.2.2.3). Modified VFS was prepared by adding mucin at a final concentration of 1.5% (w/v), namely VFS/mucin [228, 229]. The pH of VFS and VFS/mucin solution were adjusted to either 7 or 4.2 by adding 0.1N HCl or NaOH. Nanosuspension (reconstituted CSIC nanocrystals) was then mixed with VFS/mucin solution (pH 7 or pH 4.2) at a ratio of 10:1. Similar samples were prepared in VFS at different pH values and compared as controls. Samples were then equilibrated in a 37°C water bath for 2h before particle size analysis. The particle sizes were determined by dynamic light scattering using a Malvern Zetasizer Nano ZS.

5.2.2.2 Plasma protein adsorption

In the current study, the total amount of protein adsorbed on the surface of free drug or CSIC nanocrystals was quantified by BCA protein assay. This method is highly sensitive and compatible with typical concentrations of most ionic and nonionic detergents. More importantly, the BCA assay is more accurate than the previously applied CBQCA assay because the color development reaction involved in the BCA assay for protein quantification does not require the detachment of the adsorbed proteins from CSIC nanocrystals [230].

To investigate the extent of protein adsorption, nanosuspension was mixed with the same volume of human plasma and incubated in a 37˚C water bath for either 5 minutes or 1h. Previous studies have shown that if nanoparticles can be recognized as foreign, they will be transported to the liver and spleen 5 minutes after systemic exposure [231]. Otherwise, these nanoparticles will show a prolonged circulation or time-dependent distribution in the body. Therefore, 5 minutes time point was selected as a standard and 1h was chosen as a representative extended time point. In addition, the sample-to-plasma ratio between drug and human plasma was optimized in preliminary studies in order to: (1) minimize the effect of lipids in human plasma on protein quantification, and (2) make sure that plasma proteins are in excess of the available nanoparticle surface area [230].

In detail, after incubation, samples were centrifuged at 15,000g for 30 minutes at 25˚C to separate CSIC nanocrystal from the majority of unbound plasma proteins. Afterwards, the sedimentary drug nanocrystal pellet was washed to remove the rest of the unbound proteins by three rounds of centrifugation (15,000g for 30 minutes at 25˚C) and resuspension in PBS containing 0.1 % v/v Triton X-100. In this washing step, a mild non-ionic detergent Triton X-100 was employed since CSIC nanocrystal-protein corona pellets cannot be re-suspended efficiently

in the standard washing solution PBS. The use of 0.1% w/v Triton X-100 was comparable to other washing solution such as 0.05% v/v Tween 20 [209]. It should not solubilize the bound plasma proteins. Preliminary study conducted in our laboratory also confirmed its limited impact on dissolving plasma proteins by quantifying the extent of protein binding with or without washing. More importantly, Triton X-100 at this concentration was found to be compatible with BCA assay (<5%). Its application would not affect protein quantification.

After washing, the residue pellets were then dispersed in 0.1 mL 0.1 % Triton X-100 and mixed with 2 mL working solutions prepared according to the Pierce BCA Protein assay protocol. The adsorbed protein reduced the copper (Cu^{2+}) in working solution to cuprous cation (Cu^{1+}) and the change was detected by BCA in solution. The amount of protein in each solution was quantified by UV-spectrophotometer at 562nm.

In comparison, to quantify the amount of protein adsorbed on the surface of free drug, all the procedures remained the same except the washing step. PBS was applied to wash off the unbound plasma proteins since the free drug pellet was easily re-dispersible.

5.2.2.3 Tissue permeability study

Excised human cervical tissues were obtained from the University of Pittsburgh Health Sciences Tissue Bank (Pittsburgh, PA) and the protocol was approved by University of Pittsburgh IRB #PRO09110431. Tissue samples were collected from healthy volunteers who were undergoing hysterectomy. Before the experiments, excess stromal tissue was removed to achieve a full thickness of epithelial layer. Tissues were set up in PermeGear In-Line Cells (7mm in diameter). Briefly, epithelial tissue was placed horizontally between the donor and receptor compartments with the epithelial side facing up. DMEM containing 1% BSA was used as the

receptor medium. The receptor medium was pumped through the receptor compartment via a coupled peristaltic pump at a rate of 50 μl/min. A fraction collector was used to collect samples from the receptor compartment. The whole system was warmed at 37°C to mimic biological conditions.

To increase the sensitivity of drug quantification, carbon-14 labelled (^{14}C) CSIC was spiked with regular CSIC. The drug mixture was then used to prepare radiolabeled drug nanocrystal and free drug samples. Free drug was uniformly suspended in DMEM containing 0.1% DMSO.

0.5ml of CSIC nanosuspension or CSIC free drug at a concentration of 800 μg/mL was loaded in each donor chamber respectively. At the end of the 8h experiment, tissues were removed from the in-line cells, and each one was cut into three pieces. One piece was sectioned consecutively using a cryostat into 100μm sections, and the amount of CSIC retained in each section was determined by liquid scintillation counter (LSC) (Beckman LS 6500 Multi-Purpose Scintillation Counter). One piece was digested directly for drug content analysis. The last piece was stained by Hematoxylin & Eosin (H&E) staining for histological evaluation of tissue morphology.

The flux (J) and the apparent permeability coefficient (Papp) of both CSIC nanocrystal and free drug were calculated based on the Fick's First Law of Diffusion, with the equations described below:

$$J = \frac{dM}{A\,d\,t} \qquad\qquad \text{(Equation 5)}$$

$$P_{app} = \frac{J}{C_d} * 60 \qquad\qquad \text{(Equation 6)}$$

130

Where, in Equation 5, M is the accumulated amount of drug collected in the receptor medium (counts per minute, cpm), A is the area of contact (cm^2), t is the time of exposure (min), dM/dt represents the slope of the curve of M versus t, and the units for J are $cpm/(cm^2*min)$. In the Equation 6, Cd is the initial dosing concentration, and the units for Papp are cm/sec.

5.2.2.4 *In vivo* drug distribution and genital lymph node drug delivery

All procedures used in the mouse drug distribution studies were approved by the University of Pittsburgh Institutional Animal Care and Use Committee (IACUC) (approval number 14114443). In general, 6 week old female Swiss Webster mice were purchased from Charles River Inc. Medroxyprogesterone (Depo-Provera) (3mg/animal, 60uL) was injected subcutaneously 7 days and 3 days prior to drug exposure. This intervention was applied in the field of microbicides and vaginal drug to synchronize the mice to the diestrous stage [105]. On the day of experiment, mice were first anesthetized in an induction chamber filled with 3% isoflurane-oxygen, and then transferred to a nosecone for continuous anesthetization by 1.5% isoflurane-oxygen. Radiolabeled free drug or CSIC nanocrystal was suspended in PBS (800 μg/mL) and then administrated by genital pipetting into the mouse vagina. After drug administration to the mice, anesthesia was maintained for one additional minute. Afterwards, the mice were removed from the nosecone, and physically restrained in 50 mL conical tubes individually for 20 minutes with their hindquarters elevated. These procedures were designed to reduce the extent of drug leakage from the mouse vagina.

At each predetermined time point after drug exposure (0.5, 1, 2, 4, 24, 48 and 72h), blood samples were collected from the submandibular vein. After the exsanguination, mice were exposed to carbon dioxide and euthanized by cervical dislocation. Vaginal fluid and adherent

131

mucus in the reproductive tract were collected by PBS lavage. Tissues or organs (lumbar lymph node, inguinal lymph node, vagina, ectocervix, endocervix, uterus horn, ovary, liver, kidney, and spleen) were harvested from each mouse and washed three times in PBS. After drying, all the samples were weighed, and digested for drug content using LSC.

5.2.2.5 The effect of Nonxynol-9 (N-9) pre-treatment on lymph node targeting

Nonxynol-9 (N-9), a well-known permeation enhancer, was applied to evaluate its effect on lymph node drug delivery. Similar studies were carried out using the same mouse model described in section 5.2.2.4. In detail, 12 h prior to drug exposure, 30 μl 1% N-9 were instilled intravaginally using the same approach as the test articles. Mice were then sacrificed 4h or 24h after drug exposure. Inguinal and lumbar nodes were collected for drug content analysis using LSC.

5.2.2.6 Statistical analyses

All results were presented as the mean ± standard deviation (SD). Pairwise differences were determined by Student's t test. $P < 0.05$ was considered as denoting significance unless otherwise stated. Two-way ANOVA with Bonferroni test was applied for *in vivo* pharmacokinetic study since two independent variables time and treatment were involved (GraphPad Prism 5).

5.3   RESULTS

5.3.1   Nanocrystal-mucin interaction

In this study, particle sizes of the nanocrystals under different equilibration conditions were determined. By comparing the sizes of the nanocrystals in the VFS and the corresponding VFS/mucin at the same pH, the potential mucin-nanocrystal interaction could be estimated [228]. At pH 4.2, the size of nanocrystals in VFS and VFS/mucin were found to be 256±36 nm and 282±14nm respectively. No significant difference was observed, indicating a limited mucin-nanocrystal interaction. Similar results were obtained at pH 7.4, and particle sizes were determined to be 266 ±31nm in VFS and 302 ±17nm in VFS/mucin.

5.3.2   Plasma protein adsorption

In this study, tested articles were incubated with human plasma for a certain period of time, and the total amounts of plasma protein adsorbed were quantified. After 5 minutes incubation, 429 ±40 μg/mL plasma proteins were adsorbed on the surface of the nanocrystals. In comparison, 769 ±164 μg/mL proteins absorbed on the surface of free drug particles. The 1 hour incubation gave similar findings: the protein concentrations in the nanocrystal treated and free drug treated samples were calculated to be 408 ±86 μg/mL and 639 ±38 μg/mL, respectively. In both scenarios, plasma proteins seem to have more interactions with free drug particles than CSIC nanocrystals.

5.3.3 Tissue permeability study

5.3.3.1 Flux (J) and apparent permeability coefficient (P_{app}).

As CSIC could be detected in the collected receptor medium all through the experiment for both CSIC nanocrystals and the free drug, their fluxes and the apparent permeability coefficients (P_{app}) were calculated based on the equations described in the methods section (Equation 5 and 6). The resulting data suggested no significant difference between the CSIC nanocrystal and free drug for both parameters. The flux of CSIC nanocrystals and the free drug were determined to be 7.3 ±5.2 and 6.6 ±3.4 cpm/(cm^2*sec) respectively (p=0.80). The P_{app} of drug nanocrystals was determined to be 3.2 ±2.3 X10^{-7} cm/sec as compared to 3.0 ±1.5 X10^{-7} cm/sec for the free drug (p=0.87).

5.3.3.2 Drug permeation in tissue

The purpose of this study was to investigate mucosal permeation properties of CSIC in nanocrystal formulation. Drug contents in the donor chamber (D_{end}), tissue wash solution, receptor chamber (R_{end}), explant tissue, and the collected receptor medium (cumulative collection) were analyzed and presented as percentages in the Table 6. Mass balance was also calculated by summing up drug contents in each compartment. As expected, the distribution of CSIC nanocrystals was significantly different from that of the free drug. In terms of mass balance, all the dosed CSIC nanocrystals could be recovered (97.4 ±3.84%), whereas only 77.4 ±7.99% of free drug could be collected. More CSIC nanocrystals remained in the donor chamber than the free drug (95.1 ±4.25% vs 67.0 ±7.06%). In contrast, substantially higher amounts of free drug were found in the tissues, tissue wash solutions, and the receptor chambers than the

CSIC nanocrystals. Specifically, in the tissues, drug concentrations for free drug and nanocrystals were calculated to be 281.3 ±71.1and 127.8 ±30.0 ug/g of tissue, respectively. In addition, the drug contents detected in the cumulative collections were found to be similar between these two test articles. This finding was consistent with the calculated flux and P_{app}.

Table 6 Drug distribution after an 8h permeability study using explanted human cervicovaginal tissues.
D_{end}: drug remained in the donor chamber in the in-line cell; Tissue wash: drug detected in the tissue wash solution; R_{end}: drug remained in the receptor chamber in the in-line cell. Tissue: drug contents determined in the cervicovaginal tissue. Cumulative collection: the amount of drug in the collected receptor medium. All the data are presented as mean±SD. ** indicated p<0.005. n≥5

Treatment	D_{End}, % **	Tissue Wash, %**	R_{End}, %**	Tissue, %**	Cumulative Collection,%	Mass Balance,%**
Nanocrystal	95.1±4.25	0.2±0.06	0.1±0.03	1.3±0.18	0.7±0.51	97.4±3.84
Free drug	67.0±7.06	5.4±2.58	0.4±0.16	4.0±1.05	0.7±0.33	77.4±7.99

Furthermore, to better understand the drug permeation profile, drug content in each tissue section from apical epithelium to basal stroma was quantitatively analyzed using LSC (Figure 27). It is evident that, for both CSIC nanocrystals and the free drug, the amounts of drug were highest in the topical 200μm-thick tissues which were mainly the epithelial cells, and gradually decreased in the underlying tissue sections. Similar trends were observed for both test articles, but much higher amounts were detected in the first 7 layers of tissue sections from the apical side after free drug exposure.
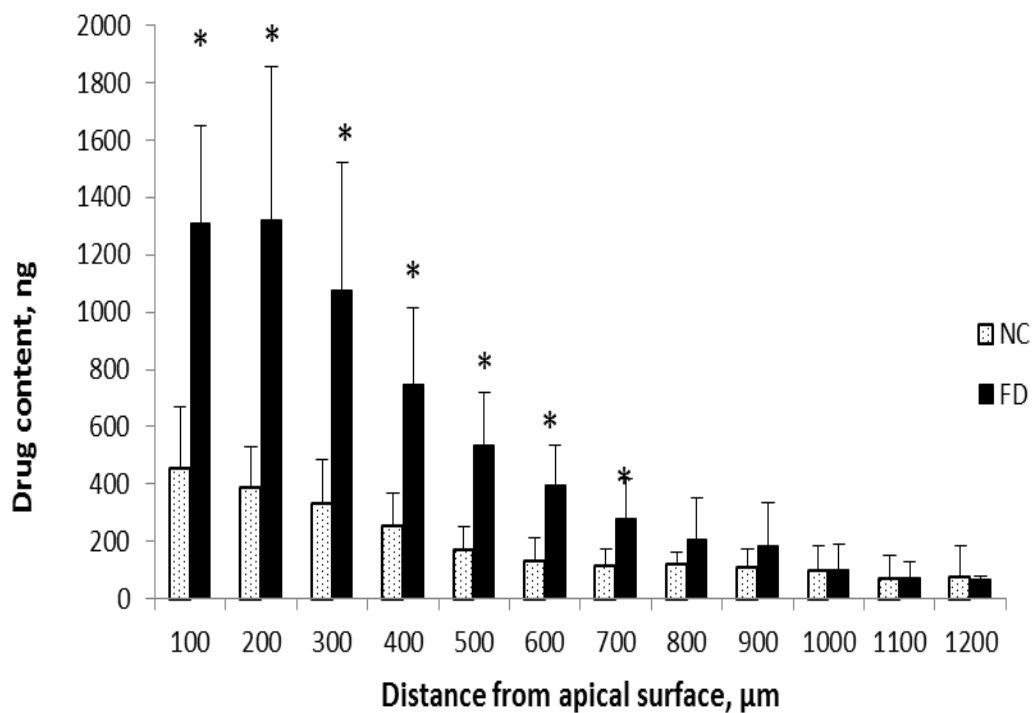
Figure 27 Drug content in per 100μm section of human ectocervical tissue from the apical epithelium to the stroma after 8 hour exposure.
For both test articles, drug contents in the tissue sections decreased from the superficial epithelium to basal layer stroma. Free drug substance was mainly accumulated in the epithelium (the top layers of tissue sections). Data is presented as mean ± SD.

5.3.3.3 Safety evaluation

In addition to the permeation study, a safety study was conducted to determine if test articles were safe for the epithelium in the female reproductive tract. CSIC nanocrystals or free drug in DMSO solution were exposed to human ectocervical tissue using an in-line cell system.

137

After 8h treatment, tissues were removed and stained for histological evaluation. H&E stained

tissue sections were presented in Figure 28. No gross changes in morphology were observed for

the tissues exposed to CSIC nanocrystals or free drug when compared to the pre-exposure tissue.

(a)   (b)   (c)
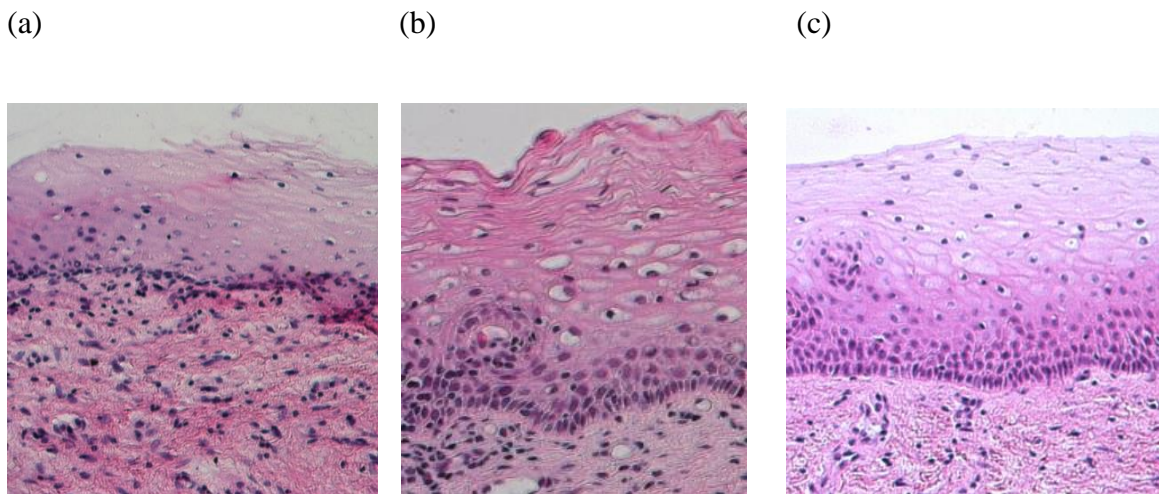
Figure 28 Representative H& E stained epithelium of human cervicovaginal tissue.

Representative histology pictures of (a) pre-exposure tissue, (b) tissue exposed to CSIC nanocrystals for 8h, and (c) tissue exposed to CSIC free drug for 8h. Nuclei of cells were colored by hematoxylin and presented in dark blue dots. Eosin was used to stain the cytoplasm in pink. The epithelia of the tissues were found to be intact, and the integrity of the tissue could be preserved after CSIC nanocrystals or free drug treatment. Micrographs were taken with a 20X objective. (n≥5)

5.3.4 *In vivo* pharmacokinetics and lymph node drug delivery

The goal of this study was to confirm that nanocrystal formulation can improve tissue penetration and, more importantly, deliver drug to genital lymph nodes, which would provide protection against HIV-1 transmission through multiple targets.

5.3.4.1 Drug distribution in the reproductive tract

After intravaginal administration of CSIC nanocrystal or CSIC API to mice, drug substances could be detected throughout the reproductive tract and presented a gradient pattern from the site of administration to the ovaries. Drug concentration in the tissue peaked at the earliest time point (0.5 h) and rapidly decreased afterwards. At 0.5h, nearly 7.3% and 1.2% of administrated nanocrystals were detected in the vagina and ectocervix, corresponding to 52% and 8.4% of the total amount recovered. As expected, substantially higher amounts of CSIC nanocrystals penetrated into the reproductive tract in contrast to the free drug, especially in the vaginal and ectocervical tissue (Figure 29). At 0.5h, drug contents in the mouse vagina for CSIC nanocrystals and free drug were found to be 23.8 ±6.64 µg/g and 2.2 ±1.46 µg/g respectively. In the ectocervix, 8.3±5.81 µg/g CSIC was detected 0.5h after nanocrystal treatment and 0.36 ±0.38 µg/g after free drug treatment. In addition, more CSIC nanocrystals were found in the uterine horn than free drug at 1h and in the ovaries at 0.5h.
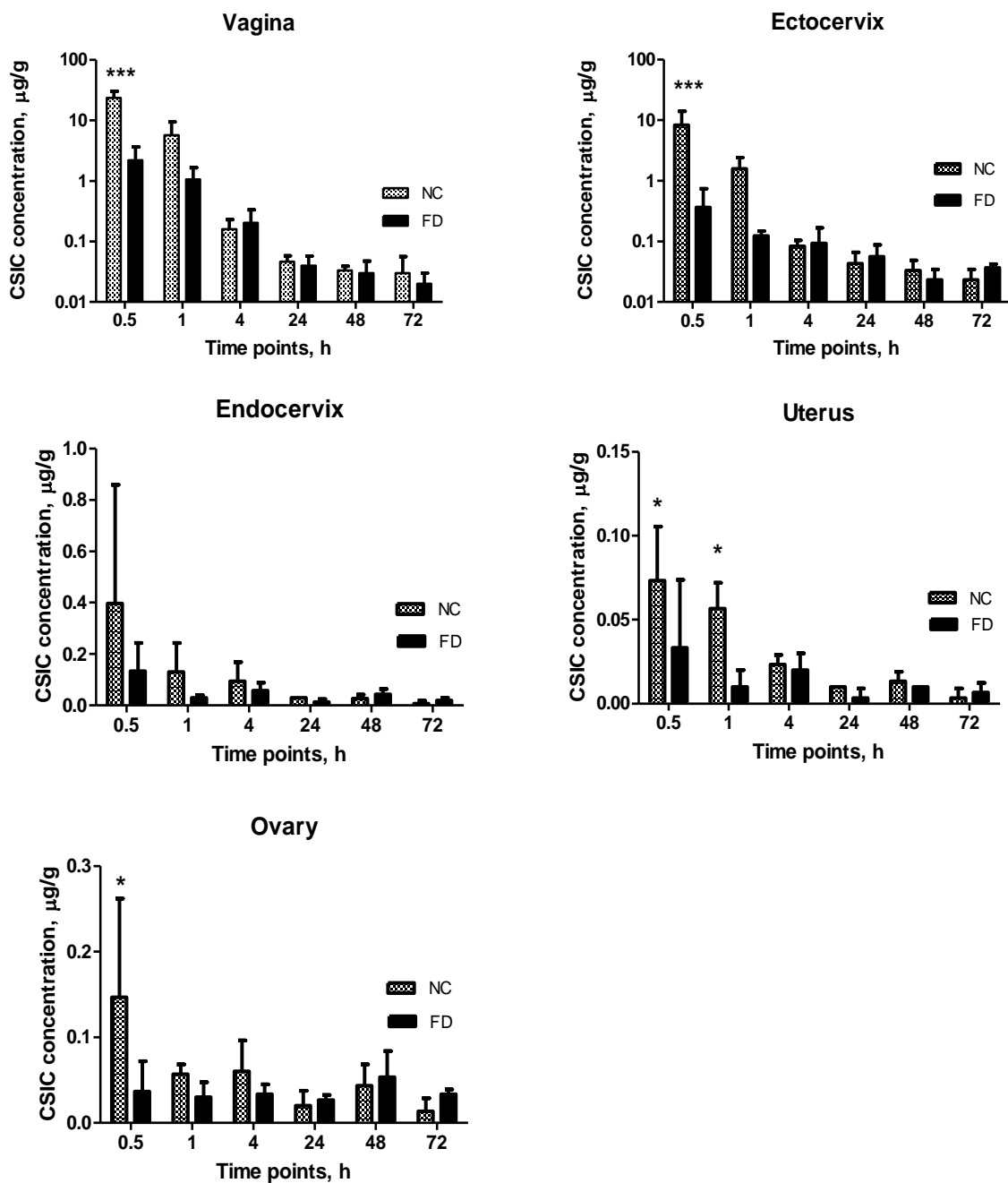
Figure 29 Drug distribution in the female reproductive tract in mice following intravaginal administration of CSIC nanocrystals (NC) or the free drug in PBS (FD).
Drug substance could be detected throughout the reproductive tract and presented a gradient pattern from the site of administration vagina to the ovaries after CSIC nanocrystals or free drug

treatment. Higher amounts of CSIC nanocrystals were detected in the vagina at 0.5h, ectocervix at 0.5h, uterus in the first 1h, and ovary at 0.5h. Note the different scales and units in y-axes, including the log-scale for vaginal and ectocervical tissue. Two-way ANOVA with Bonferroni test was applied for statistical analysis. * and * denote significant difference with p<0.05 and p <0.001 respectively between CSIC nanocrystals and free drug treatment. (n=3)**

5.3.4.2 Drug in the vaginal lavage

The amount of drug remaining in the vaginal lumen is estimated through assessment of the drug content in the collected vaginal lavage. By 0.5h, drug concentration in the lavage for CSIC nanocrystal treatment group was about 7.3 ± 11.3 μg/mL. Drug contents then rapidly decreased to 0.81 ± 0.5 μg/mL and 0.04 ± 0.02 μg/mL after 1h and 4h respectively (Figure 30). In comparison, even though there was no significant difference observed between CSIC nanocrystal treatment and free drug treatment. The free drug particles seemed to remain longer in the vaginal lumen.
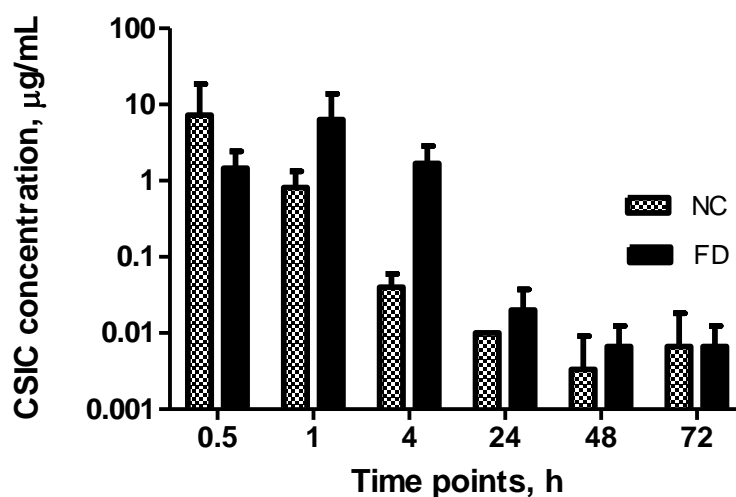
Figure 30 Drug remained in the vaginal lavage after intravaginal administration of CSIC nanocrystals or CSIC free drug.
No significant difference between these two test articles was observed in terms of drug content remained in vaginal lavage. Data is presented in log-scale. Two-way ANOVA with Bonferroni test was applied for statistical analysis. No significant difference was observed between CSIC nanocrystal and free drug. (n=3)

5.3.4.3 Systemic exposure

Drug exposure in the plasma and elimination organs, such as liver, kidney, and spleen were also determined (Figure 31). The application of CSIC nanocrystals resulted in a greater systemic exposure than the free drug. In the plasma, nanocrystal concentration was much higher than that of free drug during the first 24h. The peak value for CSIC nanocrystals was observed at 1h with a plasma concentration of 0.031 ± 0.005 µg/mL. As for liver, kidney and spleen, CSIC nanocrystals migrated to these elimination organs in a much faster mode with higher amounts of

drug exposure. The peak nanocrystal concentration was observed at 1h, while the peak concentration for CSIC free drug was detected at 24h. Among these three organs, drug exposure in the liver for both test articles was found to be higher at all times than that in the kidney, followed by the spleen, which might indicate a liver-mediated elimination. Moreover, the higher mount of drug exposure detected in spleen after nanocrystal treatment can be an indication for lymph node targeting since spleen is a primary lymphoid organ [232].
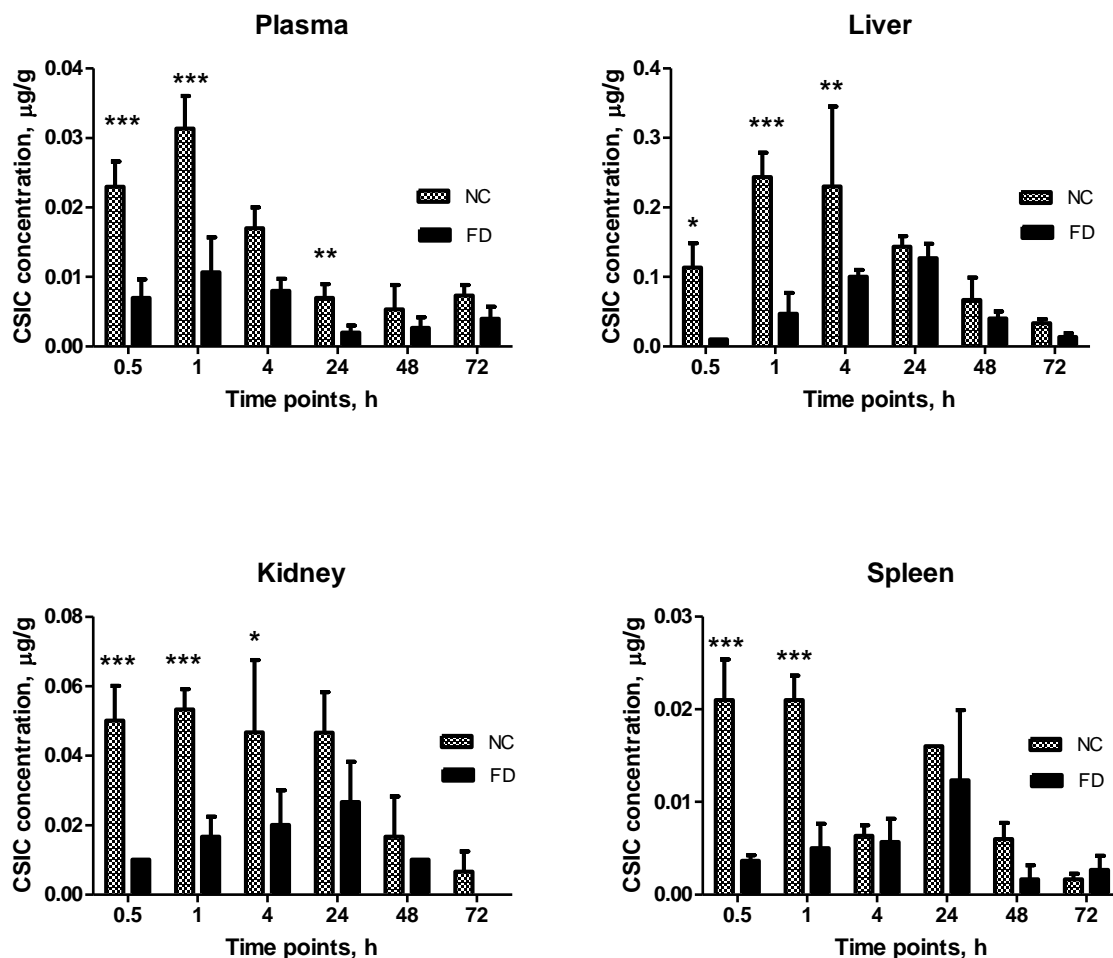
Figure 31 Systemic exposure to CSIC following vaginal administration of CSIC nanocrystals or the free drug.
For both CSIC nanocrystal and free drug treatment, drug substance could be detected in the blood and the elimination organs at the earliest time point (0.5h). Compared with CSIC free drug, higher amounts of CSIC nanocrystals were detected at 0.5, 1, and 24h in the blood, first 4h in the liver and kidney, and the first 1h in the spleen. Drug concentrations in the liver were found to be higher than that in the kidney and spleen which might indicate a liver-mediated clearance. Two-way ANOVA with Bonferroni test was applied for statistical analysis. *, ** and *** denote significant difference when comparing CSIC nanocrystal with free drug at the same time point with $p < 0.05$, $p < 0.01$, and $p < 0.001$. (n=3)

5.3.4.4 Lymph node drug delivery

Drug exposure in the genital lymph nodes was relatively low compared with that in the cervicovaginal tissue. No drug could be detected in the inguinal lymph nodes at all the time points for both test articles (Figure 32). In comparison, the nanocrystal formation was able to deliver antiretroviral drug CSIC to the lumber lymph nodes at 48h (Figure 32). However, as the amount of drug detected in the lymph nodes were very low, the quantification method available could not conclusively indicate the superiority of CSIC nanocrystals in terms of lymphatic targeting. Additionally, the application of permeation enhancer N-9 12h before treatment did not enhance lymph node drug delivery of CSIC nanocrystals or free drug at 4h and 24h (Data not shown).

145
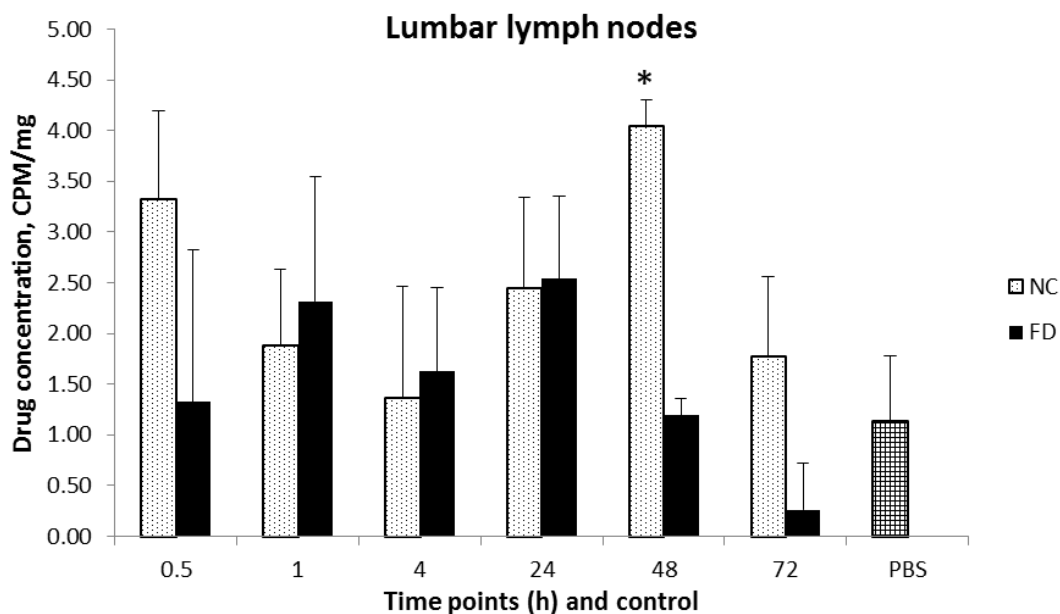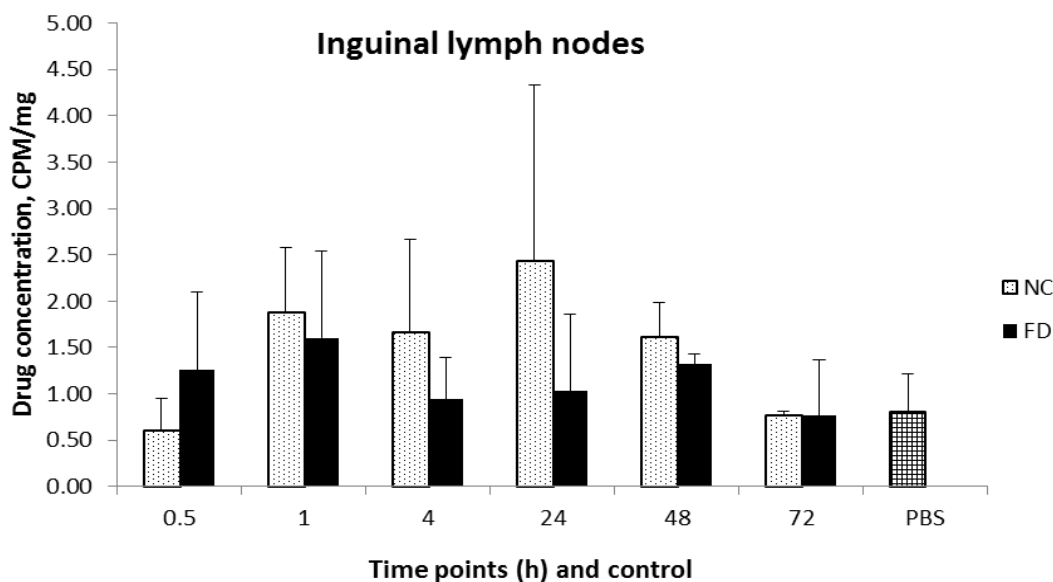
Figure 32 Drug exposure in lumbar lymph nodes and inguinal lymph nodes over a 72h period of time.
Drug substance was detected in the lumbar lymph nodes 48h after CSIC nanocrystal treatment. No CSIC nanocrystals or free drug could be found in the inguinal lymph nodes at any of the time point investigated. A control study using PBS was conducted to indicate the background level. * denotes a significant difference ($p<0.01$) when compared with the PBS control. (n=3)

5.4   DISCUSSION AND CONCLUSION

The overall goal of this chapter is to improve drug permeation in the cervicovaginal tissue and subsequently deliver drug to the genital lymph nodes after intravaginal instillation using the developed CSIC nanocrystal formulation. To achieve this objective, first of all, drug

146

formulations must penetrate through the mucus and be accessible to the female reproductive tissue. Previous studies have shown that the test formulations may interact with the mucin in the vaginal fluid and this interaction could significantly alter drug retention, release rate, delivery kinetics, and bioactivity in the body [233-235]. Therefore, it is important to investigate the potential interaction between CSIC nanocrystal and mucin from the perspective of formulation development. Based on the data generated in this chapter, CSIC nanocrystals did not seem to interact with mucin molecules, since the particle size of the CSIC nanocrystal remained unchanged after mucin treatment at both pH 4.2 and 7.0. As the interactions between mucin and drug particles are generally induced by hydrophobic and electrostatic forces, these findings suggested a complete coverage of the hydrophobic nanocrystal surface by stabilizer HPMC and Pluronic 98. Additionally, the minimal negative surface charge (-7.8mV) of CSIC nanocrystals might further inhibit their interaction with the negatively charged mucin via electrical repulsion. It was worth noting that, however, as the CSIC nanocrystal-mucin mixtures were diluted before particle size analysis, even if there was an interaction, it might not be recorded as a size increase.

It was also found that the mucin-nanocrystal interaction at higher pH (pH 7.0) was similar to that at pH4.2. This result was inconsistent with a previous study which showed a lower interaction between DPV nanoparticles and mucin at pH 7.0 compared to pH 4.2 [228]. This disparity could be a result of different surface charges for CSIC nanocrystals and DPV nanoparticles. As for the DPV nanoparticle, the intensity of its surface charge was > -30mV, which was much higher than that of CSIC nanocrystals (near neutral, <-10mV). Thus, when the ionization of mucin would increase at a higher pH (pH 7.0), meaning it would become more negatively charged, and its interaction with the highly negatively charged DPV nanoparticles would be further decreased due to the larger electrical repulsion.

In addition to the mucus penetration properties, the extents of protein adsorption at two different time points were also determined. The resulting data showed that the protein concentration after 1 hour of incubation was similar to that after 5 minutes incubation. In addition, the extent of protein adsorption on the surface of CSIC nanocrystals was much less than that on the free drug particles for both incubation times. This phenomenon could be explained by the utilization of Pluronic F98 (a PEG containing polymer) in the nanocrystal formulation, which decreased the overall hydrophobicity of the product. This finding is in accordance with previous studies showing that PEG could be applied to suppress protein adsorption by blocking the protein binding site on the surface of nanoparticles and creating a thermodynamic barrier to protein diffusion [236, 237]. Chan and his colleague also reported that increasing PEG grafting density on the surface of nanoparticles significantly reduced the extent of protein adsorption and changed the composition of the adsorbed proteins when compared to the un-grafted nanoparticles [209]. The variation in protein adsorption led to different mechanisms and efficiency of nanoparticle uptake by macrophages in the blood. It is worth noting that, as the identities of the adsorbed proteins in each sample remained unknown in our scenario, no significant conclusions can be drawn at this stage for CSIC nanocrystals or CSIC free drug regarding to their macrophage uptake in blood and subsequent biodistribution *in vivo*.

To verify the advantage of nanocrystal formulation in terms of tissue penetration, the next step was to evaluate drug permeation properties using excised human ectocervical tissue. The results have shown that both CSIC free drug and nanocrystals were able to penetrate though the cervicovaginal tissues. The flux (J) and the P_{app} were found to be similar between these two test articles. This result is in agreement with another permeability study, which investigated the permeation properties of free drug DPV and DPV encapsulated polymeric nanoparticles using

pig vaginal mucosa [40]. The P_{app} of free drug DPV was calculated to be 1.75 ±0.17 cm·s^{-1}x10^{-6}, which was of a similar magnitude but slightly higher than the P_{app} of the CSIC free drug (3.0 ±1.5cm·s^{-1}x10^{-7}). Strikingly, the P_{app} of DPV free drug was found to be lower than that of the positively charged DPV nanoparticles, but higher than that of the negatively charged DPV nanoparticles. Thus, surface charge seems to play a critical role in determining the P_{app}. In our scenario, CSIC nanocrystals have a near-neutral charge which is similar to that of the free drug molecules. This similarity in surface charge could contribute to the comparable P_{app} values between the CSIC free drug and CSIC nanocrystals.

In terms of the amount of drug retained in the tissue, drug concentrations determined after nanocrystal exposure were found to be significantly lower than the free drug treatment, which is not unexpected. This difference could be explained by the precipitation and accumulation of free drug on the surface of the tissue. The drug accumulation could significantly increase the concentration gradient in the apical layers of epithelium, which facilitated drug permeation. In contrast, CSIC nanocrystals were well stabilized and homogenously suspended in the solution (95.1 ±4.25%) with a very small fraction of the nanocrystals (0.2 ±0.06%) in contact with the tissue. This hypothesis can also be confirmed by the amount of drug detected in the most superficial 100 μm-thick tissue: the amounts of free drug were found to be 1309.5 ±341.8 ng, 2-3 times higher than that after nanocrystal treatment (459 ±212.5 ng).

The low drug nanocrystal concentration in the tissue could also be attributed to its sustained drug release profile [48]. As drug molecules have to be released first to be absorbed and CSIC is released from the nanocrystals in a controlled manner, the concentration of soluble drug that is free to be absorbed could be low. In contrast, in the case of CSIC free drug, the concentration of soluble drug could be relatively higher due to the presence of the solubilizing agent DMSO.

Along with the differing extents of drug penetration, these two test articles showed distinct drug penetration efficiency. Very encouraging, CSIC nanocrystals seem to penetrate throughout the tissue more efficiently than the free drug. By comparing the amounts of CSIC remaining in the first and last piece of tissue section from the apical epithelium to the basal layer stroma, it was determined that over 17% of the CSIC nanocrystal was able to migrate to the stroma side, however, only 5% of free drug penetrated through the tissue and located in the bottom layers.

In light of these findings, it was assumed that the impact of the free drug accumulation on tissue exposure could be compromised if a reduced dosing level and a shorter period of incubation time could be applied. To test this hypothesis, extended study was conducted using 0.1ml test articles and 0.5h incubation time. As expected, no difference was observed between the two test articles in terms of the total amounts of drug remaining in the tissue and the cumulative amount of drug collected in the receptor chamber.

Notably, in the *ex vivo* drug permeation study, cervicovaginal mucus was not involved in the experimental setup, and the effect of tissue permeation on lymphatic drug delivery could not be investigated. Therefore, it is worthwhile to explore the permeation properties *in vivo* using an animal model and verify drug exposure in the genital lymph nodes. The animal study performed in this chapter is the first pharmacokinetic study for the anti-retroviral drug CSIC.

The resulting data has shown that CSIC nanocrystals presented mainly in the vagina and ectocervix, and to some extent in the uterus and ovaries. Drug exposure in the entire FRT was favorable since the upper FRT might also contribute to viral transmission [9]. The existence of drug in the ovary, despite it only accounted for 0.01% of the dosed drug, was consistent with a previous study conducted by Hope's group. They found that SIV-based dual reporter particles could reached macaque ovaries 48h after vaginal inoculation [70]. Other studies investigating drug distribution of PLGA nanoparticles and Qdots in mouse FRT did not report the presence of drug in the ovaries [105, 238]. The disparity between different investigations could be attributed to the following reasons. First of all, to prevent drug leakage, the mice in current study were physical restrained in cornicle tubes with their hindquarters elevated for 20 minutes after drug instillation. This body position might induce the formulations to migrate down to the ovaries. In addition, first-uterine-pass effect might play a role in the transfer of vaginally administered hydrophobic drugs to the uterus/ovary. Evidence of this effect can be confirmed by other drugs such as progesterone, terbutaline, and danazol [23]. In the case of the CSIC nanocrystal formulation, the pure drug particles were stabilized by the stabilizers but not encapsulated in surface modified nanocarrrier systems. Therefore, the hydrophobic property of CSIC was somehow reserved and induced the first-uterine-pass effect. Furthermore, the limited mucin-nanocrystal interactions described earlier might also facilitate the wide distribution of

nanocrystals within the whole reproductive tract. Lastly, the quantification method applied in the present work (LSC) was more sensitive than measuring the intensity of fluorescent signals so that extremely low amounts of drug exposure could be detected.

To better understand the elimination rate of CSIC nanocrystals in the reproductive tract, the total amount of drug remaining in the vaginal lavage and the genital tissue at various time points were determined. As early as 0.5h, over 85% of the loaded nanocrystals had already been cleared. The amount of drug detected at 1h had further decreased to 2%. After 24h, only a trace amount of drug could be quantified. The clearance rate of CSIC nanocrystals was found to be similar but faster than other nanoparticles [238, 239]. Previous studies have shown that over 30% surface modified PLGA nanoparticles and rhodamine-loaded poly(epsilon-caprolactone) (PCL) nanoparticles could be recovered after 0.5h administration, and about 10% detected by 2h. In our case, other than vaginal leakage, another plausible explanation for the fast drug loss could be the stress induced by physical restraints. The stress might increase the frequency of urination and the bowel activity, which in turn accelerated the elimination of the administered drug.

Compared with the CSIC nanocrystals, the residence of free drug in the vagina and ectocervix were one order of magnitude lower, especially at earlier time points (Figure 29). This result was in line with the biodistribution of free dapivirine (DPV, another tight binding NNRTI as CSIC), which presented a lower tissue exposure in the vagina and lower uterus compared to the corresponding DPV-loaded nanoparticles [239]. More importantly, a previous study by Ensign et al. has demonstrated that mucus penetrating PEG-coated nanoparticles could provide more protection against Herpes Simplex virus after intravaginal administration than the soluble drug. This increased protection from nanoparticles was attributed to the more uniform drug distribution on the vaginal epithelial and rapid penetration into rugae with more drug retained in

the tissue [240]. This finding thus suggests that the increased CSIC concentration in the tissue after CSIC nanocrystal treatment is beneficial and would lead to a better protection against HIV transmission in the female reproductive tract. In addition, Ensign et al. further showed that the application in a hypotonic medium enhanced drug uptake due to a more uniform and intimate contact with the vaginal surface. In future work, it would be interesting to see whether their method would result in a still greater drug uptake from our nanoparticles [241].

The amounts of drug present in the vaginal lavage after CSIC nanocrystals or free drug administration were also analyzed (Figure 30). Unexpectedly, the difference between the two treatments was not statistically significant. Only at 4h, drug concentrations obtained in the free drug treated mice were found to be slightly higher than the nanocrystal treated ones. This result could be explained by their different mucus penetrating properties. Considering that CSIC is very hydrophobic, it was likely that mucin proteins entangled with the free drug aggregates and hindered their migration to the cervicovaginal tissues. In contrast, CSIC nanocrystals, as a type of mucus-penetrating nanoparticle, penetrated through the mucus rapidly and eventually enter the vaginal folds [240].

In addition, drug concentrations in the plasma and elimination organs were evaluated as criteria of systemic exposure (Figure 31). It was found that drug contents in plasma after both treatments were extremely low. At 0.5h, plasmatic level of CSIC nanocrystal was only about 0.02 µg/mL corresponding to 0.03% of initial dose, which was much lower than the DPV free dug (0.099 µg/g, 3%) and DPV nanoparticles (0.026 µg/g, 0.8%) at 15 minutes after vaginal administration [239]. As for drug exposure in the liver and kidney, CSIC concentrations for both formulations were determined to be relatively higher than DPV nanoparticles, but still at very low levels. Drug concentrations detected in the plasma were found to be very low compared with

the amount of drug remained in the cervicovaginal tissue. This result is desirable since the limited systemic drug exposure can curb the progress of drug resistance, especially for non-nucleoside reverse transcriptase inhibitors (NNRTIs). NNRTIs have the longest half-life in plasma compared with other classes of antiretroviral drug [242, 243]. When the drug concentration in plasma reaches to a threshold, there is an increased risk of developing drug resistance. More importantly, NNRTIs have a low genetic barrier to the viral mutants selected from other within-class drugs. Therefore, existing NNRTI resistance could potentially compromise the efficacy of future regimens that containing other NNRTIs. Accordingly, it is critical to monitor NNRIT plasma concentration and maintain a low systemic concentration. For drug CSIC, however, there is no information available about its resistance threshold. Therefore, we have to use the threshold determined for nevirapine (0.25µg/mL) [244], which is another NNRTI with a similar half-life compared to CSIC. It was found that CSIC plasma concentration (0.02µg/mL) was much lower than this threshold and should not induce drug resistance.

In the current animal study, we were also interested in drug transport in the genital lymph nodes. Very encouragingly, without N-9 pretreatment, CSIC could be detected in the lumbar nodes 48h after nanocrystal administration, whereas neither of the two test articles was observed in the inguinal lymph nodes at any of the time points. Similarly, a previous study investigated the lymphatic transport of Qdots from vaginal lumen to draining lymph nodes after N-9 pretreatment. This study showed the drainage of Qdots to both the inguinal lymph nodes and the lumbar lymph, with peak concentrations observed at 36 hr [105]. In comparison, the lymphatic trafficking of CSIC nanocrystal was found to be slower than that for Qdots, which could be explained by the much larger particle size of the nanocrystals and the tissue damage caused by N-9 intervention in the Qdots study.

To understand the mechanism of lymph node drug targeting, another set of studies were carried out using the same mouse model, while mouse vagina were pretreated with the permeation enhance N-9 intravaginally. Unexpectedly, N-9 treatment 12h prior to drug exposure did not enhance the lymph node drug delivery for CSIC nanocrystals. This observation differed from the Qdots study which reported an enhanced transport of Qdots to lumbar lymph nodes by prior vaginal installation of N-9 [105]. As the driving force of Qdots migration was the secretion of inflammatory cytokines, the mechanism behind for CSIC nanocrystals should not be the same [245]. Another possible interpretation is the solubilization effect of N-9 on drug. If both CSIC nanocrystals and CSIC free drug were dissolved in N-9, no difference will be expected between these two treatments. Last but not the least, considering that the amounts of drug detected in the nodes were extremely low, the effect of N-9 on nanocrystal lymph node delivery cannot be determined due to the limitation of the current techniques.

Another limitation of this study is that there is no direct or indict evidence to confirm the presence of the intact nanocrystals in the draining lymph nodes. In another word, CSIC molecules might be released from the nanocrystals on the way of migration and existed as free drug substance in the lymph nodes. To answer this question, one possible approach is to administrate free drug intravaginally and determine the amount of drug exposure in the nodes. As free drug solution can be easily leaked out from the vagina, alternative formulation such as CSIC containing vaginal film will be applied to control the actual dosing level. In this case, if no drug or less amount of drug is detected in the lymph nodes after CSIC vaginal films intervention, then it can be concluded that CSIC nanocrystals can make it to the lymph nodes or at least facilitate the lymphatic draining of the hydrophobic drug CSIC. Collectively, these control studies would demonstrate enhanced drug exposure in the lymph nodes by nanocrystal instillation is not simply due to the higher local concentration achieved.

In conclusion, CSIC nanocrystals act as mucus penetrating nanoparticles presenting limited interactions with mucin. Formulating free CSIC into nanocrystals did not improve the drug permeation in the explanted cervicovaginal tissue due to the free drug accumulation and the application of a solubilizing agent to prepare free drug suspension. However, enhanced drug exposure in the reproductive tract and lumbar lymph nodes were observed in a mouse model. CSIC nanocrystals showed limited systemic exposure and a reduced protein adsorption profile after intravaginal administration. Overall, CSIC nanocrystals are a promising formulation for the purpose of vaginal drug delivery and lymph node targeting.

ACKNOWLEDGEMENT

6.0   MAJOR FINDINGS AND FUTURE DIRECTIONS

6.1   MAJOR FINDINGS AND IMPLICATIONS

Throughout the last decade, HIV/AIDS remains a major health concern globally. Over half of the people living with HIV are women. Due to this high percentage, prevention approaches focused on sexual transmission in the female reproductive tract, such as vaginal microbicides, are in development. The CSIC containing microbicide products developed in this dissertation display substantially increased drug solubility, which is a crucial parameter to increase their efficacy. Furthermore, this work proved for the first time the possibility of lymphatic targeting after intravaginal administration. These improvements will allow a much higher drug dosing level, increased drug concentration at the site of viral entry and additional protection in the regional lymph nodes. All these factors will lead to an improved anti-HIV efficacy having significant contribution to the microbicide field.

The work conducted in this dissertation was based on the hypotheses that (1) the hydrophobic microbicide drug candidate CSIC can be formulated in a polymeric vaginal film and a nanocrystal formulation with high loading capacities using multiple solubilization strategies; and (2) the nano-delivery strategy can improve cervicovaginal tissue drug penetration and achieve lymphatic drug delivery. The studies performed to address these hypotheses included preformation study, film formulation development using a co-solvent strategy, rational

design of a nanocrystal formulation, drug permeation investigation through excised human tissue, and *in vivo* distribution in the cervicovaginal tissue and genital lymph nodes following CSIC nanocrystal instillation. The major findings of the dissertation are summarized below.

6.1.1   Major findings

6.1.1.1 Preformulation evaluation of CSIC

The microbicide drug candidate CSIC is practically insoluble in aqueous solutions, with an octanol/water partition coefficient (Log $P_{oct/wat}$) of 3.7. CSIC aqueous solubility was enhanced through utilization of a co-solvent system comprised of PEG400, propylene glycol, and glycerin. Use of this system resulted in enhancement of aqueous solubility by over 1000 fold. The raw crystalline drug substance was found to be extremely stable under various pH, temperature and oxidization conditions. The only susceptibility identified for this drug in terms of stability was photosensitivity. For this reason, special care should be taken to protect CSIC from light during the process of handling, manufacturing, and packaging. The cytotoxic profile of CSIC in the epithelial cell line HEC-1A and macrophage-like cell line J774A.1 were determined to be concentration dependent with CC_{50} values around 5 µg/mL. This concentration should provide sufficient anti-HIV activity since it is several orders of magnitude higher than the EC_{50} of CSIC. The results generated in the preformulation study were applied subsequently in the formulation development and evaluation.

6.1.1.2 CSIC containing vaginal film

A co-solvent system consisting of PEG 400, propylene glycol and glycerin was optimized using a ternary phase diagram. The optimized co-solvent system was employed to disperse CSIC uniformly in a water-soluble film dosage form. The utilization of these cosolvents not only enhanced the solubility of the hydrophobic drug but also improved the flexibility and softness of the vaginal film product. More importantly, by optimizing the ratio among the co-solvents, the total amount of solvents being used was controlled to avoid any potential side effects such as epithelial damage, which may lead to increased risk of HIV infection. The vaginal film formulation developed utilizing the co-solvent system for enhanced solubilization of the hydrophobic drug CSIC has the potential to be applied as a platform to deliver other hydrophobic drugs with a high loading capacity. In regards to drug release, an initial burst effect was observed for CSIC films. This property will allow the development of a coitally dependent microbicide product providing a sufficient drug concentration at the site of HIV entry.

6.1.1.3 CSIC nanocrystal: preparation and intracellular uptake

The CSIC nanocrystal formulation was prepared for vaginal administration using a nanoprecipitation method. Pluronic F98 and HPMC E5 were chosen in this formulation to stabilize the drug nanocrystals and prevent them from crystal aggregation. A particle size of 243nm and a near neutral surface charge were achieved. These properties were desired to achieve rapid mucus penetration. Different from the film formulation, the CSIC nanocrystals feature a controlled and sustained drug release profile lasting for 4 days. This release profile indicates its potential application as a coitally independent microbicide product that might significantly increase the dosing interval and improve user adherence. CSIC nanocrystals were found to be readily internalized by macrophages and get into the cytoplasm via a clathrin mediated endocytosis pathway.

6.1.1.4 CSIC nanocrystal: drug permeation and lymph node drug delivery

Limited interactions between CSIC nanocrystal and mucin were found in this study, which indicates that the nanocrystal formulation can readily penetrate the mucus present at the cervicovaginal epithelium. Because mucus is the major barrier for vaginal drug delivery, the mucus penetration property will ensure drug access to the underlying epithelial cells. In addition, formulating CSIC into nanocrystals significantly enhanced its permeation efficiency across cervicovaginal tissue. When CSIC nanocrystals were topically administrated in the mouse vagina, increased drug concentration was detected in the mouse reproductive tissue, especially in the vagina and ectocervix, compared with the free drug treatment. The increased drug exposure at the site of HIV entry is favorable for increased anti-HIV efficacy. More importantly, results showed the presence of drug in the lumber lymph nodes after nanocrystal treatment. This is the first study that confirmed the feasibility of lymph node drug targeting after vaginal instillation without the use of the permeation enhancer N-9 in the microbicide field.

6.1.2   Contribution to the field of vaginal microbicide

In this dissertation project, the data generated from the preformation studies provides the most critical information required for the development of vaginal products. Therefore, research can be extended to other dosage forms, such as vaginal gels, tablets, rings, or other vaginal applied nanocarrrier systems. The existence of multiple dosage forms will provide women with more choices, which in turn will improve user adherence.

Since an increasing number of microbicide drug candidates are hydrophobic in nature, the co-solvent strategy presented in this dissertation contributes to the advancement of

162

microbicides by offering a strategy for facilitating formulation development of hydrophobic drugs for vaginal delivery. The utilization of this cosolvent strategy will increase drug loading capacity substantially while the safety properties required for microbicide products remain unaffected.

It is well known that potential users are more likely to adhere to drug dosing regimens which require limited times of product administration [246, 247]. Sustained and controlled delivery of a microbicide holds significant potential as a cost-effective strategy for the treatment of sexually transmitted HIV-1. This release profile can improve user adherence and maintain a therapeutic drug concentration in the vaginal fluid and the cervicovaginal tissue over a long period of time. More importantly, controlled release microbicide products can be applied in a coitally independent fashion which may enable greater coverage of all sexual contacts, especially those that are unanticipated or coerced. Hence such a regimen may provide better overall product effectiveness. Currently, the intravaginal ring (IVR) is the main device being investigated for this purpose. However, not all women may choose to use a ring product, more options need to be provided to further improve user compliance. In the current dissertation work, a CSIC nanocrystal formulation was developed that can release the drug in a sustained and controlled manner. Considering that nanocrystals can be incorporated into other dosage forms such as hydrogels and polymeric films [248, 249], sustained drug release from traditional vaginal dosage forms can be achieved. These products can be applied as promising alternatives to vaginal rings. Additionally, as nanocrystal technology is a universal approach to formulate hydrophobic drugs, this formulation strategy can be applied as a novel platform for the sustained delivery of many other hydrophobic microbicides after vaginal administration.

The pharmacokinetic study performed in this dissertation project is the first piece of work in the microbicide field investigating drug delivery to both cervicovaginal tissue and genital lymph nodes. We were able to prove the possibility of achieving lymph node drug targeting after intravaginal instillation without N-9 intervention. Our accomplishment reinforces the importance of lymphatic drug delivery. The distribution of microbicides in the genital lymph nodes warrants future investigation when considering vaginal instillation.

6.2   FUTURE DIRECTIONS

Although CSIC nanocrystal formulation is found to be promising as a vaginal microbicide product and it has the capacity to deliver drug to both cervicovaginal tissue and lumber lymph nodes, a number of studies need to be completed to further evaluate this formulation and elucidate the mechanism of lymph node targeting. In addition, as nanocrystals can be formulated in a final dosage form, such as vaginal film or gel, further studies are warranted to develop formulations for nanocrystals incorporation and delivery.

Further evaluation of CSIC Nanocrystal formulation:

In the current dissertation study, the stability of CSIC nanocrystal was evaluated at room temperature in both solid and liquid states. To expand the assessment as per ICH guidelines and published literatures [213, 250, 251], nanocrystal product needs be stored at different temperature and humidity conditions including 4°C, 25°C/60% RH, 30°C/65% RH and 40°C/60% RH for 12 months. At various time points, physicochemical parameters such as particle size, size distribution, surface charge, crystal morphology, drug content, and *in vitro* release will be evaluated and compared with time zero.

To translate this formulation to clinical application, the safety profile of CSIC nanocrystals must be investigated. First, the nanocrystals need to be incubated with lactobacillus cultures to evaluate its effect on lactobacillus colonization. This acute toxicity study can only be performed *in vitro* since no vaginal environment in an animal model has been reported to be lactobacillus dominant and acidic [42, 252]. In addition, it is important to investigate the toxic effect of CSIC nanocrystal in mouse vagina. The study can be conducted by measuring the levels of proinflammatory cytokines, chemokines and granulocyte elastase in the vaginal lavage [253]. The selected markers must be able to represent a broad range of inflammatory processes. The data collected will provide a good rationale for designing a safe dosing regimen.

Additionally, it will be very interesting to investigate the memory effect of CSIC nanocrystals. Since drug can be released from the nanocrystals in a sustained mode for 96h, we expect to see a much longer protection period against HIV acquisition in comparison with CSIC containing vaginal film.

To better visualize the advantage of CSIC nanocrystals for tissue permeation, tissue permeability study of CSIC nanocrystals and CSIC free drug need to be conducted using a Side-

Bi-Side cell system (Figure 33). In contrast to the in-line cell system applied in this dissertation, the free drug aggregates will accumulate at the bottom of the donor chamber in the Side-Bi-Side cells, thus avoiding direct contact with the cervicovaginal tissue. In this way, the effect of free drug accumulation on drug permeation in the tissue can be circumvented.
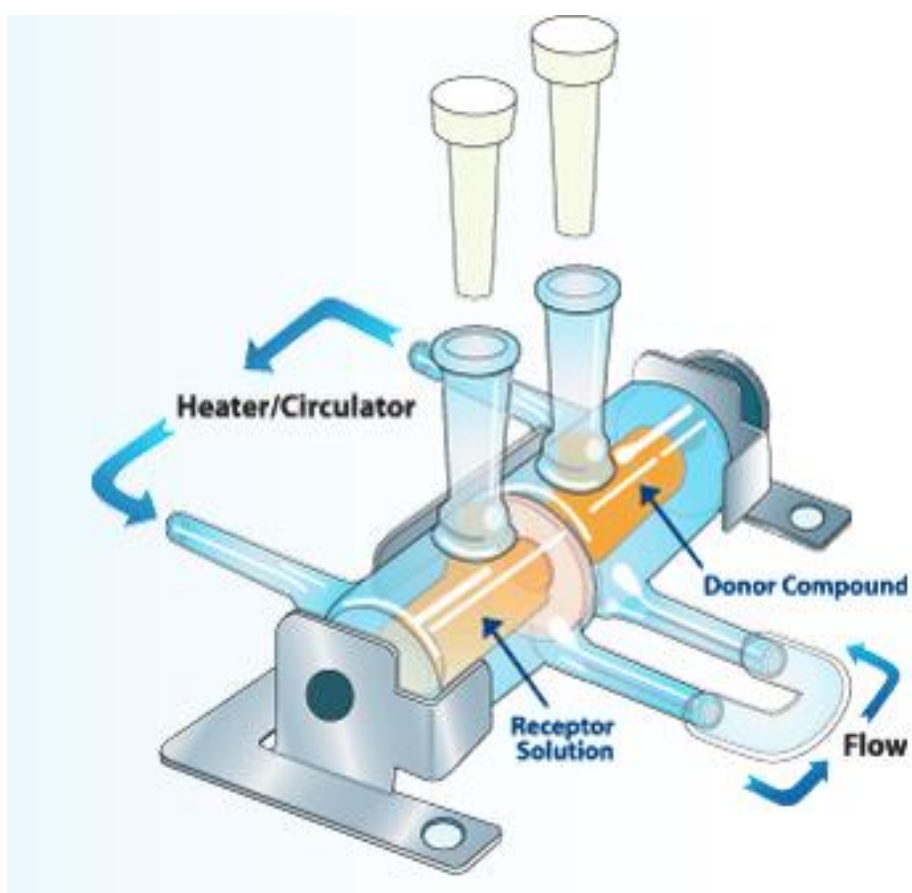
Figure 33 Side-Bi-Side Cell

In the future studies, excised human cervicovaginal tissue will be placed between the donor chamber and receptor chamber and displayed horizontally.

In the pharmacokinetic study, drug distribution from vagina to ovary has been accurately quantified. In the next step, this study needs to be extended to investigate the depth of drug penetration from the apical epithelium to stroma. To further investigate drug distribution in mouse, the whole female reproductive tract collected will be cut into a reasonable number of pieces in sequential orders. Each individual piece of tissue will be fixed and sectioned consecutively to 100μm sections as the method described in the human tissue permeability study. Drug content in each tissue section will be determined by a liquid scintillation counter. By encoding the amounts of drug available together with their in situ position, a three-dimensional drug localization profile can be obtained. These results will allow a more comprehensive understanding of drug distribution and penetration in the reproductive tissue after vaginal administration.

Further elucidation of mechanisms:

The pharmacokinetic study performed in the current dissertation has proved the presence of CSIC in the lumbar lymph nodes. To continue this project, it will be very interesting to explore the mechanism/pathway associated with the lymphatic trafficking. Previous studies have shown that $CD4^+$ T cells exist abundantly in the cervicovaginal epithelium, and they normally drain to the T cell zone in the lymph nodes [16]. Thus, the uptake of CSIC nanocrystals in $CD4^+$ T cells might contribute to the drug transport in the lumber nodes. In addition, antigen presenting cells such as macrophages and dendritic cells (Langerhans cells) also have the capability to uptake and transport antigens/particles to the draining lymph nodes. Therefore, to better understand the mechanism/pathway of lymph node drug delivery, it is important to test (1) the uptake profile of CSIC nanocrystal in at least $CD4^+$ T cells, and dendritic cells (Langerhans cells), and (2) isolate each type of cell from mouse reproductive tissue after intravaginal administration of CSIC nanocrystals and analysis drug content individually.

Further development of dosage form:

Research on incorporation of CSIC nanocrystal/nanosuspension in a final formulation is warranted. The final products could be vaginal films, gels or tablets. This transformation will allow the final products for easy application and less leakage. It might also improve drug retention in the vaginal lumen and increase drug concentration in the vaginal lavage and cervicovaginal tissue. It is worth noting that the stabilizers used in the nanocrystal formulation might be incompatible with the new excipients employed in the final dosage form. Therefore, drug particle size, crystal properties, dissolution profile, and mucus penetration characteristics must be evaluated in the final formulation to ensure desirable tissue penetration and biodistribution.

BIBLIOGRAPHY

1.   UNAIDS, *Global report: UNAIDS report on the global AIDS epidemic 2013.*
2.   Abdool Karim, Q., et al., *Effectiveness and Safety of Tenofovir Gel, an Antiretroviral Microbicide, for the Prevention of HIV Infection in Women.* Science, 2010. **329**(5996): p. 1168-1174.
3.   Romano, J., et al., *Safety and availability of dapivirine (TMC120) delivered from an intravaginal ring.* AIDS Res Hum Retroviruses, 2009. **25**(5): p. 483-8.
4.   Nel, A., et al., *Safety and Pharmacokinetics of Dapivirine Delivery From Matrix and Reservoir Intravaginal Rings to HIV-Negative Women.* JAIDS Journal of Acquired Immune Deficiency Syndromes, 2009. **51**(4): p. 416-423 10.1097/QAI.0b013e3181acb536.
5.   *<UNAIDS. AIDS epidemic update [global summary]. UNAIDS; 2004.pdf>.*
6.   AIDS.gov. *U.S. Statistics*. 2015 [cited 2015 24 June].
7.   Quinn, T.C. and J. Overbaugh, *HIV/AIDS in Women: An Expanding Epidemic.* Science, 2005. **308**(5728): p. 1582-1583.
8.   HIV, E.S.G.o.H.T.o., *Comparison of female to male and male to female transmission of HIV in 563 stable couples.* BMJ, 1992. **304**(6830): p. 6.
9.   Wira, C.R. and J.V. Fahey, *A new strategy to understand how HIV infects women: identification of a window of vulnerability during the menstrual cycle.* AIDS (London, England), 2008. **22**(15): p. 1909-1917.
10.   Heffron, R., et al., *Use of hormonal contraceptives and risk of HIV-1 transmission: a prospective cohort study.* The Lancet Infectious Diseases, 2012. **12**(1): p. 19-26.
11.   Baeten, J.M., et al., *Hormonal contraceptive use, herpes simplex virus infection, and risk of HIV-1 acquisition among Kenyan women.* AIDS, 2007. **21**(13): p. 1771-1777.
12.   Baeten, J.M., L. Lavreys, and J. Overbaugh, *The Influence of Hormonal Contraceptive Use on HIV-1 Transmission and Disease Progression.* Clinical Infectious Diseases, 2007. **45**(3): p. 360-369.
13.   Fleming, D.T. and J.N. Wasserheit, *From epidemiological synergy to public health policy and practice: the contribution of other sexually transmitted diseases to sexual transmission of HIV infection.* Sexually transmitted infections, 1999. **75**(1): p. 3-17.
14.   Haase, A.T., *Targeting early infection to prevent HIV-1 mucosal transmission.* Nature, 2010. **464**(7286): p. 217-223.
15.   Shattock, R.J. and J.P. Moore, *Inhibiting sexual transmission of HIV-1 infection.* Nat Rev Micro, 2003. **1**(1): p. 25-34.
16.   Miller, C.J. and R.J. Shattock, *Target cells in vaginal HIV transmission.* Microbes and Infection, 2003. **5**(1): p. 59-67.
17.   Zhang, Z.-Q., et al., *Sexual Transmission and Propagation of SIV and HIV in Resting and Activated CD4+ T Cells.* Science, 1999. **286**(5443): p. 1353-1357.
18.   Pace, M.J., et al., *Directly infected resting CD4+ T cells can produce HIV Gag without spreading infection in a model of HIV latency.* PLoS Pathog, 2012. **8**(7): p. e1002818.

19.   Haase, A.T., *Early events in sexual transmission of HIV and SIV and opportunities for interventions.* Annual review of medicine, 2011. **62**: p. 127-139.

20.   Barnhart, K.T., et al., *Baseline dimensions of the human vagina.* Human Reproduction, 2006. **21**(6): p. 1618-1622.

21.   Richardson, J.L. and L. Illum, *(D) Routes of delivery: Case studies: (8) The vaginal route of peptide and protein drug delivery.* Advanced Drug Delivery Reviews, 1992. **8**(2–3): p. 341-366.

22.   Knuth, K., M. Amiji, and J.R. Robinson, *Hydrogel delivery systems for vaginal and oral applications: Formulation and biological considerations.* Advanced Drug Delivery Reviews, 1993. **11**(1–2): p. 137-167.

23.   Krogstad, E.A., M.J. Rathbone, and K.A. Woodrow, *Vaginal Drug Delivery*, in *Focal Controlled Drug Delivery*, M.J. Rathbone, Editor. 2014, Springer: Advances in Delivery Science and Technolog.

24.   Owen, D.H. and D.F. Katz, *A vaginal fluid simulant.* Contraception, 1999. **59**(2): p. 91-95.

25.   Wagner, G. and B. Ottesen, *Vaginal physiology during menstruation.* Annals Of Internal Medicine, 1982. **96**(6 Pt 2): p. 921-923.

26.   Boskey, E.R., et al., *Origins of vaginal acidity: high d/l lactate ratio is consistent with bacteria being the primary source.* Human Reproduction, 2001. **16**(9): p. 1809-1813.

27.   Brannon-Peppas, L., *Novel vaginal drug release applications.* Advanced Drug Delivery Reviews, 1993. **11**(1–2): p. 169-177.

28.   Caillouette, J.C., et al., *Vaginal pH as a marker for bacterial pathogens and menopausal status.* American Journal of Obstetrics and Gynecology, 1997. **176**(6): p. 1270-1277.

29.   Srikrishna, S. and L. Cardozo, *The vagina as a route for drug delivery: a review.* International Urogynecology Journal, 2013. **24**(4): p. 537-543.

30.   Hussain, A. and F. Ahsan, *The vagina as a route for systemic drug delivery.* Journal of Controlled Release, 2005. **103**(2): p. 301-313.

31.   das Neves, J., M.H. Amaral, and M.F. Bahia, *Vaginal Drug Delivery*, in *Pharmaceutical Sciences Encyclopedia*. 2010, John Wiley & Sons, Inc.

32.   Abdool Karim, S.S., et al., *Drug concentrations after topical and oral antiretroviral pre-exposure prophylaxis: implications for HIV prevention in women.* Lancet, 2011. **378**(9787): p. 279-281.

33.   Hendrix, C.W., et al., *MTN-001: Randomized Pharmacokinetic Cross-Over Study Comparing Tenofovir Vaginal Gel and Oral Tablets in Vaginal Tissue and Other Compartments.* PLoS ONE, 2013. **8**(1): p. 1-11.

34.   Garg, S., et al., *Advances in development, scale-up and manufacturing of microbicide gels, films, and tablets.* Antiviral research, 2010. **88**: p. S19-S29.

35.   das Neves, J. and M.F. Bahia, *Gels as vaginal drug delivery systems.* International Journal of Pharmaceutics, 2006. **318**(1–2): p. 1-14.

36.   Akil, A., et al., *Development and characterization of a vaginal film containing dapivirine, a non-nucleoside reverse transcriptase inhibitor (NNRTI), for prevention of HIV-1 sexual transmission.* Drug Delivery and Translational Research, 2011. **1**(3): p. 209-222.

37.   Malcolm, R.K., et al., *Long-term, controlled release of the HIV microbicide TMC120 from silicone elastomer vaginal rings.* Journal of Antimicrobial Chemotherapy, 2005. **56**(5): p. 954-956.

38.   Rohan, L., B. Devlin, and H. Yang, *Microbicide dosage forms*, in *Microbicides for Prevention of HIV Infection*. 2014, Springer. p. 27-54.

39.   Ham, A., et al., *Targeted Delivery of PSC-RANTES for HIV-1 Prevention using Biodegradable Nanoparticles.* Pharmaceutical Research, 2009. **26**(3): p. 502-511.

40.   das Neves, J., et al., *In Vitro and Ex Vivo Evaluation of Polymeric Nanoparticles for Vaginal and Rectal Delivery of the Anti-HIV Drug Dapivirine.* Molecular Pharmaceutics, 2013. **10**(7): p. 2793-2807.

41.   Zhang, T., T.F. Sturgis, and B.-B.C. Youan, *pH-responsive nanoparticles releasing tenofovir intended for the prevention of HIV transmission.* European Journal of Pharmaceutics and Biopharmaceutics, 2011. **79**(3): p. 526-536.

42.   Ensign, L.M., R. Cone, and J. Hanes, *Nanoparticle-based drug delivery to the vagina: A review.* Journal of Controlled Release, 2014. **190**(0): p. 500-514.

43.   Mallipeddi, R. and L.C. Rohan, *Nanoparticle-based vaginal drug delivery systems for HIV prevention.* Expert opinion on drug delivery, 2010. **7**(1): p. 37-48.

44.   M El-Hammadi, M. and J. L Arias, *Nano-Sized Platforms for Vaginal Drug Delivery.* Current pharmaceutical design, 2015. **21**(12): p. 1633-1644.

45.   Gupta, K.M., et al., *Polyurethane intravaginal ring for controlled delivery of dapivirine, a nonnucleoside reverse transcriptase inhibitor of HIV‑1.* Journal of pharmaceutical sciences, 2008. **97**(10): p. 4228-4239.

46.   Woolfson, A.D., et al., *Freeze-dried, mucoadhesive system for vaginal delivery of the HIV microbicide, dapivirine: optimisation by an artificial neural network.* International journal of pharmaceutics, 2010. **388**(1): p. 136-143.

47.   Damian, F., et al., *Approaches to improve the stability of the antiviral agent UC781 in aqueous solutions.* International journal of pharmaceutics, 2010. **396**(1): p. 1-10.

48.   Merisko-Liversidge, E.M. and G.G. Liversidge, *Drug Nanoparticles: Formulating Poorly Water-Soluble Compounds.* Toxicologic Pathology, 2008. **36**(1): p. 43-48.

49.   Serajuddin, A.T., *Salt formation to improve drug solubility.* Advanced drug delivery reviews, 2007. **59**(7): p. 603-616.

50.   Kawabata, Y., et al., *Formulation design for poorly water-soluble drugs based on biopharmaceutics classification system: Basic approaches and practical applications.* International Journal of Pharmaceutics, 2011. **420**(1): p. 1-10.

51.   JOHN, M.K., et al., *Development and Pharmacokinetic Evaluation of a Curcumin Co-solvent Formulation.* Anticancer Research, 2013. **33**(10): p. 4285-4291.

52.   Bendas, B., U. Schmalfuβ, and R. Neubert, *Influence of propylene glycol as cosolvent on mechanisms of drug transport from hydrogels.* International journal of pharmaceutics, 1995. **116**(1): p. 19-30.

53.   Watkinson, R., et al., *Influence of ethanol on the solubility, ionization and permeation characteristics of ibuprofen in silicone and human skin.* Skin pharmacology and physiology, 2009. **22**(1): p. 15-21.

54.   Del Valle, E.M., *Cyclodextrins and their uses: a review.* Process biochemistry, 2004. **39**(9): p. 1033-1046.

55.   Davis, M.E. and M.E. Brewster, *Cyclodextrin-based pharmaceutics: past, present and future.* Nature Reviews Drug Discovery, 2004. **3**(12): p. 1023-1035.

56.   Chen, H., et al., *Nanonization strategies for poorly water-soluble drugs.* Drug Discovery Today, 2011. **16**(7): p. 354-360.

57.   Murdande, S.B., D.A. Shah, and R.H. Dave, *Impact of Nanosizing on Solubility and Dissolution Rate of Poorly Soluble Pharmaceuticals.* Journal of Pharmaceutical Sciences, 2015. **104**(6): p. 2094-2102.

58.   Date, A.A., et al., *Development and evaluation of a thermosensitive vaginal gel containing raltegravir+ efavirenz loaded nanoparticles for HIV prophylaxis.* Antiviral research, 2012. **96**(3): p. 430-436.

59.   Pavelić, Ž., N. Škalko-Basnet, and I. Jalšenjak, *Characterisation and in vitro evaluation of bioadhesive liposome gels for local therapy of vaginitis.* International journal of pharmaceutics, 2005. **301**(1): p. 140-148.

60.   Pavelic, Z., N. Skalko-Basnet, and I. Jalsenjak, *Liposomal gel with chloramphenicol: Characterisation and in vitro release.* Acta Pharm, 2004. **54**(4): p. 319-330.

61.   Lai, S.K., Y.-Y. Wang, and J. Hanes, *Mucus-penetrating nanoparticles for drug and gene delivery to mucosal tissues.* Advanced Drug Delivery Reviews, 2009. **61**(2): p. 158-171.

62.   Tang, B.C., et al., *Biodegradable polymer nanoparticles that rapidly penetrate the human mucus barrier.* Proceedings of the National Academy of Sciences, 2009. **106**(46): p. 19268-19273.

63.   Lee, S.K., et al., *Immune Cells in the Female Reproductive Tract.* Immune Netw, 2015. **15**(1): p. 16-26.

64.   Givan, A.L., et al., *Flow cytometric analysis of leukocytes in the human female reproductive tract: comparison of fallopian tube, uterus, cervix, and vagina.* American journal of reproductive immunology, 1997. **38**(5): p. 350-359.

65.   Ma, Z., et al., *The number and distribution of immune cells in the cervicovaginal mucosa remain constant throughout the menstrual cycle of rhesus macaques.* Clinical Immunology, 2001. **100**(2): p. 240-249.

66.   Trifonova, R.T., J. Lieberman, and D. Baarle, *Distribution of immune cells in the human cervix and implications for HIV transmission.* American Journal of Reproductive Immunology, 2014. **71**(3): p. 252-264.

67.   Salamonsen, L.A. and D.E. Woolley, *Menstruation: induction by matrix metalloproteinases and inflammatory cells.* Journal of reproductive immunology, 1999. **44**(1): p. 1-27.

68.   Wira, C.R., et al., *Regulation of mucosal immunity in the female reproductive tract: the role of sex hormones in immune protection against sexually transmitted pathogens.* American Journal of Reproductive Immunology, 2014. **72**(2): p. 236-258.

69.   Hu, J., M.B. Gardner, and C.J. Miller, *Simian Immunodeficiency Virus Rapidly Penetrates the Cervicovaginal Mucosa after Intravaginal Inoculation and Infects Intraepithelial Dendritic Cells.* Journal of Virology, 2000. **74**(13): p. 6087-6095.

70.   Stieh, D.J., et al., *Vaginal challenge with an SIV-based dual reporter system reveals that infection can occur throughout the upper and lower female reproductive tract.* 2014.

71.   Li, Q., et al., *Glycerol monolaurate prevents mucosal SIV transmission.* Nature, 2009. **458**(7241): p. 1034-1038.

72.   Cohen, O., et al., *Studies on lymphoid tissue from HIV-infected individuals: implications for the design of therapeutic strategies*, in *Immunopathogenesis of HIV Infection*, A. Fauci and G. Pantaleo, Editors. 1997, Springer Berlin Heidelberg. p. 53-70.

73.   Torchilin, V.P., *Nanoparticles as drug carriers*. 2006: Imperial College Press. 724.

74.   Gao, X., et al., *In vivo cancer targeting and imaging with semiconductor quantum dots.* Nature biotechnology, 2004. **22**(8): p. 969-976.

75.   Luo, G., et al., *LyP-1-conjugated nanoparticles for targeting drug delivery to lymphatic metastatic tumors.* International Journal of Pharmaceutics, 2010. **385**(1–2): p. 150-156.

76.   Xie, Y., et al., *Drug delivery to the lymphatic system: importance in future cancer diagnosis and therapies.* 2009.

77.   Kim, S., et al., *Near-infrared fluorescent type II quantum dots for sentinel lymph node mapping.* Nature biotechnology, 2004. **22**(1): p. 93-97.

78.   Ballou, B., et al., *Noninvasive imaging of quantum dots in mice.* Bioconjugate chemistry, 2004. **15**(1): p. 79-86.

79.   Giuliano, A.E., et al., *Lymphatic mapping and sentinel lymphadenectomy for breast cancer.* Annals of surgery, 1994. **220**(3): p. 391.

80.   Nishioka, Y. and H. Yoshino, *Lymphatic targeting with nanoparticulate system.* Advanced drug delivery reviews, 2001. **47**(1): p. 55-64.

81. Damge, C., et al., *Nanocapsules as carriers for oral peptide delivery.* Journal of Controlled Release, 1990. **13**(2): p. 233-239.

82. Eldridge, J.H., et al., *Controlled vaccine release in the gut-associated lymphoid tissues. I. Orally administered biodegradable microspheres target the Peyer's patches.* Journal of Controlled Release, 1990. **11**(1): p. 205-214.

83. Désormeaux, A. and M. G. Bergeron, *Lymphoid Tissue Targeting of Anti-HIV Drugs Using Liposomes*, in *Methods in Enzymology*, D. Nejat, Editor. 2005, Academic Press. p. 330-351.

84. Reddy, S.T., et al., *In vivo targeting of dendritic cells in lymph nodes with poly(propylene sulfide) nanoparticles.* Journal of Controlled Release, 2006. **112**(1): p. 26-34.

85. Sheue Nee Ling, S., et al., *Enhanced Oral Bioavailability and Intestinal Lymphatic Transport of a Hydrophilic Drug Using Liposomes.* Drug Development and Industrial Pharmacy, 2006. **32**(3): p. 335-345.

86. Cai, S., et al., *Lymphatic drug delivery using engineered liposomes and solid lipid nanoparticles.* Advanced drug delivery reviews, 2011. **63**(10): p. 901-908.

87. Kaminskas, L.M. and C.J. Porter, *Targeting the lymphatics using dendritic polymers (dendrimers).* Advanced drug delivery reviews, 2011. **63**(10): p. 890-900.

88. Singh, I., et al., *Delivery Systems for Lymphatic Targeting*, in *Focal Controlled Drug Delivery*, A.J. Domb and W. Khan, Editors. 2014, Springer US. p. 429-458.

89. O'Hagan, D., N. Christy, and S. Davis, *Particulates and lymphatic drug delivery*, in *Lymphatic transport of drugs*. 1992, CRC Press Boca Raton, FL. p. 279-315.

90. Velinova, M., et al., *Morphological observations on the fate of liposomes in the regional lymph nodes after footpad injection into rats.* Biochimica et Biophysica Acta (BBA)-Lipids and Lipid Metabolism, 1996. **1299**(2): p. 207-215.

91. Kaur, C.D., M. Nahar, and N.K. Jain, *Lymphatic targeting of zidovudine using surface-engineered liposomes.* Journal of drug targeting, 2008. **16**(10): p. 798-805.

92. Dufresne, I., et al., *Targeting lymph nodes with liposomes bearing anti-HLA-DR Fab′ fragments.* Biochimica et Biophysica Acta (BBA)-Biomembranes, 1999. **1421**(2): p. 284-294.

93. Tacken, P.J., et al., *Targeted delivery of TLR ligands to human and mouse dendritic cells strongly enhances adjuvanticity*. Vol. 118. 2011. 6836-6844.

94. Hawley, A., S. Davis, and L. Illum, *Targeting of colloids to lymph nodes: influence of lymphatic physiology and colloidal characteristics.* Advanced Drug Delivery Reviews, 1995. **17**(1): p. 129-148.

95. McLennan, D.N., C.J. Porter, and S.A. Charman, *Subcutaneous drug delivery and the role of the lymphatics.* Drug Discovery Today: Technologies, 2005. **2**(1): p. 89-96.

96. Hawley, A.E., L. Illum, and S.S. Davis, *Preparation of biodegradable, surface engineered PLGA nanospheres with enhanced lymphatic drainage and lymph node uptake.* Pharmaceutical research, 1997. **14**(5): p. 657-661.

97. Lamka, J., et al., *Influence of the composition of rat central lymph on the pharmacokinetics (the steady state during infusion, bioavailability, absorption) of diazepam, studied in the blood and lymph.* Physiologia Bohemoslovaca, 1989. **39**(5): p. 403-408.

98. Oussoren, C., et al., *Lymphatic uptake and biodistribution of liposomes after subcutaneous injection.: II. Influence of liposomal size, lipid composition and lipid dose.* Biochimica et Biophysica Acta (BBA)-Biomembranes, 1997. **1328**(2): p. 261-272.

99. Moghimi, S., *The effect of methoxy-PEG chain length and molecular architecture on lymph node targeting of immuno-PEG liposomes.* Biomaterials, 2006. **27**(1): p. 136-144.

100. Videira, M.A., et al., *Lymphatic uptake of pulmonary delivered radiolabelled solid lipid nanoparticles.* Journal of drug targeting, 2002. **10**(8): p. 607-613.

101. Latimer, P., et al., *Aerosol delivery of liposomal formulated paclitaxel and vitamin E analog reduces murine mammary tumor burden and metastases.* Experimental Biology and Medicine, 2009. **234**(10): p. 1244-1252.

102. Botelho, M.F.R.R., et al., *Nanoradioliposomes molecularly modulated to study the lung deep lymphatic drainage.* Revista Portuguesa de Pneumologia (English Edition), 2009. **15**(2): p. 261-293.

103. Kraft, S.L., et al., *Magnetic resonance imaging of pulmonary lesions in guinea pigs infected with Mycobacterium tuberculosis.* Infection and immunity, 2004. **72**(10): p. 5963-5971.

104. Çuburu, N., et al., *Intravaginal immunization with HPV vectors induces tissue-resident CD8+ T cell responses.* The Journal of clinical investigation, 2012. **122**(12): p. 4606.

105. Ballou, B., et al., *Nanoparticle transport from mouse vagina to adjacent lymph nodes.* PloS one, 2012. **7**(12): p. e51995.

106. Howe, S.E. and V.H. Konjufca, *Protein-coated nanoparticles are internalized by the epithelial cells of the female reproductive tract and induce systemic and mucosal immune responses.* PloS one, 2014. **9**(12): p. e114601.

107. Porter, C.J., *Drug delivery to the lymphatic system.* Critical reviews in therapeutic drug carrier systems, 1997. **14**(4): p. 333-394.

108. Bergqvist, L., et al., *The characterisation of radio colloids used for administration to the lymphatic system.* Davis SS, Ilium L, 1984. **1206**: p. 263-267.

109. Hlrano, K. and C. Anthony Hunt, *Lymphatic transport of liposome-encapsulated agents: Effects of liposome size following intraperitoneal administration.* Journal of Pharmaceutical Sciences, 1985. **74**(9): p. 915-921.

110. Patel, H.M., B. Katherine M, and R. Vaughan-Jones, *Assessment of the potential uses of liposomes for lymphoscintigraphy and lymphatic drug delivery failure of 99m-technetium marker to represent intact liposomes in lymph nodes.* Biochimica et Biophysica Acta (BBA) - General Subjects, 1984. **801**(1): p. 76-86.

111. Patel, H.M., *Serum opsonins and liposomes: their interaction and opsonophagocytosis.* Critical reviews in therapeutic drug carrier systems, 1992. **9**(1): p. 39-90.

112. Stafford, M.K., et al., *Safety Study of Nonoxynol-9 as a Vaginal Microbicide: Evidence of Adverse Effects.* JAIDS Journal of Acquired Immune Deficiency Syndromes, 1998. **17**(4): p. 327-331.

113. Moncla, B.J. and S.L. Hillier, *Why nonoxynol-9 may have failed to prevent acquisition of Neisseria gonorrhoeae in clinical trials.* Sexually transmitted diseases, 2005. **32**(8): p. 491-494.

114. Hillier, S.L., et al., *In vitro and in vivo: the story of nonoxynol 9.* JAIDS Journal of Acquired Immune Deficiency Syndromes, 2005. **39**(1): p. 1-8.

115. Abdool Karim, S.S., et al., *Safety and effectiveness of BufferGel and 0.5% PRO2000 gel for the prevention of HIV infection in women.* AIDS, 2011. **25**(7): p. 957-66.

116. Garg, S., et al., *Properties of a new acid-buffering bioadhesive vaginal formulation (ACIDFORM).* Contraception, 2001. **64**(1): p. 67-75.

117. Skoler-Karpoff, S., et al., *Efficacy of Carraguard for prevention of HIV infection in women in South Africa: a randomised, double-blind, placebo-controlled trial.* Lancet, 2008. **372**(9654): p. 1977-87.

118. Van Damme, L., et al., *Lack of effectiveness of cellulose sulfate gel for the prevention of vaginal HIV transmission.* N Engl J Med, 2008. **359**(5): p. 463-72.

119. Lacey, C.J., et al., *Unacceptable side-effects associated with a hyperosmolar vaginal microbicide in a phase 1 trial.* Int J STD AIDS, 2010. **21**(10): p. 714-7.

120. McCormack, S., et al., *PRO2000 vaginal gel for prevention of HIV-1 infection (Microbicides Development Programme 301): a phase 3, randomised, double-blind, parallel-group trial.* Lancet, 2010. **376**(9749): p. 1329-37.

121. AIDSinfo. *The HIV Life Cycle*. 2015; Available from: https://aidsinfo.nih.gov/education-materials/fact-sheets/19/73/the-hiv-life-cycle.

122. Emau, P., et al., *Griffithsin, a potent HIV entry inhibitor, is an excellent candidate for anti-HIV microbicide.* Journal of Medical Primatology, 2007. **36**(4-5): p. 244-253.

123. Fatkenheuer, G., et al., *Efficacy of short-term monotherapy with maraviroc, a new CCR5 antagonist, in patients infected with HIV-1.* Nat Med, 2005. **11**(11): p. 1170-1172.

124. Kawamura, T., et al., *PSC-RANTES Blocks R5 Human Immunodeficiency Virus Infection of Langerhans Cells Isolated from Individuals with a Variety of CCR5 Diplotypes.* Journal of Virology, 2004. **78**(14): p. 7602-7609.

125. Bangsberg, D.R., et al., *Adherence to protease inhibitors, HIV-1 viral load, and development of drug resistance in an indigent population.* AIDS, 2000. **14**(4): p. 357-366.

126. Reeves, J. and A. Piefer, *Emerging Drug Targets for Antiretroviral Therapy.* Drugs, 2005. **65**(13): p. 1747-1766.

127. Motakis, D. and M.A. Parniak, *A Tight-Binding Mode of Inhibition Is Essential for Anti-Human Immunodeficiency Virus Type 1 Virucidal Activity of Nonnucleoside Reverse Transcriptase Inhibitors.* Antimicrobial Agents and Chemotherapy, 2002. **46**(6): p. 1851-1856.

128. Motakis, D. and M. Parniak, *A tight-binding mode of inhibition is essential for anti-human immunodeficiency virus type 1 virucidal activity of nonnucleoside reverse transcriptase inhibitors.* Antim Agent Chem, 2002. **6**(46): p. 1851 - 1856.

129. Paul Lewi, J.H., *Reverse Transcriptase Inhibitors as Microbicides.* Current HIV Research, 2012. **10**: p. 27-35.

130. Das, K., et al., *High-resolution structures of HIV-1 reverse transcriptase/TMC278 complexes: Strategic flexibility explains potency against resistance mutations.* Proceedings of the National Academy of Sciences, 2008. **105**(5): p. 1466-1471.

131. Williams, T.M., et al., *5-Chloro-3-(phenylsulfonyl)indole-2-carboxamide: a novel, non-nucleoside inhibitor of HIV-1 reverse transcriptase.* Journal of Medicinal Chemistry, 1993. **36**(9): p. 1291-1294.

132. Parniak, M.A., *Nonnucleoside reverse transcriptase inhibitors as anti-HIV-1 microbicides.* AIDS, 2001. **15**: p. S56.

133. ICH, *Stability Testing Guidelines: Stability Testing of New Drug Substances and Products* 2003.

134. das Neves, J., M.H. Amaral, and M.F. Bahia, *Vaginal Drug Delivery*, in *Pharmaceutical Manufacturing Handbook*. 2007, John Wiley & Sons, Inc. p. 809-878.

135. GUIDELINE, I.H.T., *VALIDATION OF ANALYTICAL PROCEDURES: TEXT AND METHODOLOGY Q2 (R1).*

136. *The United States Pharmacopeia, USP 30-NF 25.* 2007.

137. *British Pharmacopoeia.* 2009.

138. Savjani, K.T., A.K. Gajjar, and J.K. Savjani, *Drug Solubility: Importance and Enhancement Techniques.* ISRN Pharmaceutics, 2012. **2012**: p. 195727.

139. Blessy, M., et al., *Development of forced degradation and stability indicating studies of drugs—A review.* Journal of Pharmaceutical Analysis, 2014. **4**(3): p. 159-165.

140. Alsante, K.M., et al., *The role of degradant profiling in active pharmaceutical ingredients and drug products.* Advanced drug delivery reviews, 2007. **59**(1): p. 29-37.

141. Quayle, A.J., *The innate and early immune response to pathogen challenge in the female genital tract and the pivotal role of epithelial cells.* Journal of Reproductive Immunology, 2002. **57**(1–2): p. 61-79.

142. D'Cruz, O.J. and F.M. Uckun, *Clinical Development of Microbicides for the Prevention of HIV Infection.* Current Pharmaceutical Design, 2004. **10**(3): p. 315-336.

143. Williams, T., et al., *5-Chloro-3- (phenylsulfonyl)indole-2-carboxamide: a novel, non-nucleoside inhibitor of HIV-1 reverse transcriptase.* J Med Chem, 1993. **36**: p. 1291 - 1294.

144. Yeh, M.-K., L.-C. Chang, and A.-J. Chiou, *Improving Tenoxicam Solubility and Bioavailability by Cosolvent System.* AAPS PharmSciTech, 2009. **10**(1): p. 166-171.

145. Rubino, J.T., *Cosolvents and Cosolvency*, in *Encyclopedia of Pharmaceutical Technology, Third Edition*. p. 806-819.

146. Nayak, A.K. and P.P. Panigrahi, *Solubility Enhancement of Etoricoxib by Cosolvency Approach.* ISRN Physical Chemistry, 2012. **2012**: p. 5.

147. Gelderblom, H., et al., *Cremophor EL: the drawbacks and advantages of vehicle selection for drug formulation.* European Journal of Cancer, 2001. **37**(13): p. 1590-1598.

148. Sinha, S., et al., *Solid dispersion as an approach for bioavailability enhancement of poorly water-soluble drug ritonavir.* AAPS PharmSciTech, 2010. **11**(2): p. 518 - 527.

149. Arunprasad, K., N. Narayanan, and G. Rajalakshmi, *Preparation and evaluation of solid dispersion of terbinafine hydrochloride.* International journal of pharmaceutical sciences review and research, 2010. **3**(1): p. 130-134.

150. Serajuddin, A.T.M., *Solid dispersion of poorly water-soluble drugs: Early promises, subsequent problems, and recent breakthroughs.* Journal of Pharmaceutical Sciences, 1999. **88**(10): p. 1058-1066.

151. Dobaria, N., A.C. Badhan, and R.C. Mashru, *A Novel Itraconazole Bioadhesive Film for Vaginal Delivery: Design, Optimization, and Physicodynamic Characterization.* AAPS PharmSciTech, 2009. **10**(3): p. 951-959.

152. Akil, A., et al., *Development and Characterization of a Vaginal Film Containing Dapivirine, a Non-nucleoside Reverse Transcriptase Inhibitor (NNRTI), for prevention of HIV-1 sexual transmission.* Drug Deliv Transl Res, 2011. **1**(3): p. 209-222.

153. Garg, S., et al., *Development and Characterization of Bioadhesive Vaginal Films of Sodium Polystyrene Sulfonate (PSS), a Novel Contraceptive Antimicrobial Agent.* Pharmaceutical Research, 2005. **22**(4): p. 584-595.

154. Neurath, A., N. Strick, and Y.-Y. Li, *Water dispersible microbicidal cellulose acetate phthalate film.* BMC Infectious Diseases, 2003. **3**(1): p. 27.

155. Akil, A., et al., *Increased Dapivirine Tissue Accumulation through Vaginal Film Codelivery of Dapivirine and Tenofovir.* Molecular Pharmaceutics, 2014. **11**(5): p. 1533-1541.

156. Christopher Elias, C.C., *Acceptability Research on Female-Controled Barrier Methods to Prevent Heterosexual Transmission of HIV: Where Have We Been? Where Are We Going?* J Wemens Health & Gender Based Med., 2001. **10**(2): p. 11.

157. Raymond, E., et al., *Acceptability of two spermicides in five countries.* Contraception, 1999. **60**(1): p. 45-50.

158. Ham, A., et al., *Vaginal Film Drug Delivery of the Pyrimidinedione IQP-0528 for the Prevention of HIV Infection.* Pharmaceutical Research, 2012. **29**(7): p. 1897-1907.

159. Freire, F.D., et al., *Compatibility study between chlorpropamide and excipients in their physical mixtures.* Journal of Thermal Analysis and Calorimetry, 2009. **97**(1): p. 355-357.

160. Roumeli, E., et al., *Compatibility study between trandolapril and natural excipients used in solid dosage forms.* Journal of Thermal Analysis and Calorimetry, 2012. **111**(3): p. 2109-2115.

161. *<Guidance for Industry Q1A(R2) Stability Testing of New Drug Substances and Products.pdf>.*

162. Morales, J.O. and J.T. McConville, *Manufacture and characterization of mucoadhesive buccal films.* European Journal of Pharmaceutics and Biopharmaceutics, 2011. **77**(2): p. 187-199.

163. Garg, S., S. Garg, and G. Kumar, *Development and evaluation of a buccal bioadhesive system for smoking cessation therapy.* Die Pharmazie - An International Journal of Pharmaceutical Sciences, 2007. **62**(4): p. 266-272.

164. Satish K. Patil, K.S.W., Venkatesh B. Parik, Anup M Akarte, Dheeraj T. Baviskar, *<Strategies for solubility enhancement of poorly soluble drugs.pdf>*. International Journal of Pharmaceutical Sciences Review and Research, 2011. **8**(2): p. 7.

165. Nel, A.M., et al., *Safety, tolerability, and systemic absorption of dapivirine vaginal microbicide gel in healthy, HIV-negative women.* AIDS, 2009. **23**(12): p. 1531-1538 10.1097/QAD.0b013e32832c413d.

166. Nel, A.M., et al., *Pharmacokinetics of 2 Dapivirine Vaginal Microbicide Gels and Their Safety Vs. Hydroxyethyl Cellulose-Based Universal Placebo Gel.* JAIDS Journal of Acquired Immune Deficiency Syndromes, 2010. **55**(2): p. 161-169 10.1097/QAI.0b013e3181e3293a.

167. Obitte, N., et al., *The utility of self-emulsifying oil formulation to improve the poor solubility of the anti HIV drug CSIC.* AIDS Research and Therapy, 2013. **10**(1): p. 14.

168. Fuchs, E.J., et al., *Hyperosmolar Sexual Lubricant Causes Epithelial Damage in the Distal Colon: Potential Implication for HIV Transmission.* Journal of Infectious Diseases, 2007. **195**(5): p. 703-710.

169. Lacey, C.J., et al., *Unacceptable side-effects associated with a hyperosmolar vaginal microbicide in a phase 1 trial.* International Journal of STD & AIDS, 2010. **21**(10): p. 714-717.

170. Dezzutti, C.S., et al., *Reformulated tenofovir gel for use as a dual compartment microbicide.* Journal of Antimicrobial Chemotherapy, 2012. **67**(9): p. 2139-2142.

171. Perissutti, B., et al., *Formulation design of carbamazepine fast-release tablets prepared by melt granulation technique.* International journal of pharmaceutics, 2003. **256**(1): p. 53-63.

172. Patel, K., et al., *Oral delivery of paclitaxel nanocrystal (PNC) with a dual Pgp-CYP3A4 inhibitor: Preparation, characterization and antitumor activity.* International Journal of Pharmaceutics, 2014. **472**(1–2): p. 214-223.

173. Rabinow, B., et al., *Itraconazole IV nanosuspension enhances efficacy through altered pharmacokinetics in the rat.* International Journal of Pharmaceutics, 2007. **339**(1–2): p. 251-260.

174. Mishra, P.R., et al., *Production and characterization of Hesperetin nanosuspensions for dermal delivery.* International Journal of Pharmaceutics, 2009. **371**(1–2): p. 182-189.

175. Sekiguchi, K. and N. Obi, *Studies on Absorption of Eutectic Mixture. I. A Comparison of the Behavior of Eutectic Mixture of Sulfathiazole and that of Ordinary Sulfathiazole in Man.* Pharmaceutical Bulletin, 1961. **9**(11): p. 866-872.

176. Leone, F. and R. Cavalli, *Drug nanosuspensions: a ZIP tool between traditional and innovative pharmaceutical formulations.* Expert Opinion on Drug Delivery. **0**(0): p. 1-19.

177. Shegokar, R. and R.H. Müller, *Nanocrystals: Industrially feasible multifunctional formulation technology for poorly soluble actives.* International Journal of Pharmaceutics, 2010. **399**(1–2): p. 129-139.

178. Salazar, J., *Combinative particle size reduction technologies for the formulation of poorly soluble drugs*. 2013, Freie Universität Berlin.

179. Rebbeck, j.E.K.J.C.T.W.M.J.D.C.L., *Microprecipitation method for preparing submicron suspensions US Patent 6607784 B2.* 2003.

180. Al Shaal, L., R.H. Müller, and R. Shegokar, *smartCrystal combination technology – scale up from lab to pilot scale and long term stability.* Die Pharmazie - An International Journal of Pharmaceutical Sciences, 2010. **65**(12): p. 877-884.

181. Muller, C.K.S.K.R.M.R.H., *Second generation of drug nanocrystals for delivery of poorly soluble drugs smartCrystal technology.* DOSIS, 2008. **24**.

182. Moschwitzer, J. and R. Muller, *Drug Nanocrystals-The Universal Formulation Approach for Poorly Soluble Drugs.* DRUGS AND THE PHARMACEUTICAL SCIENCES, 2007. **166**: p. 71.

183.   Baert, L., et al., *Development of a long-acting injectable formulation with nanoparticles of rilpivirine (TMC278) for HIV treatment.* European Journal of Pharmaceutics and Biopharmaceutics, 2009. **72**(3): p. 502-508.

184.   Clift, M.J., et al., *The impact of different nanoparticle surface chemistry and size on uptake and toxicity in a murine macrophage cell line.* Toxicology and applied pharmacology, 2008. **232**(3): p. 418-427.

185.   Janát-Amsbury, M., et al., *Geometry and surface characteristics of gold nanoparticles influence their biodistribution and uptake by macrophages.* European Journal of Pharmaceutics and Biopharmaceutics, 2011. **77**(3): p. 417-423.

186.   Zahr, A.S., C.A. Davis, and M.V. Pishko, *Macrophage uptake of core-shell nanoparticles surface modified with poly (ethylene glycol).* Langmuir, 2006. **22**(19): p. 8178-8185.

187.   Jøraholmen, M.W., et al., *Chitosan-coated liposomes for topical vaginal therapy: Assuring localized drug effect.* International Journal of Pharmaceutics, 2014. **472**(1–2): p. 94-101.

188.   Abram, M.E., S.G. Sarafianos, and M.A. Parniak, *The mutation T477A in HIV-1 reverse transcriptase (RT) restores normal proteolytic processing of RT in virus with Gag-Pol mutated in the p51-RNH cleavage site.* Retrovirology, 2010. **7**(6).

189.   Lu, J., et al., *Mesoporous Silica Nanoparticles for Cancer Therapy: Energy-Dependent Cellular Uptake and Delivery of Paclitaxel to Cancer Cells.* NanoBiotechnology, 2007. **3**(2): p. 89-95.

190.   Fernando, L.P., et al., *Mechanism of Cellular Uptake of Highly Fluorescent Conjugated Polymer Nanoparticles.* Biomacromolecules, 2010. **11**(10): p. 2675-2682.

191.   Zhang, L.W. and N.A. Monteiro-Riviere, *Mechanisms of Quantum Dot Nanoparticle Cellular Uptake.* Toxicological Sciences, 2009. **110**(1): p. 138-155.

192.   Tahara, K., et al., *Improved cellular uptake of chitosan-modified PLGA nanospheres by A549 cells.* International Journal of Pharmaceutics, 2009. **382**(1–2): p. 198-204.

193.   Banquy, X., et al., *Effect of mechanical properties of hydrogel nanoparticles on macrophage cell uptake.* Soft Matter, 2009. **5**(20): p. 3984-3991.

194.   Sandvig, K., et al., *Clathrin-independent endocytosis: from nonexisting to an extreme degree of complexity.* Histochemistry and Cell Biology, 2008. **129**(3): p. 267-276.

195.   Deng, J., L. Huang, and F. Liu, *Understanding the structure and stability of paclitaxel nanocrystals.* International Journal of Pharmaceutics, 2010. **390**(2): p. 242-249.

196.   Yang, M., et al., *Biodegradable Nanoparticles Composed Entirely of Safe Materials that Rapidly Penetrate Human Mucus.* Angewandte Chemie International Edition, 2011. **50**(11): p. 2597-2600.

197.   Moghimi, S., *Modulation of lymphatic distribution of subcutaneously injected poloxamer 407-coated nanospheres: the effect of the ethylene oxide chain configuration.* FEBS letters, 2003. **540**(1): p. 241-244.

198.   Oussoren, C. and G. Storm, *Lymphatic uptake and biodistribution of liposomes after subcutaneous injection: III. Influence of surface modification with poly (ethyleneglycol).* Pharmaceutical research, 1997. **14**(10): p. 1479-1484.

199.   Illum, L., et al., *Development of systems for targeting the regional lymph nodes for diagnostic imaging: in vivo behaviour of colloidal PEG-coated magnetite nanospheres in the rat following interstitial administration.* Pharmaceutical research, 2001. **18**(5): p. 640-645.

200.   Oussoren, C., et al., *Lymphatic uptake and biodistribution of liposomes after subcutaneous injection: IV. Fate of liposomes in regional lymph nodes.* Biochimica et Biophysica Acta (BBA)-Biomembranes, 1998. **1370**(2): p. 259-272.

201.   Verma, S., et al., *Physical stability of nanosuspensions: investigation of the role of stabilizers on Ostwald ripening.* International journal of pharmaceutics, 2011. **406**(1): p. 145-152.

202.   Woodrow, K.A., et al., *Intravaginal gene silencing using biodegradable polymer nanoparticles densely loaded with small-interfering RNA.* Nat Mater, 2009. **8**(6): p. 526-533.

203.	Lai, S.K., et al., *Rapid transport of large polymeric nanoparticles in fresh undiluted human mucus.* Proceedings of the National Academy of Sciences, 2007. **104**(5): p. 1482-1487.
204.	Rao, D.A., et al., *Biodegradable PLGA based nanoparticles for sustained regional lymphatic drug delivery.* Journal of pharmaceutical sciences, 2010. **99**(4): p. 2018-2031.
205.	O'Driscoll, C.M., *Anatomy and physiology of the lymphatics*, in *Lymphatic transport of drugs*. 1992, Boca Raton, FL: CRC Press Inc. p. 1-35.
206.	Khan, A.A., et al., *Advanced drug delivery to the lymphatic system: lipid-based nanoformulations.* International journal of nanomedicine, 2013. **8**: p. 2733.
207.	Siegel, R.A. and M.J. Rathbone, *Overview of controlled release mechanisms*, in *Fundamentals and Applications of Controlled Release Drug Delivery*. 2012, Springer. p. 19-43.
208.	Liu, Y., L. Huang, and F. Liu, *Paclitaxel nanocrystals for overcoming multidrug resistance in cancer.* Molecular pharmaceutics, 2010. **7**(3): p. 863-869.
209.	Walkey, C.D., et al., *Nanoparticle Size and Surface Chemistry Determine Serum Protein Adsorption and Macrophage Uptake.* Journal of the American Chemical Society, 2012. **134**(4): p. 2139-2147.
210.	Moghimi, S.M. and J. Szebeni, *Stealth liposomes and long circulating nanoparticles: critical issues in pharmacokinetics, opsonization and protein-binding properties.* Progress in Lipid Research, 2003. **42**(6): p. 463-478.
211.	Immordino, M.L., F. Dosio, and L. Cattel, *Stealth liposomes: review of the basic science, rationale, and clinical applications, existing and potential.* International journal of nanomedicine, 2006. **1**(3): p. 297.
212.	Nowacek, A.S., et al., *Analyses of nanoformulated antiretroviral drug charge, size, shape and content for uptake, drug release and antiviral activities in human monocyte-derived macrophages.* Journal of Controlled Release, 2011. **150**(2): p. 204-211.
213.	Mauludin, R., R.H. Müller, and C.M. Keck, *Development of an oral rutin nanocrystal formulation.* International Journal of Pharmaceutics, 2009. **370**(1–2): p. 202-209.
214.	Kassem, M., et al., *Nanosuspension as an ophthalmic delivery system for certain glucocorticoid drugs.* International journal of pharmaceutics, 2007. **340**(1): p. 126-133.
215.	Müller, R., et al., *Nanocrystals: Production, Cellular Drug Delivery, Current and Future Products*, in *Intracellular Delivery*, A. Prokop, Editor. 2011, Springer Netherlands. p. 411-432.
216.	Mauludin, R. and R.H. Müller, *Physicochemical properties of hesperidin nanocrystal.* Int J Pharm Pharm Sci, 2013. **5**(Suppl 3): p. 954-60.
217.	Petersen, R., *Nanocrystals for use in topical cosmetic formulations and method of production thereof*. 2010, Google Patents.
218.	Squier, C.A., et al., *Porcine vagina Ex Vivo as a model for studying permeability and pathogenesis in mucosa.* Journal of Pharmaceutical Sciences, 2008. **97**(1): p. 9-21.
219.	Machado, R.M., et al., *Studies and methodologies on vaginal drug permeation.* Advanced Drug Delivery Reviews, (0).
220.	Rohan, L.C., et al., *In Vitro and Ex Vivo Testing of Tenofovir Shows It Is Effective As an HIV-1 Microbicide.* PLoS ONE, 2010. **5**(2): p. e9310.
221.	Popov, A., et al., *Nanocrystals, compositions, and methods that aid particle transport in mucus*. 2013, Google Patents.
222.	Lieleg, O. and K. Ribbeck, *Biological hydrogels as selective diffusion barriers.* Trends in cell biology, 2011. **21**(9): p. 543-551.
223.	Olmsted, S.S., et al., *Diffusion of macromolecules and virus-like particles in human cervical mucus.* Biophysical journal, 2001. **81**(4): p. 1930-1937.

224. Shogren, R., T.A. Gerken, and N. Jentoft, *Role of glycosylation on the conformation and chain dimensions of O-linked glycoproteins: light-scattering studies of ovine submaxillary mucin.* Biochemistry, 1989. **28**(13): p. 5525-5536.

225. Gipson, I.K., et al., *Mucin genes expressed by human female reproductive tract epithelia.* Biology of reproduction, 1997. **56**(4): p. 999-1011.

226. Sigurdsson, H.H., J. Kirch, and C.-M. Lehr, *Mucus as a barrier to lipophilic drugs.* International Journal of Pharmaceutics, 2013. **453**(1): p. 56-64.

227. Lai, S.K., et al., *Nanoparticles reveal that human cervicovaginal mucus is riddled with pores larger than viruses.* Proceedings of the National Academy of Sciences, 2010. **107**(2): p. 598-603.

228. das Neves, J., et al., *Interactions of Microbicide Nanoparticles with a Simulated Vaginal Fluid.* Molecular Pharmaceutics, 2012. **9**(11): p. 3347-3356.

229. Albertini, B., et al., *Polymer–lipid based mucoadhesive microspheres prepared by spray-congealing for the vaginal delivery of econazole nitrate.* European Journal of Pharmaceutical Sciences, 2009. **36**(4–5): p. 591-601.

230. Klein, J., *Probing the interactions of proteins and nanoparticles.* Proceedings of the National Academy of Sciences, 2007. **104**(7): p. 2029-2030.

231. Shegokar, R., et al., *In vitro protein adsorption studies on nevirapine nanosuspensions for HIV/AIDS chemotherapy.* Nanomedicine: Nanotechnology, Biology and Medicine, 2011. **7**(3): p. 333-340.

232. Trevaskis, N.L., L.M. Kaminskas, and C.J.H. Porter, *From sewer to saviour [mdash] targeting the lymphatic system to promote drug exposure and activity.* Nat Rev Drug Discov, 2015. **14**(11): p. 781-803.

233. Bhatta, R., et al., *Mucoadhesive nanoparticles for prolonged ocular delivery of natamycin: In vitro and pharmacokinetics studies.* International journal of pharmaceutics, 2012. **432**(1): p. 105-112.

234. Arangoa, M.A., et al., *Gliadin nanoparticles as carriers for the oral administration of lipophilic drugs. Relationships between bioadhesion and pharmacokinetics.* Pharmaceutical research, 2001. **18**(11): p. 1521-1527.

235. Sarmento, B., et al., *Alginate/chitosan nanoparticles are effective for oral insulin delivery.* Pharmaceutical research, 2007. **24**(12): p. 2198-2206.

236. Jeon, S.I., et al., *Protein—surface interactions in the presence of polyethylene oxide: I. Simplified theory.* Journal of Colloid and Interface Science, 1991. **142**(1): p. 149-158.

237. Szleifer, I., *Protein Adsorption on Surfaces with Grafted Polymers: A Theoretical Approach.* Biophysical Journal, 1997. **72**(2 Pt 1): p. 595-612.

238. Cu, Y., C.J. Booth, and W.M. Saltzman, *In vivo distribution of surface-modified PLGA nanoparticles following intravaginal delivery.* Journal of Controlled Release, 2011. **156**(2): p. 258-264.

239. das Neves, J., et al., *Biodistribution and Pharmacokinetics of Dapivirine-Loaded Nanoparticles after Vaginal Delivery in Mice.* Pharmaceutical Research, 2014. **31**(7): p. 1834-1845.

240. Ensign, L.M., et al., *Mucus-Penetrating Nanoparticles for Vaginal Drug Delivery Protect Against Herpes Simplex Virus.* Science Translational Medicine, 2012. **4**(138): p. 138ra79.

241. Ensign, L.M., et al., *Enhanced vaginal drug delivery through the use of hypotonic formulations that induce fluid uptake.* Biomaterials, 2013. **34**(28): p. 6922-6929.

242. Moore, K.H., et al., *The pharmacokinetics of lamivudine phosphorylation in peripheral blood mononuclear cells from patients infected with HIV-1.* Aids, 1999. **13**(16): p. 2239-2250.

243. Taylor, S., et al. *Stop Study: After discontinuation of efavirenz, plasma concentrations may persist for 2 weeks or longer*. in *11th Conference on Retroviruses and Opportunistic Infections*. 2004.

244. Cressey, T.R., et al., *Plasma Drug Concentrations and Virologic Evaluations after Stopping Treatment with Nonnucleoside Reverse-Transcriptase Inhibitors in HIV Type 1–Infected Children.* Clinical infectious diseases : an official publication of the Infectious Diseases Society of America, 2008. **46**(10): p. 1601-1608.

245. Cone, R.A., et al., *Vaginal microbicides: detecting toxicities in vivo that paradoxically increase pathogen transmission.* BMC infectious diseases, 2006. **6**(1): p. 90.

246. van den Berg, J.J., et al., *"Set it and forget it": Women's perceptions and opinions of long-acting topical vaginal gels.* AIDS and Behavior, 2014. **18**(5): p. 862-870.

247. Turner, A.N., et al., *Predictors of adherent use of diaphragms and microbicide gel in a four-arm, randomized pilot study among female sex workers in Madagascar.* Sexually transmitted diseases, 2009. **36**(4): p. 249-257.

248. Rana, P. and R. Murthy, *Formulation and evaluation of mucoadhesive buccal films impregnated with carvedilol nanosuspension: a potential approach for delivery of drugs having high first-pass metabolism.* Drug delivery, 2013. **20**(5): p. 224-235.

249. Lin, Z., et al., *Novel thermo-sensitive hydrogel system with paclitaxel nanocrystals: High drug-loading, sustained drug release and extended local retention guaranteeing better efficacy and lower toxicity.* Journal of Controlled Release, 2014. **174**(0): p. 161-170.

250. Teeranachaideekul, V., et al., *Development of ascorbyl palmitate nanocrystals applying the nanosuspension technology.* International Journal of Pharmaceutics, 2008. **354**(1–2): p. 227-234.

251. das Neves, J., et al., *Assessing the physical–chemical properties and stability of dapivirine-loaded polymeric nanoparticles.* International journal of pharmaceutics, 2013. **456**(2): p. 307-314.

252. Mirmonsef, P., et al., *A comparison of lower genital tract glycogen and lactic acid levels in women and macaques: implications for HIV and SIV susceptibility.* AIDS research and human retroviruses, 2012. **28**(1): p. 76-81.

253. Anderson, D.J., et al., *Safety analysis of the diaphragm in combination with lubricant or acidifying microbicide gels: effects on markers of inflammation and innate immunity in cervicovaginal fluid.* American Journal of Reproductive Immunology, 2009. **61**(2): p. 121-129.